AD_____

Award Number: DAMD17-01-1-0820

TITLE: Effects of Low Level Radiation Exposure on Neurogenesis and Cognitive Function: Mechanisms and Prevention

PRINCIPAL INVESTIGATOR: John R. Fike, Ph.D.

CONTRACTING ORGANIZATION: University of California, San Francisco
San Francisco, CA 94143-0962

REPORT DATE: September 2004

TYPE OF REPORT: Annual

PREPARED FOR: U.S. Army Medical Research and Materiel Command
Fort Detrick, Maryland 21702-5012

REPORT DOCUMENTATION PAGE

Form Approved
OMB No. 074-0188

1. AGENCY USE ONLY (Leave blank)	2. REPORT DATE	3. REPORT TYPE AND DATES COVERED
	September 2004	Annual (1 Aug 2003 - 1 Aug 2004)

4. TITLE AND SUBTITLE
Effects of Low Level Radiation Exposure on Neurogenesis and Cognitive Function: Mechanisms and Prevention

5. FUNDING NUMBERS
DAMD17-01-1-0820

6. AUTHOR(S)
John R. Fike, Ph.D.

7. PERFORMING ORGANIZATION NAME(S) AND ADDRESS(ES)
University of California, San Francisco
San Francisco, CA 94143-0962

E-Mail: jfike@itsa.ucsf.edu

8. PERFORMING ORGANIZATION REPORT NUMBER

9. SPONSORING / MONITORING AGENCY NAME(S) AND ADDRESS(ES)
U.S. Army Medical Research and Materiel Command
Fort Detrick, Maryland 21702-5012

10. SPONSORING / MONITORING AGENCY REPORT NUMBER

11. SUPPLEMENTARY NOTES

12a. DISTRIBUTION / AVAILABILITY STATEMENT
Approved for Public Release; Distribution Unlimited

12b. DISTRIBUTION CODE

13. ABSTRACT (Maximum 200 Words)

Studies were carried out to investigate the radiation response of neural precursor cells *in vitro* and *in vivo*, to determine the role of reactive oxygen species (ROS) in the reactions of those cells, and to determine if antioxidant treatment could modify those responses. Our data show that proliferating precursor cells and their progeny are extremely sensitive to low/moderate x-ray doses (2-10 Gy), and that ROS play a major role in the sensitivity on these cells and may act in concert with p53 and cell cycle-dependent processes. In addition, conditions of reduced cell density, such as that seen after radiation exposure of the dentate subgranular zone, are associated with increased ROS, which may stimulate proliferation in surviving cells. Modulating ROS using antioxidant compounds may provide a means to control proliferation in damaged cells allowing for repair and recovery after radiation injury. We have begun to address specific mechanistic factors that are not only associated with oxidative processes, but that may provide additional targets for interventional treatment. The ability to ameliorate the radiation effects on neural precursor cells may provide a potential protective strategy for individuals exposed to unplanned exposure to low/moderate doses of irradiation.

14. SUBJECT TERMS
Ionizing irradiation, central nervous system, neurogenesis, neural precursor cells, oxidative stress, antioxidants

15. NUMBER OF PAGES
61

16. PRICE CODE

17. SECURITY CLASSIFICATION OF REPORT	18. SECURITY CLASSIFICATION OF THIS PAGE	19. SECURITY CLASSIFICATION OF ABSTRACT	20. LIMITATION OF ABSTRACT
Unclassified	Unclassified	Unclassified	Unlimited

Table of Contents

PAGE

Cover..... 1

SF 298..... 2

Table of Contents 3

Introduction..... 4

Body..... 4

Key Research Accomplishments..... 10

Reportable Outcomes..... 10

Conclusions..... 11

Figures..... 12

References..... 16

Appendices..... 18

INTRODUCTION: Uncontrolled radiation exposure from a nuclear battlefield will lead to a wide range of delivered doses and subsequent tissue/body effects. However, such exposure does not have to be lethal to have significant consequences. The depletion of stem/precursor cells, for instance could lead to prolonged effects in some tissues, particularly if those cells have limited regenerative potential. Because of the role of hippocampal neuronal precursor cells in the development and maintenance of memory, we hypothesize that these cells are critical targets in the radiation-induced impairment of cognitive function. We contend that radiation-induced loss of these cells will decrease neurogenesis and lead to cognitive changes. We hypothesize that such effects are mediated through oxidative stress, and that by reducing oxidative injury we can ameliorate radiation-induced cognitive impairment. This research project involves a series of *in vitro* and *in vivo* laboratory studies to assess the effects of ionizing irradiation on neural precursor cells, neurogenesis and cognitive function. The experiments will assess the role of oxidative processes in the development of radiation injury and determine the efficacy of antioxidant strategies in reducing that injury.

BODY: This research project consists of 3 objectives which are: 1) using low to moderate radiation doses to simulate a battlefield exposure, quantify the effects of x-rays on dentate subgranular zone (SGZ) neurogenesis, and determine if such exposure is associated with the development of cognitive deficits; 2) using biochemical measures of oxidative stress determine the effects of x-rays on neural precursor cells in culture and test the ability of antioxidant compounds to reduce those effects; and 3) determine if antioxidant treatment during exposure to x-rays will ameliorate radiation-induced effects on neural precursor cells, neurogenesis and subsequent cognitive impairment.

The Statement of Work for the third, and last, year of funding listed 2 primary goals: 1) continue our long term radiation studies; and 2) continue *in vitro* studies to determine the role of oxidative stress in radiation injury. We were able to complete the experimental portion of these tasks and are continuing our analysis of neurogenesis.

In vitro studies:

In the first year of funding we elucidated a number of important characteristics of neural precursor cells in culture. Briefly, these cells are very sensitive to low doses of irradiation, undergoing apoptosis within 12 hours of exposure. The apoptotic changes are associated in time and radiation dose with elevations in reactive oxygen species (ROS) indicating that oxidative damage plays an important role in the acute and chronic radiation response of neural precursors. We also were able to provide preliminary evidence that ROS and apoptosis could be modulated using a superoxide dismutase (SOD) mimetic compound, Euk-134. In year 2 we showed that irradiation affected cell cycle progression of proliferating precursor cells and that the response of these cells was regulated in part by p53. Further, we showed that there were striking differences between neural precursor cells and other primary and established cells lines with respect to their ROS production as a function of culture density. This suggested that these cells may be particularly sensistive to changes in ROS, such as that seen after radiation exposure.

There are data suggesting that oxidative species may function as signaling molecules. Radiation, and other noxious stimuli elicit fluctuating changes in ROS, growth factors, and cytokine levels within the CNS and these factors can dictate the attrition and repopulation of cells within a damaged tissue. While most studies that address the effects of damaging agents focus on intracellular events, it is easy to overlook the impact of cell loss on the microenvironment and on the remaining surviving cell population. Therefore, we hypothesized that the mere absence of cells constituted an integral component of the general CNS stress response, affecting redox state and subsequent physiologic parameters. We modeled this latter effect *in vitro*, by simple manipulations of culture density. While an *in vitro* neural precursor cell model does not simulate the complexity of

the hippocampal microenvironment, it provides a unique system whereby the mechanisms governing these interactions can be addressed independently.

General methods:

Standard growth conditions for maintaining multipotential neural precursor cells derived from the rat hippocampus have recently been described by us (1). Neural precursor cells were cultured on polyornithine/laminin coated plasticware in the presence of serum-free DMEM/F12 (1:1) containing N2 supplement and 20 ng/ml of fibroblast growth factor-2 (FGF2). For all cell density experiments described, cells were seeded 2 days prior to analysis unless noted otherwise, and counted the day of assay to confirm actual cell numbers. For the purposes of this report, low density (LD) refers to $<1x10^4$ cells/cm^2 and high density (HD) refers to $>1x10^5$ cells/cm^2.

For those experiments investigating the effects of α-lipoic acid (ALA), the antioxidant was added at the time of plating and left in culture until the time of assay. Stock solutions were prepared in ethanol (10 mM) and diluted in full media the day of use.

Measurement of reactive oxygen species (ROS)

We hypothesized that changes in cell density would alter ROS levels which are critical in regulating neural precursor cell function. To show this, we monitored redox sensitive endpoints as a function of cell density. Exponentially growing cultures of neural precursor cells were seeded over a range of subconfluent cell densities ($0.4x10^4$ – $1.6x10^5$ cells/cm^2), and analyzed for ROS levels by FACS 48h after plating. To detect intracellular ROS, anchored cultures of variable cell density were treated for 1h at 37°C with 5 μM of the ROS sensitive dye 5-(and-6)-chloromethyl-2',7'-dichlorodihydrofluorescein diacetate (CM-H_2DCFDA). Oxidation of this ROS sensitive dye yielded a fluorescent analog that could be quantified by fluorescent automated cell sorting (FACS). Analysis by FACS was done immediately after dye treatment, and all measurements were repeated at least three times. Histograms of FACS sorted cells cultured at LD showed significantly more ROS than the same cells cultured at HD (Fig 1a). As cell cultures grew and expanded from LD, ROS levels dropped rapidly and then leveled off (Fig 1b). This marked dependence of ROS production on cell density was atypical of other cell lines tested. The opposite trend was observed in immortalized neural precursors (Fig. 1c) and other transformed cells (Fig. 1d,e), where increasing cell density was associated with *increasing* ROS levels. While other primary cells (Fig. 1f, g) did show the same general trend in ROS vs. cell density as primary neural precursors, the effect was much less pronounced, given that the absolute levels of ROS were at least an order of magnitude lower. These data suggest that neural precursor cells may be uniquely predisposed to redox regulation. Given their mitotic activity and multipotentiality, these cells must possess the capability to respond to multiple endogenous and exogenous cues (including oxidative stress) to control their ability to divide and/or differentiate. We suggest that ROS are critical to this decision. Given that radiation is a strong oxidizing agent, this information will be critical to understanding and perhaps ameliorating radiation effects on these cells.

Determination of cell growth and metabolic activity

The response of ROS to changes in cell density (Fig. 1) suggested that ROS are involved in regulating proliferation. To determine the potential physiological impact of ROS, cells were cultured at different densities in the presence or absence of the antioxidant ALA and analyzed for changes in growth rate and cell cycle distribution by FACS analysis. In the absence of ALA, LD cultures tended to show more rapid population growth (Fig. 2a) and higher S-phase fractions (Fig.

2b) than HD cultures. In the presence of ALA, both LD and HD cultures showed a significant and concentration-dependent inhibition of growth (~3-fold longer doubling times and ~1.5-fold reduction in S-phase cells at 100 μM).

To more thoroughly examine the potential consequences imparted by differences in cell density, metabolic activity and proliferation were measured after cells were reseeded at equal densities. Cells cultured at LD and HD as described (*i.e.* for 2 days) were harvested and either immediately assayed using the XTT assay or reseeded for subsequent analysis. Cells derived from LD cultures showed a significantly higher XTT absorbance (26%, $p<0.05$), indicating an increased metabolic activity compared to cells derived from HD. However, when these cells (i.e. LD and HD) were reseeded (on day 2) at equal densities ($1.2x10^4/cm^2$), those derived from LD cultures exhibited a persistent inhibition of growth (Fig. 3). Analysis of cultures derived from LD conditions by XTT assay showed lower absorbance at days 4, 5, and 6 compared to cultures derived from HD conditions. When day 6 cultures were harvested and reseeded again at equal densities, lower XTT readings still persisted in cultures derived from LD conditions (Fig. 3a). Cell counts confirmed that the XTT data reflected reduced cell numbers in cultures from LD. When cell counts were compared between each condition, the ratio (LD/HD) of total cells was always less than unity (Fig. 3b), indicating that cultures derived from LD conditions showed slower growth than their HD counterparts, both before and after reseeding at day 6. Similar data were also obtained when higher numbers of cells were reseeded ($4.0x10^4/cm^2$) from LD and HD cultures (Fig. 3b), suggesting that the persistent inhibition of growth was more likely a consequence of changes and/or damage incurred during the initial period of growth at low density. Given the prevalence of ROS and increased metabolic activity of the mitochondria that is associated with LD cultures, and based on the knowledge of the critical role mitochondria play in the intracellular metabolism of ROS we suspected that many of our density dependent effects were associated with alterations at the mitochondrial level.

Assay of mitochondria by FACS analysis

Our ALA data suggested that under certain conditions (i.e. LD) there are pools of ROS that are variably accessible to ALA scavenging, and hence more amenable to regulation. The most potent antioxidant form of ALA, dihydrolipoic acid, is generated by the mitochondrial α-keto acid dehydrogenase complexes, suggesting that the mitochondria are key sites of action of ALA in cells. Given the more significant impact of ALA on LD cultures, and the pivotal role of mitochondria in the generation of ROS, we postulated that mitochondrial ROS might be critical regulators of density-dependent redox changes observed in neural precursor cells. To determine the status of mitochondria under our different culture conditions, LD and HD cultures were assessed for mitochondrial content and function by FACS analysis, using the dyes nonyl acridine orange (NAO) and rhodamine 123 (R123) respectively. Analysis of FACS histograms showed no significant differences between LD and HD cultures with respect to mitochondrial content (Fig. 4a), yielding a LD/HD ratio of NAO fluorescence near unity (Fig. 4b). This result was confirmed by western analysis of mitochondrial porin levels (Fig 4c). However, analysis of cells treated with R123 at different densities showed a significant drop in fluorescence in LD cultures (Fig 4a), suggesting that those conditions favored a state of altered mitochondrial function (Fig. 4b). To demonstrate further that the drop in R123 fluorescence observed at LD represented an actual change in mitochondrial Ψ_m, cells cultured at different densities were also analyzed with the dye tetrametylrhodamine methyl ester (TMRM). Fluorescence in LD cultures treated with TMRM was not reduced to the same extent as found with R123 (Fig. 4b), and may reflect both differences in dye uptake and some

concentration dependent quenching of R123 fluorescence. Despite these differences, both dyes showed lower fluorescence suggesting real, physiologic changes in mitochondrial Ψ_m in LD cultures. In addition to the impact of density upon mitochondrial function, the levels of proteins specific to these organelles were also found to be different. Low density cultures had 3-4 times less MnSOD than HD cultures (Fig. 4c), as well as significantly lower levels of the metabolic enzyme aconitase (Fig. 4c). These data suggest that as cells expand to HD, there is a direct upregulation of MnSOD that reduces ROS and slows proliferation. However, high levels of ROS can also be damaging, and likely contribute to the degradation of mitochondrial aconitase, since message levels of this protein as determined by RT-PCR show little variation with cell density (data not shown). Changes in mitochondrial proteins noted above clearly show that redox state impacts the physiology of these cells.

The dual nature of ROS and their impact upon the mitochondria may underlie many of the density dependent changes we observed. Conditions of LD trigger a rise in metabolic activity accompanied by an elevation of ROS that can promote proliferation. However, the high levels of ROS found at LD can also be damaging (e.g. aconitase degradation) and may also lead to changes that cause the persistent inhibition of growth observed in cells reseeded from LD as opposed to HD cultures. While the precise cause of this effect is uncertain, heritable changes in the mitochondria caused by elevated ROS may provide one clue. Oxidative damage to the mitochondrial DNA could compromise the proliferative capacity of daughter cells derived from LD. Others have found that certain mitochondrial defects can hasten the onset of aging and degenerative conditions. This information along with the data presented here suggests that the memory of past insult in neural precursor cells can be transmitted through damaged mitochondria. This concept awaits further experimental validation.

In Vivo Studies

In the first 2 years of funding we were able to show that: 1) neural precursor cells and their progeny are extremely sensitive to irradiation; 2) acute changes in these cells were associated with altered neurogenesis, i.e. the production of new neurons; 3) altered neurogenesis was strongly linked with hippocampal-dependent cognitive impairments. The quantification of cell fate after irradiation (neurogenesis) was accomplished using immunohistochemistry and confocal microscopy. In the original proposal we had not proposed to use this approach, but during the initial studies the technology became available to us and allowed us to do analyses far more sophisticated than those originally proposed. In the last year of funding we carried out more fractionated irradiations and followed those animals for 3 months, at which time we did a comprehensive battery of cognitive tests. We also collected tissues after paraformaldehyde perfusion for confocal analyses of neurogenesis as previously described by us (2, 3). While the cognitive testing is complete, the neurogenesis analyses are ongoing.

General Methods:

Young adult male C57BL mice were used in most studies. In some studies (see below) we also irradiated very young mice (21 day old). Anesthesia was required for irradiation and perfusion procedures; intraperitoneal (i.p.) injections of ketamine hydrochloride (65 mg/kg) and medetomidine (0.5 mg/kg) were used. Whole brain irradiation was done as previously described (2, 3) and dose rate was about 175 cGy/min: single and fractionated doses were used. At specified times after exposure, animals were anesthetized and perfused with 10 % buffered formalin using parameters previously described (2,3). After fixation, brains were processed for

immunohistochemistry using paraffin embedding; a standardized counting region and protocol were used when quantifying cells in paraffin embedded tissues (2, 3). Quantification was made of all positively-labeled cells within the dentate SGZ of the superior and inferior blades of the dentate gyrus; both hemispheres were counted for each animal. The total number of positively-labeled cells was determined by summing the values from all 3 tissue sections from a given brain. Proliferating cells were detected using an antibody against Ki-67, a nuclear antigen that is expressed during all proliferative stages of the cell cycle except G_0 (4). Immature neurons were detected using an antibody against Doublecortin (Dcx), a protein required for neuronal migration (5). Numbers of cells exhibiting cell-specific staining were scored blind. For studies of neurogenesis, one month prior to tissue collection, mice received a single injection of the thymidine analog BrdU for each of 7 consecutive days (2, 3, 6). Three weeks after the last injection mice were perfused with paraformaldehyde and tissues prepared for confocal microscopy. The fate of newly born (i.e. BrdU+ cells) was determined using cell-specific antibodies for neurons, astrocytes, oligodendrocytes and activated microglia (2, 3, 6).

Proliferation and oxidative stress in the hippocampus

To substantiate the relevance of our *in vitro* observations described above, studies were undertaken in mice to determine the relationship between redox state and number of neural precursor cells *in vivo*. To accomplish this, we reduced neural precursor cells in the mouse dentate SGZ using ionizing irradiation (5 Gy, single dose). Irradiation led to a significant drop in the number of proliferating (Ki67 positive) precursor cells by two days (Fig. 5a); this cell loss was followed by a subsequent increase in proliferation that lasted over a week (Fig. 5a). Over this same post-irradiation interval, measurements of lipid peroxidation showed an increase in the amount of MDA, as detected by bulk measurements of hippocampal tissues (Fig. 5b) or immunohistochemistry of tissue sections (Fig. 5 c, d). Thus, as observed in LD cultures, reducing the number of neural precursor cells *in vivo* was followed by an increased proliferation that was associated with an elevated oxidative stress in the dentate SGZ.

Elevated ROS persisting within the irradiated hippocampus may function as a neurotrophic signal to stimulate cell proliferation following the depletion of precursor cells within the SGZ. To analyze this possibility, mice were given ALA and analyzed for changes in proliferation and oxidative stress in the dentate SGZ. Administration of ALA *in vivo* was found to reduce cell proliferation; unirradiated mice given ALA exhibited reduced numbers of proliferating (Ki67 positive) cells (Fig. 5a), while the effect of ALA in irradiated animals was less pronounced due to the marked radiation-induced depletion of precursor cell numbers. Following irradiation, ALA also lowered MDA levels in hippocampal tissue (Fig. 5b), indicating that this antioxidant can ameliorate radiation-induced oxidative stress *in vivo*.

Long-term effects of fractionated irradiation

In previous years we carried out radiation studies using single doses in order to define dose response characteristics, establish reproducible endpoints, and correlate the histologic findings with cognitive changes; these data have been recently published (see reportable outcomes). Given that in an uncontrolled radiation exposure the dose received will likely be relatively low and protracted, we hypothesized that a fractionated paradigm would better simulate such an exposure. However, in our year 2 progress report we showed data relating to the response of the dentate SGZ after fractionated doses of x-rays and showed little difference between single and fractionated doses, at least in terms

of proliferating cells and immature neurons. These latter studies were relatively acute, i.e. 1-2 wks post-irradiation, and we wanted to determine more long-term effects of fractionation. We irradiated mice with 5 fractions of 2 Gy and followed them for 1-3 months. At 3 months we initiated a comprehensive battery of behavioral tests to assess hippocampal dependent and hippocampal independent functions. The details of how each test were run and analyzed have been recently published by us (7).

At the present time we have data regarding changes in SGZ cells 1 month after our proposed fractionation regimen (Fig. 6). At that time the number of proliferating cells and their progeny, immature neurons, were significantly reduce in irradiated animal. However, the magnitude of cell loss was less than that seen after a single 10 Gy dose suggesting that there is some sparing due to dose fractionation. Regardless, there still is a significant reduction in the neurogenic population after a relatively modest dose of fractionated irradiation. How these change relate to actual measures of neurogenesis will be determined in the analyses that are still underway.

Our studies of cognitive impairment after fractionated irradiation parallel our previous studies in very young (21 day old) and young adult (2 month old) mice after single dose irradiation. Results from those studies have been recently published (2, 3, 7). While we saw significant impairments in hippocampal dependent memory and spatial information processing after single dose irradiation, we did not see similar changes in mice that received fractionated treatment. However, in these latter mice we did see substantial deficits in the zero maze, a test associated with measures of anxiety. The elevated zero maze is a circular maze that consists of 2 enclosed areas and 2 open areas and has a diameter of 53.3 cm. Mice are place in the closed part of the maze and allowed free access for 10 minutes. A video tracking system is used to calculate the time spend in both areas; since the open area is anxiogenic for mice, less time in that area represents higher levels of anxiety. In this test non-irradiated mice spent an average of 54 ± 11 sec (n = 12), in the open area while irradiated mice spent an average of 95± 22 sec (n = 12). This suggests that irradiated mice are less anxious than controls. Whether this represents a specific lesion in or around the amygdala or hippocampus remains unclear. Because glucocorticoid receptors and/or GABA may also associated with anxiety, these factors may also be involved in some way. More work is required to determine the mechanisms behind our observation that fractionated irradiation resulted in reduced anxiety and those changes in some way are associated with altered neurogenesis.

In addition to the long-term studies described above we also collaborated with other investigators looking at split-dose irradiation of the brain of gerbils; this study has recently been published (8). In that study we showed that two 5 Gy doses separated by 7 days resulted in significantly reduced neurogenesis in the dentate SGZ but no changes in vascular or dendritic morphology. At the time of decreased neurogenesis there was impaired performance in the Morris water maze, suggesting a hippocampal-dependent cognitive impairment. This split dose study agrees with our single and multi-fraction studies in mice showing that low to modest doses of x-rays have significant effects on neurogenesis which are associated with altered cognitive performance.

While this proposal is primarily focused on neurogenesis and oxidative stress, preliminary findings also directed us toward other, related factors that might play a role in radiation-induced alterations in neurogenesis and cognitive function. In particular, work supported by this grant showed that altered neurogenesis was associated with changes in the microenvironment, particularly inflammatory changes (2, 3, 6). In this context we have been able to show, after single doses of x-rays in the SGZ of both very young and young adult mice that there is an upregulation of CCR2, a chemokine receptor associate with monocyte chemoattractant protein (9)

(Fig. 7). This receptor is up regulated shortly after irradiation (1-2 wks), reaches maximum expression 3-4 weeks after exposure and stays elevated for many months. Because the receptor is associated with the attraction and activation of monocytic cells, we have looked at endogenous (microglia) and circulating monocytes in the brain after irradiation and have been able to show a significant increase in these cells. While we still cannot prove cause and effect, this finding, along with our findings regarding oxidative stress in neural precursor cells in the SGZ, suggests that we may be able to modulate specific adverse effects of irradiation using relatively simple approaches such as anti-oxidants and/or anti-inflammatory agents. More work is necessary to understand how ROS and/or inflammatory factors may mediate alterations in neurogenesis and cognitive impairment, and to develop effective countermeasures.

KEY RESEARCH ACCOMPLISHMENTS:

- An in vitro neural precursor system facilitates the investigation of microenvironmental factors in hippocampal radiation response;
- Our results suggest that ROS are involved in the regulation of proliferation of neural precursor cells;
- Treatment with the antioxidant ALA inhibits growth of precursor cells in vitro;
- ROS effects on neural precursor cells appear to be mediated through altered mitochondrial function;
- Under conditions of cell loss stress, such as that seen after irradiation, neural precursor cells appear to upregulate MnSOD which reduces ROS and slows proliferation;
- Stresses associated with reduced cell density in vitro are reflected in vivo by radiation-induced changes in cellularity in the dentate SGZ;
- In vitro and in vivo, elevated ROS as a result of exposure to irradiation are reduced by treatment with ALA;
- Fractionated doses of irradiation result in significantly reduced cellularity in the SGZ but the extent of cell loss is less than the same dose delivered in a single fraction;
- Fractionated doses of irradiation result in specific cognitive impairments, particularly those associated with anxiety;
- The pathogenesis of the neurocognitive effects is not yet clear;
- In addition to increase oxidative stress after irradiation, there is a significant and persistent inflammatory response that is associated in time with reduced neurogenesis and impaired cognitive functions.

REPORTABLE OUTCOMES

Only published papers are submitted as appendices.

C. L. Limoli, E. Giedzinski, R. Rola, S. Otsuka, T. D. Palmer, and J. R. Fike, Radiation response of neural precursor cells: linking cellular sensitivity to cell cycle checkpoints, apoptosis and oxidative stress. *Radiation Research.* **161**, 17-27 (2004).

R. Rola, J. Raber, A. Rizk, S. Otsuka, S. R. VandenBerg, D. R. Morhardt, and J. R. Fike, Radiation-induced impariment of hippocampal neurogenesis is associated with cognitive deficits in young mice. *Exp. Neurol.* **188**, 316-330 (2004).

J. Raber, R. Rola, A. LeFevour, D. R. Morhardt, J. Curley, S. Mizumatsu, S. R. VandenBerg, and J. R. Fike, Radiation-Induced cognitive impairments are associated with changes in indicators of hippocampal neurogenesis. *Radiation Research.* **162**, 39-47 (2004).

J. Raber, Y. Fan, Y. Matsumori, Z. Liu, P.R. Weinstein, J.R.Fike, J. Liu, Irradiation attenuates neurogenesis and exacerbates cerebral ischemia-induced functional deficits. *Ann. Neurol.* **55**: 381-38. (2004).

C.L. Limoli, R. Rola, E. Giedzinski, S. Mantha, T-T. Huang, J.R. Fike, Cell density dependent regulation of neural precursor cell function. *PNAS*, Submitted.

CONCLUSIONS

The last 3 years of funding have provided considerable data regarding how neural precursor cells respond to low/moderate doses of ionizing irradiation. While it is difficult to simulate an uncontrolled exposure to irradiation, we used single and fractionated doses that did not induce any overt morphologic changes such as vascular injury, demyelination, etc. Therefore we feel that the changes we observed are compatible with what might happen after significant but non-lethal doses of irradiation. In 3 rodent models and 1 in vitro system we have consistently seen that neural stem cells are extremely sensitive to irradiation. That sensitivity is manifest as an acute apoptotic response after doses as low as 1 Gy. Both in vitro and in vivo, this acute cell death is associated with indications of oxidative stress. Precursor cells seem to be extremely sensitive to reactive oxygen species (ROS), which can act both as damaging agents and also as signaling molecules. By using our in vitro system we were able to address relationships between ROS, cell density and mitochondrial function and have made important inroads into understanding how neural precursor cells response to stress such as that imposed by ionizing irradiation. Based on our in vitro findings we identified potential antioxidant agents that could have an impact on the development of cell injury and/or death, and have shown that treatment with α-lipoic acid appears to reduce some effects of irradiation on neural precursor cells and their progeny. Our newest data show that in addition to increased oxidative stress, there is also a substantial inflammatory response that is persistent for months after irradiation.

While there still are many questions that remain to be answered, we have been able to clearly show that early cell losses in the dentate subgranular zone are associated with altered neurogenesis and also with impaired cognitive function. Given the observations of increased oxidative stress and inflammation after relatively low single or fractioned doses, it may be that relatively simple approaches could be implemented to reduce radiation-induced damage to the dentate SGZ. If and how prolonged treatment with anti-oxidant or anti-inflammatory agents will impact the adverse effects of low dose irradiation on neurogenesis and cognitive function should be addressed in future research endeavors. The ability to ameliorate non-lethal radiation effects would not only provide a

potential protective strategy for military personnel exposed to moderate doses of irradiation, but it would also have a clinical impact on patients undergoing therapeutic irradiation involving the brain.

FIGURES

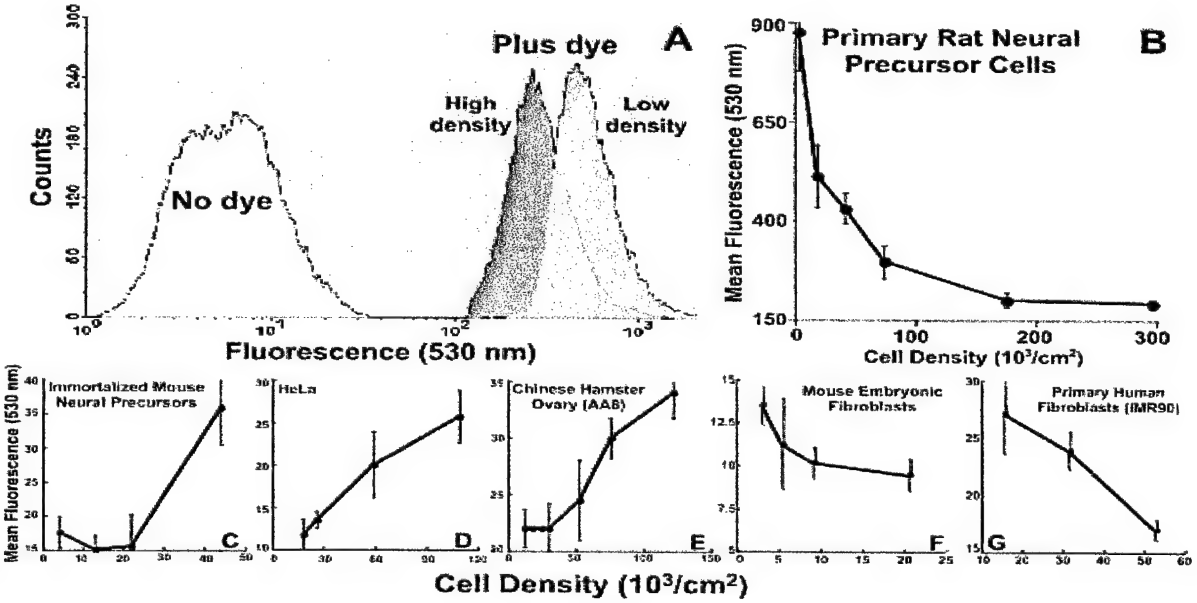

Figure. 1: Cell density dependent production of ROS. Cells grown at different densities were treated while anchored with the fluorogenic dye CM-H_2DCFDA (5 μM, 1h), and assessed for intracellular ROS by FACS analysis. FACS histograms (a) show that neural precursor cells are not autofluorescent and have elevated ROS at LD versus HD. ROS levels drop rapidly as neural precursors grow to HD (b), but are significantly higher at all densities when compared to other cells (c-g). The observation of elevated ROS at LD is atypical of other transformed or immortalized cells (c-e) that show the opposite trend, but is similar but much less pronounced in other primary cells (f, g). All data (b-g) averaged from ≥4 experiments (±SEM).

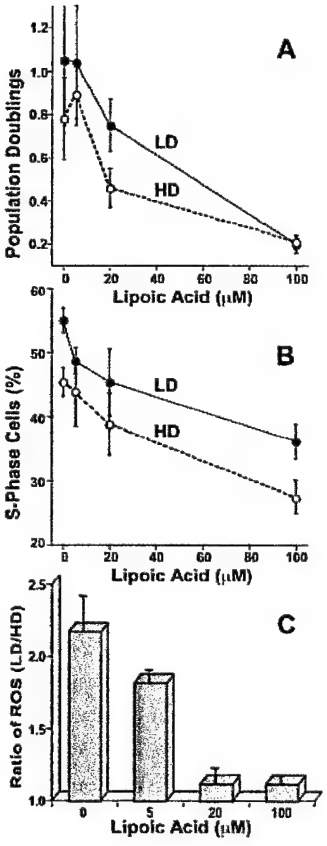

Figure 2: Cell growth depends on ROS levels. Cells grown at varying densities were assessed for population doubling, cell cycle distribution and ROS levels in the presence (5-100 μM) and absence of lipoic acid. In the presence of lipoic acid, LD and HD cultures showed concentration dependent decreases in population doubling (assessed over 48-72h, a) and S-phase fractions (measured by FACS analysis of BrdU-labeled cells, b), suggesting that ROS levels could exert some control over proliferation. Increasing concentrations of LA were found to progressively reduce the LD/HD ratio of ROS found at different densities (3c) suggesting that ROS at LD were more easily scavenged. All data averaged from ≥3 experiments (±SEM).

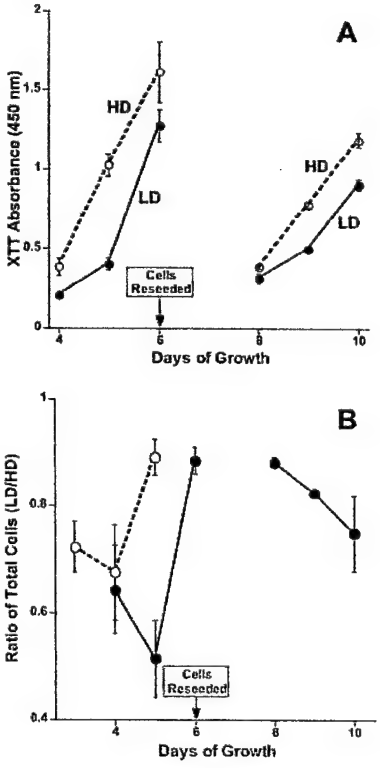

Figure 3: Cells cultured under LD conditions exhibit a persistent inhibition of growth. Cells were cultured at LD or HD for 2 days before reseeding at equal densities and subsequent analysis over the course of 10 days. Cultures derived from LD conditions (a, solid lines) exhibited reduced XTT absorbance compared to cultures derived from HD (a, dashed lines), even after cells were reseeded again at equal densities on day 6. Cell counts showed that cultures grown from LD conditions had significantly fewer cells than those grown from HD conditions, yielding a LD/HD ratio that was always less than unity (b). The slow growth of cells from LD conditions persisted over all times analyzed, and was observed at two different densities (*i.e.* $1.2x10^4/cm^2$ solid line, b; or $4.0x10^4/cm^2$ dashed line, b). Experiments were averaged from 3 experiments (±SEM).

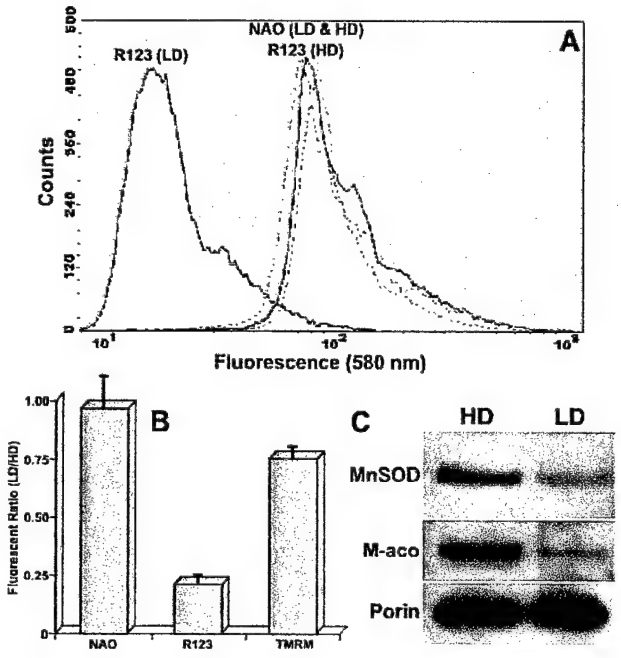

Figure 4: Mitochondrial (MT) alterations correspond to density dependent changes in oxidative stress. FACS analysis of anchored cells treated with the MT probe NAO (10 μM, 0.5h) indicated little density-dependent fluctuation in mitochondrial content (a, dashed lines), yielding a LD/HD ratio of NAO fluorescence near unity (b). This result was confirmed by western analysis of mitochondrial porin levels, (that also served as loading controls for these blots), and showed that mitochondrial content varied little with cell density (c). However, FACS analysis of LD anchored cells treated with the mt function probe R123 (10 μM, 0.5h) showed a dramatic drop in R123 fluorescence (a, solid lines) that resulted in a considerable decline in the LD/HD ratio of R123 fluorescence (b). Qualitatively similar results (Fig. b) obtained with the dye TMRM (10 μM, 0.5h) suggested further that reduced cell densities lead to physiologic changes in mitochondrial Ψ_m. Further analysis of MT proteins showed that aconitase was significantly lower (10-fold) in LD cultures (c), supporting the idea that LD conditions favored the generation of mt-derived ROS that contribute to the degradation of mt-aconitase. Western analysis of MnSOD levels (c) showed that HD cultures contained more (3-4 fold) of this mt-localized antioxidant, thereby providing one explanation for why ROS levels are lower at HD. All data (b) averaged from ≥4 experiments (±SEM).

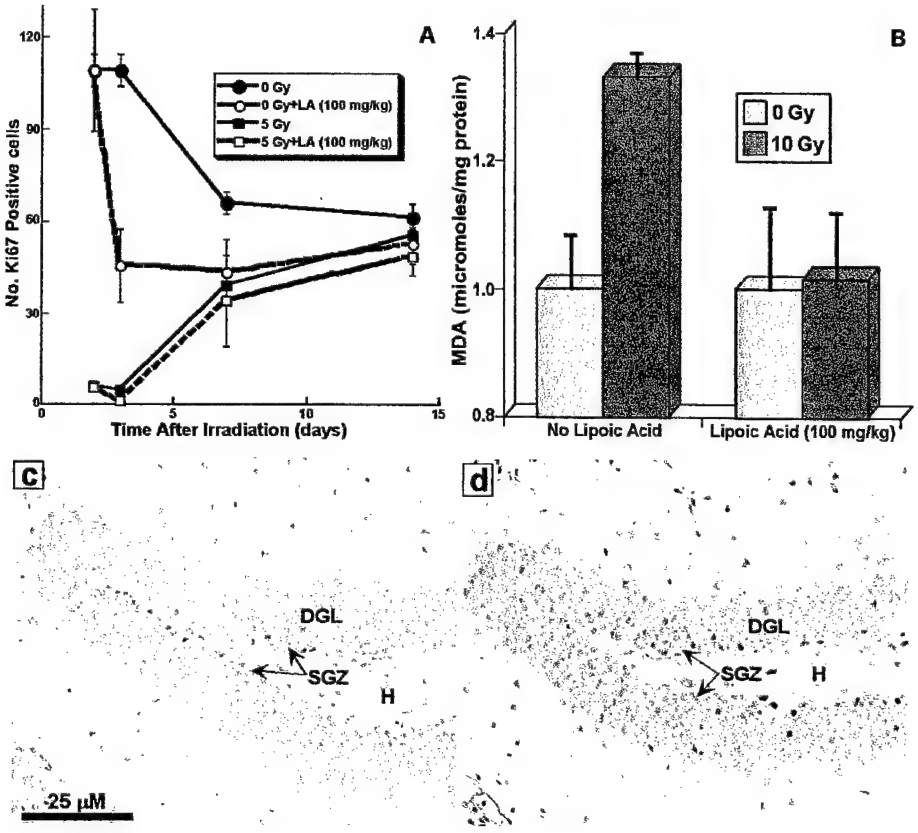

Figure 5: Proliferation and oxidative stress within the hippocampus. Brain tissues from irradiated (5 - 10 Gy) and non-irradiated mice with or without concomitant treatment with LA (100 mg/kg) were processed for immunohistochemical analysis or MDA levels as previously described. Numbers of proliferating cells within the SGZ of the dentate gyrus were quantified as described. Unirradiated controls showed a typical age-dependent decline in the number of proliferating precursors (a, closed circles) that was markedly enhanced by LA treatment (a, open circles). Analysis of tissues from irradiated mice demonstrated the effectiveness of X-irradiation to reduce the numbers of proliferating neural precursors in the SGZ (a, squares). Proliferating cells then recover over the next 2 weeks; this was not affected by the presence of LA (a, squares). During this increased proliferation, oxidative stress increased as measured by MDA levels of hippocampal tissue (10Gy, 2 weeks), an effect that could be reversed by LA (b). Compared to unirradiated controls (c), tissue sections from irradiated mice showed that MDA staining was concentrated in both blades of the dentate SGZ (d). All data (a) averaged from ≥5 experiments (±SEM).

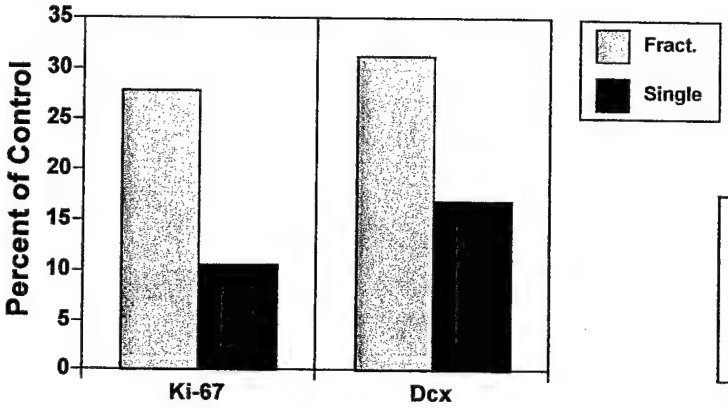

Figure 6: Changes in proliferating cells (Ki67) and immature neurons 1 month after either a single dose of 10 Gy (black bar) or 5 fractions of 2 Gy. Each bar represents the decrease in cell number as a percent of age match controls; mice/group = 4.

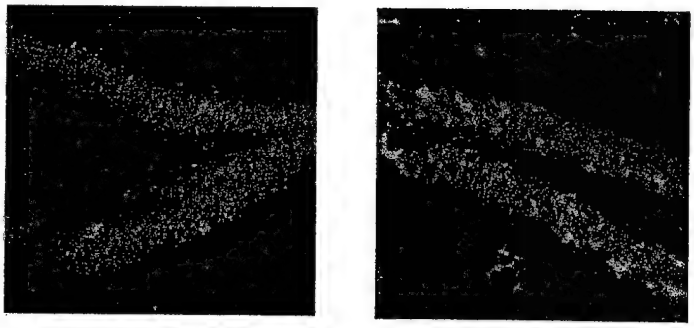

Figure 7: Immunohistochemical labeling of the CCR2 receptor (red) in the dentate gyrus of control (left) and irradiated (5 Gy) brain 3 months after treatment. The expression of the receptor in throughout the granule cell layer (blue).

REFERENCES

1. C. L. Limoli, E. Giedzinski, R. Rola, S. Otsuka, T. D. Palmer, and J. R. Fike, Radiation response of neural precursor cells: linking cellular sensitivity to cell cycle checkpoints, apoptosis and oxidative stress. *Radiation Research.* **161**, 17-27 (2004).

2. S. Mizumatsu, M. L. Monje, D. R. Morhardt, R. Rola, T. D. Palmer, and J. R. Fike, Extreme sensitivity of adult neurogenesis to low doses of x-irradiation. *Can Res.* **63**, 4021-4027 (2003).

3. R. Rola, J. Raber, A. Rizk, S. Otsuka, S. R. VandenBerg, D. R. Morhardt, and J. R. Fike, Radiation-induced impariment of hippocampal neurogenesis is associated with cognitive deficits in young mice. *Exp. Neurol.* **188**, 316-330 (2004).

4. K. Kee, S. Sivalingam, R. Boonstra, The utility of Ki-67 and BrdU as proliferative markers of adult neurogenesis. *J. Neurosci. Methods*. **115**, 97-105. (2002).

5. J. Nacher, C. Crespo, B.S. McEwen, Doublecortin expression in the adult rat telencephalon. *Eur. J. Neurosci*. **14**, 629-644. (2001).

6. M. L. Monje, S. Mizumatsu, J. R. Fike, and T. D. Palmer, Irradiation induces neural precursor-cell dysfunction. *Nat Med*. **8**, 955-962. (2002).

7. J. Raber, R. Rola, A. LeFevour, D. R. Morhardt, J. Curley, S. Mizumatsu, S. R. VandenBerg, and J. R. Fike, Radiation-Induced cognitive impairments are associated with changes in indicators of hippocampal neurogenesis. *Radiation Research*. **162**, 39-47 (2004).

8. J. Raber, Y. Fan, Y. Matsumori, Z. Liu, P.R. Weinstein, J.R.Fike, J. Liu . Irradiation attenuates neurogenesis and exacerbates cerebral ischemia-induced functional deficits. *Ann. Neurol*. **55**: 381-38. (2004).

9. M. Mack, J. Cihak, C. Simonis, B. Luckow, A.E.I. Proudfoot, J. Poachy, H. Bruhl, M. Frink, H-J. Anders, V. Vielhauer, J. Pfirstinger, M. Stangassinger, D. Schlondorff, Expression and characterization of the chemokine receptors CCR2 and CCR5 in mice. *J. Immunology*. **166**, 4697-4704. (2001).

RADIATION RESEARCH 161, 17–27 (2004)
0033-7587/04 $15.00

Radiation Response of Neural Precursor Cells: Linking Cellular Sensitivity to Cell Cycle Checkpoints, Apoptosis and Oxidative Stress

Charles L. Limoli,[a,1] Erich Giedzinski,[a] Radoslaw Rola,[c] Shinji Otsuka,[c] Theo D. Palmer[b] and John R. Fike[a,c]

[a] *Departments of Radiation Oncology and Neurological Surgery, University of California, San Francisco, California 94103-0806;* [b] *Department of Neurosurgery, Stanford University, California 94305-5487; and* [c] *Department of Neurological Surgery, University of California, San Francisco, California 94143-0520*

Limoli, C. L., Giedzinski, E., Rola, R., Otsuka, S., Palmer, T. D. and Fike, J. R. Radiation Response of Neural Precursor Cells: Linking Cellular Sensitivity to Cell Cycle Checkpoints, Apoptosis and Oxidative Stress. *Radiat. Res.* 161, 17–27 (2004).

Therapeutic irradiation of the brain can cause a progressive cognitive dysfunction that may involve defects in neurogenesis. In an effort to understand the mechanisms underlying radiation-induced stem cell dysfunction, neural precursor cells isolated from the adult rat hippocampus were analyzed for acute (0–24 h) and chronic (3–33 days) changes in apoptosis and reactive oxygen species (ROS) after exposure to X rays. Irradiated neural precursor cells exhibited an acute dose-dependent apoptosis accompanied by an increase in ROS that persisted over a 3–4-week period. The radiation effects included the activation of cell cycle checkpoints that were associated with increased Trp53 phosphorylation and Trp53 and p21 (Cdkn1a) protein levels. *In vivo,* neural precursor cells within the hippocampal dentate subgranular zone exhibited significant sensitivity to radiation. Proliferating precursor cells and their progeny (i.e. immature neurons) exhibited dose-dependent reductions in cell number. These reductions were less severe in Trp53-null mice, possibly due to the disruption of apoptosis. These data suggest that the apoptotic and ROS responses may be tied to Trp53-dependent regulation of cell cycle control and stress-activated pathways. The temporal coincidence between *in vitro* and *in vivo* measurements of apoptosis suggests that oxidative stress may provide a mechanistic explanation for radiation-induced inhibition of neurogenesis in the development of cognitive impairment.

INTRODUCTION

Therapeutic irradiation of the brain can result in significant injury to normal brain structures. Severe morphological and functional damage generally occurs after relatively high radiation doses (*1–3*), while lower doses can induce changes that can lead to cognitive dysfunction (*4–7*). Such cognitive changes occur in both pediatric and adult patients, and they often appear as deficits in hippocampal-dependent functions of learning, memory and spatial information processing (*4, 5, 7, 8*). The hippocampus is one of two sites in the mammalian forebrain that are characterized by active neurogenesis throughout life (*9–13*), and recently it has been proposed that loss of hippocampal neural precursors and changes in the microenvironment may play a contributory if not causal role in radiation-induced cognitive impairment (*14–17*). Understanding the factors involved in the radiation sensitivity of neural precursor cells and the overall process of neurogenesis may provide keys to developing approaches to ameliorate cognitive impairments after radiation exposure.

Irradiation produces a variety of DNA and other cellular lesions that collectively elicit a global stress response in mammalian cells (*18*). This stress response is characterized by the activation of damage-inducible signaling pathways, DNA repair, cell cycle checkpoints, apoptosis and altered gene expression profiles (*18–20*). These end points are certain to be critical to the overall radiation response of the central nervous system (CNS), and they may be influenced in part by the presence of reactive oxygen species (ROS). ROS and reactive nitrogen species are also common intermediates implicated in other types of CNS pathology, including traumatic and ischemic brain injury (*21–25*). Multiple cellular pathways associated with CNS injury such as excitotoxicity, calcium release, mitochondrial dysfunction, and apoptosis can lead to a predominance of short-lived ROS and a generalized state of oxidative stress (*26–28*). ROS have a profound effect on the basal redox state of cells (*29, 30*), and there is evidence that oxidative stress may constitute a biochemical mechanism regulating the fate of neural precursors (*31*). In fact, data exist showing that ROS levels influence the balance between proliferation and differentiation in glial precursors (*31*). Given that information and our own data regarding radiation and neurogenesis (*14–16*), we hypothesize that ROS play a critical role in the radiation response of neural precursor cells.

While considerable data are available regarding the biology of neural precursor cells *in vivo,* addressing regula-

[1] Address for correspondence: Department of Radiation Oncology, Radiation Oncology Research Laboratory, University of California San Francisco, 1855 Folsom Street, MCB-200, CA 94103-0806; e-mail: Limoli@itsa.ucsf.edu.

tory mechanisms in animal systems is quite complicated. Therefore, to facilitate a mechanistic approach for the investigation of precursor cell biology, *in vitro* models have been developed (*32–35*). These models provide an effective means by which we can address the radiation response of neural precursor cells. In the present study, we used a precursor cell line derived from the rat hippocampus in conjunction with our existing animal models to provide *in vitro* and *in vivo* evidence implicating oxidative stress and Trp53 in the acute and chronic radiation response of neural precursor cells exposed to X rays.

MATERIALS AND METHODS

Neural Precursor Cells

Neural precursor cells were derived from the rat hippocampus, as described previously (*33*). These cells, which exhibited doubling times of 20–28 h, were maintained in exponential growth and passaged twice weekly. Cells were grown in the presence of serum-free DMEM/F12 medium (1:1, Gibco) containing N2 supplement (Gibco) and 20 ng/ml of fibroblast growth factor 2 (FGF2, Peprotec). All cultures were grown on polyornithine/laminin (Sigma/Gibco) coated plasticware (*33*) and were refed every other day using a ratio of 3:1 new:conditioned medium.

To demonstrate that the cells were indeed multipotential precursors, they were plated onto laminin-coated chambered slides and maintained in differentiation medium for 5 days. The differentiation medium was prepared in the absence of FGF2 and was supplemented with 1% fetal bovine serum and 0.5 μM all-trans retinoic acid (Sigma). After 5 days, adherent cells were fixed and immunohistochemistry was used to determine their phenotypic characteristics. The cell-specific antibodies used included nestin (an intermediate filament protein expressed in neural precursors; 1:1000, Chemicon International, Temecula, CA), NeuN (a nuclear antigen in mature neurons; 1:500, Chemicon International), type III β-tubulin (Tuj-1, a microtubule-associated protein specifically expressed by immature neurons; 1:5000, Chemicon International), doublecortin (Dcx, another marker expressed by immature neurons; 1:250, Santa Cruz Biotechnology, Santa Cruz, CA), glial fibrillary acidic protein (GFAP, an intermediate filament protein expressed by astrocytes; 1:1000, Chemicon International), and O4 (a ganglioside marker expressed by immature oligodendrocytes; 1:1000, Chemicon International). All fluorophore-conjugated secondary antibodies were diluted 1:500, and cells were counterstained with 4′,6-diamidino-2-phenylindole (DAPI, 0.3 μg/ml) in Vectashield (Vector Laboratories, Burlingame, CA).

X Irradiation

One day prior to irradiation, neural precursor cells were split 1:3 and seeded into 25-cm² flasks. Exponentially growing cultures were either sham-irradiated or exposed to X rays (Westinghouse Quadronex X-ray machine; 250 kVp, 15 mA) at a dose rate of 4.5 Gy/min. Immediately after irradiation, cells were placed back in incubators until the time of assay. Further cell passage was not required.

Cell Cycle Analysis

Exponentially growing cultures of neural precursor cells were either sham-irradiated or exposed to 5 Gy and at various times after irradiation (6, 12, 18, 24 and 48 h), fixed in 70% ethanol, and stored at −20°C. On the day of assay, samples were resuspended for 1 h at ambient temperature in isotonic phosphate-buffered saline (PBS) supplemented with RNase (50 U/ml) and propidium iodide (PI, 10 μg/ml). Subsequently, cells were assayed for DNA content by FACS analysis of PI fluorescence. Raw data were gated to eliminate debris and doublets and to calculate the distribution of cells throughout the cell cycle. A minimum of 30,000 cells were analyzed at each time using the ModFit LT™ analysis software (Verity Software House). Reverse χ^2 values were routinely under 5, indicating that the cell cycle data were within the parameters of the ModFit algorithm.

Measurement of Reactive Oxygen Species (ROS)

The detection of intracellular ROS was based on the ability of cells to oxidize a fluorogenic dye to its corresponding fluorescent analog. Exponentially growing cultures were treated for 1 h at 37°C with 5 μM of the ROS-sensitive dye 5-(and-6)-chloromethyl-2′,7′-dichlorodihydrofluorescein diacetate (CM-H_2DCFDA, Molecular Probes, Eugene OR). Immediately after dye incubation, cells were harvested and subjected to fluorescence-activated cell sorting (FACS). For each postirradiation time, measurements of ROS in irradiated and sham-irradiated control cultures were performed in parallel. All measurements were performed in duplicate or triplicate (12 h time) and were derived from independently irradiated cell cultures.

Measurement of Apoptosis

Apoptosis assays were performed using FACS analysis and were done in parallel with measurements of ROS. To normalize the experimental conditions for each of the end points assayed, cells to be assayed for apoptosis were passaged and refed at the same time as those in the flasks used for the ROS measurements. At each postirradiation time, cells were harvested, rinsed in PBS, and incubated for 20 min at ambient temperature in limiting volumes (~0.2–0.5 ml) of binding buffer (Clontech) containing FITC-conjugated annexin V. Cells suspensions were brought to 0.5–1.0 × 10^6 cells/ml in PBS and were immediately subjected to FACS analysis. As with ROS measurements, apoptosis assays were performed in duplicate or triplicate and derived from independently irradiated cultures of cells. FACS data were also analyzed using the ModFit LT™ program to estimate the percentage of apoptotic cells from cell cycle histograms.

Western Blot Analysis of Trp53 and Ckdn1a (p21) Protein Levels

Nuclear lysates were prepared from exponentially growing precursor cell cultures at 2, 6 or 12 h after a single dose of 5 Gy using standard procedures (*36*). Samples were quantified for protein levels using a detergent-compatible Lowry assay (Bio-RadDc assay) and frozen at −70°C until electrophoresis and blotting. Sample volumes were adjusted for protein content, denatured, loaded onto 10% precast polyacrylamide gels (Bio-Rad), electrophoresed (125 V), and transferred (100 V, 1 h) to nylon membranes. Membranes were probed with a mouse monoclonal anti-Trp53 antibody (D0-1, Santa Cruz Biotechnology), a rabbit polyclonal serine 15 phospho-specific anti-Trp53 antibody (Santa Cruz Biotechnology), and a mouse monoclonal anti-p21 (Cdkn1a) antibody (Santa Cruz Biotechnology). Primary antibodies were diluted 1:500 and were detected by alkaline phosphatase or horseradish peroxidase-conjugated anti-mouse/rabbit secondary antibodies (Santa Cruz Biotechnology) used in conjunction with the WesternBreeze Immunodetection Kit (Invitrogen, Carlsbad, CA).

Data Analysis and Statistics

Significance between data sets obtained by FACS analysis was determined by the Kolmogorov-Smirnov test (K-S test) provided with the Cell Quest™ software. This two-sample test returns a P value based upon the differences between data sets. Fluorescence values derived from FACS data are presented as relative fluorescence units (RFU). For all other data sets, means were calculated and assessed for significance (assigned at the $P = 0.05$ level) by analysis of variance (ANOVA).

In Vivo Studies

Two-month-old male wild-type C57BL/J6 mice and homozygous Trp53 knockout mice (B6.129S2-Trp53^{tm1Tyj}) mice (weight ~20 g) were

purchased from a commercial vendor (The Jackson Laboratory, Bar Harbor, ME). The Trp53 knockout mice were from a C57BL/J6 background. Mice were housed and cared for in accordance with the U.S. Department of Health and Human Services Guide for the Care and Use of Laboratory Animals; all protocols were approved by the institutional Committee for Animal Research. All mice were anesthetized for the irradiation and perfusion procedures; anesthesia consisted of an i.p. injection of ketamine (60 mg/kg) and medetomidine (0.25 mg/kg). Sham-irradiated mice were anesthetized as described.

Irradiation was done using a Philips orthovoltage X-ray system as described previously (*16*). Mice received head-only irradiation and the body was shielded with lead; the dose rate was ~1.75 Gy/min at a source-to-skin distance of 21 cm. Single doses of 0, 1, 2, 5 and 10 Gy were used.

Forty-eight hours after irradiation, mice were anesthetized and infused with 10% buffered formalin (*16*). After 5 min, brains were removed and immersed in a 10% buffered formalin solution for 3 days; tissue was stored in 70% ethanol until gross sectioning and paraffin embedding as described (*16*).

To determine radiation-induced changes in the cellular composition of the dentate subgranular zone (SGZ), proliferating cells were labeled with an antibody against Ki-67, a nuclear antigen that is expressed during all stages of the cell cycle except G_0 (*37, 38*). Immature neurons were detected using an antibody against Doublecortin (Dcx), a protein required for neuronal migration (*39*). For all immunostaining, binding of biotinylated secondary antibodies was detected using an avidin-biotinylated peroxidase complex system (ABC; Vector, Burlingame, CA). To quench endogenous peroxidase activity, deparaffinized specimens were soaked for 30 min in 0.3% H_2O_2 (Sigma) in 70% ethanol. After the primary and secondary antibodies were applied, the specimens were incubated with the ABC reagent for 30 min and developed with 0.025% 3,3′-diaminobenzidine (DAB, Sigma) dissolved in double-distilled water containing 0.005% H_2O_2. Sections were then counterstained with Gill's hematoxylin, dehydrated and mounted.

Ki-67

After deparaffinization and quenching of endogenous peroxidase, tissue sections were soaked in 10 m*M* sodium citrate buffer (pH 6.0) and boiled for 10 min using a microwave oven. Sections were left in the citrate buffer for another 20 min, washed in PBS, and incubated with 2% normal rabbit serum for 30 min. Sections were incubated overnight at 4°C with primary antibody (DakoCytomation, Carpinteria, CA) diluted 1:100 with PBS with 2% normal rabbit serum. After washing, sections were incubated for 30 min at room temperature with biotin-conjugated rabbit anti-rat IgG (Vector Laboratories) diluted 1:200 in PBS with 2% normal rabbit serum. Finally, the specimens were incubated with ABC reagent, developed with DAB, and counterstained.

Doublecortin

After deparaffinization and quenching, sections were treated in citrate buffer in a microwave oven as described above. After they were washed with PBS, and blocked for 30 min using 5% normal horse serum, sections were incubated overnight at 4°C with primary antibody (Santa Cruz Biotechnology) diluted 1:500 in PBS with 5% normal horse serum. Sections were washed and incubated for 60 min at room temperature in biotinylated anti-goat IgG (Vector Laboratories) diluted 1:500 in 5% normal horse serum. Sections were finally incubated with ABC reagent, developed with DAB, and counterstained.

The numbers of proliferating cells and immature neurons were scored blind using a histomorphometric approach (*14, 40*). A standardized counting area was used as described previously (*14*). Briefly, 6-μm-thick coronal sections were mounted from three different brain levels representing the rostral/mid hippocampus. The brain levels were approximately 50 μm apart; the most rostral brain level corresponded to a point approximately 2.5 mm behind the bregma. For each mouse, three non-overlapping sections were analyzed, one each from the three regions of the hippocampus. Quantification was made of all positively labeled cells within the SGZ of the suprapyrimidal and infrapyrimidal blades of the dentate gyrus. The total number of positively labeled cells was determined by summing the values from both hemispheres in all three tissue sections.

Assay of Malonaldehyde (MDA)

To quantify oxidative stress *in vivo*, a commercial kit was used (Lipid Peroxidation Kit, Calbiochem) that measures malonaldehyde (MDA) in cells, tissue sections and tissue homogenates by colorimetric assay. Tissue sections and homogenates were derived from hippocampi dissected from mice 24 h and 1 week after a 10-Gy dose of X rays. MDA levels in irradiated and unirradiated brains were determined in triplicate and calibrated against a standard curve generated the day of the assay.

Data Analysis and Statistics

For immunohistochemical end points, values for all animals in a given treatment group were averaged, and standard errors (SE) were calculated. A Wilcoxon-Mann-Whitney test for two independent samples stratified by dose was used to determine whether cellular changes in radiation response were statistically significant. For MDA data, means were calculated and assessed for significance by Student's *t* test. The *P* level for statistical significance was assigned at 0.05.

RESULTS

Differentiation of Rat Neural Precursor Cells

Primary cultures of neural precursor cells were differentiated using retinoic acid to verify their multipotentiality. This treatment induced significant morphological changes and resulted in cells expressing lineage-specific markers. The distributions of cell types were approximately 1% mature neurons, 5–10% immature neurons, 5–10% astrocytes, and 1% oligodendrocytes; the rest of the cells remained relatively undifferentiated. Differentiated cells showed the typical development of numerous processes that stain positive for GFAP, a marker for astrocytes (green), and β-III-tubulin, a neuronal marker (red) (Fig. 1). As found previously (*15, 33*), astrocytes and mature neurons were not found at significant levels (<0.1%) in undifferentiated cultures (data not shown).

X Irradiation Leads to Increased Apoptosis in Primary Rat Neural Precursor Cells

To determine whether cultured precursor cells exhibited a similar sensitivity to radiation as that observed *in vivo* (*14*), cells were irradiated and assayed for apoptosis by annexin V binding. Analysis of cells by FACS showed significant increases in the number of apoptotic cells after irradiation, particularly at 12 and 24 h (Fig. 2). At those times the number of apoptotic cells exhibited a dose-dependent increase relative to controls. At 12 and 24 h after 1 Gy, apoptosis was elevated relative to control levels by an average of 8.2%, while after 5 Gy, the levels increased to 37 and 21% at 12 and 24 h, respectively. Annexin V staining of adherent cells showed very little background apoptosis (<1%). Additional measurements were undertaken to substantiate that increases in relative fluorescence

FIG. 1. Differentiation of multipotential neural precursor cells. Neural precursor cells were subjected to differentiation in the presence of retinoic acid for 5 days. Lineage-specific markers found after differentiation include GFAP-positive astrocytes (green) and β-III-tubulin-positive neurons (red).

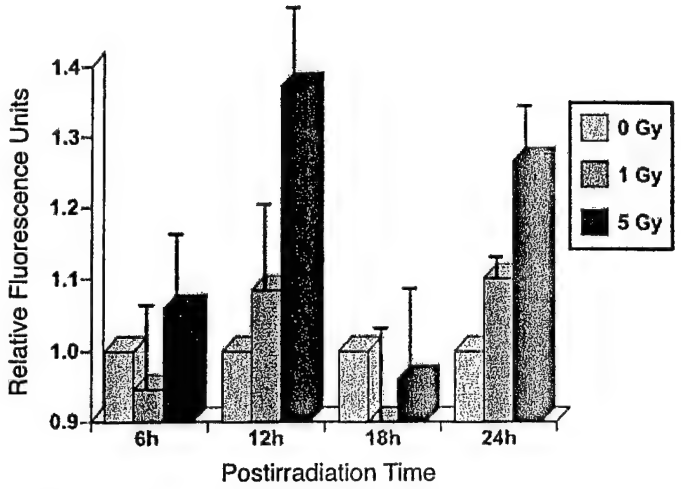

FIG. 2. Induction of apoptosis after X irradiation in primary rat neural precursor cells. Exponentially growing cultures of rat neural precursor cells were X-irradiated and harvested for the assessment of apoptosis by annexin V binding at the indicated times. The data obtained by FACS analysis show that relative to sham-irradiated cultures, precursor cells given 1 or 5 Gy of X rays exhibit a dose-dependent rise in apoptosis over a 24-h period, with a relative maximum occurring 12 h after irradiation. Bars represent the average of three to six independent measurements ± SD, and all values were normalized to controls (set to unity) run the same day.

from annexin V occurred in a significant fraction of the total cell population. Analysis of FACS data using the ModFit LT™ program provided an estimate of the percentage of apoptotic cells in the irradiated population. The percentages of apoptotic cells found over background levels (0.52%) at 6, 12, 18, 24 and 48 h after exposure to 5 Gy were 4.2, 28, 0.6, 12 and 4.0%, respectively. These values were in good agreement with annexin V data, which also showed peak apoptosis occurring 12 and 24 h after X irradiation.

X Irradiation Activates Functional Cell Cycle Checkpoints in Primary Rat Neural Precursor Cells

In further experiments, we examined the relationship between the induction of apoptosis and the inhibition of cell cycle progression. Compared to unirradiated controls, the number of cells containing a 2n complement of DNA at 6 and 12 h after irradiation increased by three- and sixfold, respectively (Fig. 3). By 18 h, the accumulation of cells G_2/M phase was reversed, leaving a population enriched for cells in G_0/G_1. This suggested either the death of cells arrested within the G_2/M-phase compartment, or the successful completion of mitosis and re-entry into the G_0/G_1 compartment resulting in a 20% increase in G_0/G_1 relative to control cultures at 18 h. Cells that were in G_0/G_1 subsequently entered a second wave of $S/G_2/M$ phase with an accompanying second peak of apoptosis, again leaving a G_0/G_1-phase-rich population at 48 h. While the apoptosis of G_2/M-phase cells at 12 and 24 h may underlie the increased fraction of G_0/G_1 cells, we cannot formally rule out the existence of a G_1/S-phase checkpoint. Cells irradiated in late S, G_2 or M or those escaping the initial G_2/M block may arrest at the G_1/S checkpoint at 18 h. Similarly, it is unlikely that the death of cells at 24 h can entirely account for the increased fraction of G_0/G_1 cells at 48 h. This suggests that neural precursor cell cycle progression is controlled in part by a G_1/S-phase checkpoint, and data shown in Fig. 3 reveal a persistent activation of radiation-responsive cell cycle checkpoints.

X Irradiation Leads to an Increase in Trp53 Levels

The presence of radiation-responsive cell cycle checkpoints suggested that hippocampal precursor cells contained a functional Trp53 protein. To substantiate this, cells were exposed to 5 Gy of X rays and analyzed by Western blotting. Compared to unirradiated controls, Trp53 protein levels were found to increase at 2 h (~twofold) and 6 h (~fourfold) after irradiation (Fig. 4). Elevations in Trp53 levels were accompanied by an increase in the phosphorylation of Trp53 at ser15 and by an increase in Cdkn1a (p21) levels (Fig. 4). Taken collectively, the increase in Trp53 and Cdkn1a protein levels and Trp53 phosphorylation provides evidence in support of a functional Trp53 response in neural precursor cells subjected to radiation-induced DNA damage.

Trp53 Regulates the Number of Proliferating Cells and Immature Neurons after Irradiation in the Dentate Subgranular Zone (SGZ)

Our *in vitro* data showed that the radiation response of precursor cells derived from the hippocampus was dependent in part upon Trp53. Based on considerable data for rats (*14*) and mice (*16*), we know that neural precursor cells *in vivo* undergo significant apoptosis after low to modest radiation doses. To determine whether Trp53 plays a role in the radiation response of SGZ precursor cells *in vivo*, we irradiated wild-type and Trp53 knockout mice and quantitatively assessed the numbers of proliferating SGZ cells and their progeny (immature neurons) 48 h after irradiation, when apoptosis is complete (*16*). Before irradiation, the numbers of proliferating cells and immature neurons in Trp53 knockout mice were ~20 and 13% higher, respectively, than those seen in wild-type controls. In addition, while relatively few, the number of apoptotic cells in our standardized region of interest (14) was 12 ± 1 (mean ± SEM) in cells from wild-type mice and 8 ± 2 in those from knockout mice. After irradiation, the numbers of proliferating cells and immature neurons decreased in a dose-dependent manner in both types of mice. Compared to wild-type mice, Trp53 knockout mice showed higher numbers of proliferating cells; while this trend was consistent, it was not significantly different at all doses (data not shown). Trp53-deficient mice did, however, exhibit statistically significant ($P < 0.05$) elevations in the numbers of immature neurons after low doses; there was no difference after the

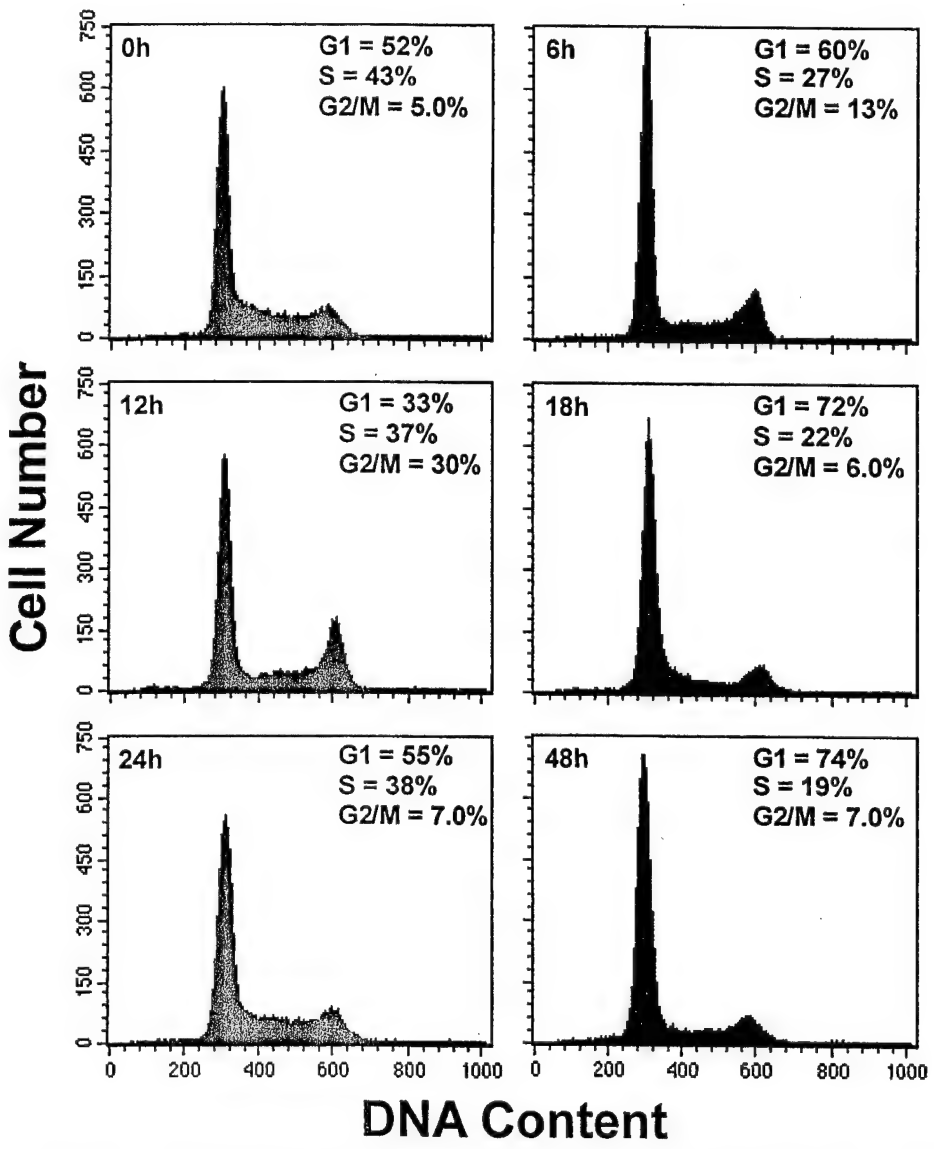

FIG. 3. Activation of cell cycle checkpoints in primary rat neural precursor cells after X irradiation. Primary rat neural precursor cells derived from hippocampal dissection were irradiated in exponential growth and fixed at the indicated times after irradiation with 5 Gy X rays. Fixed cells were treated with RNase incubated with propidium iodide and analyzed by FACS for DNA content. Histograms from a single experiment illustrate functional G_2/M and G_1/S checkpoints as seen in the pronounced buildup of cells in the G_2/M- (12 h) and G_1- (18 h) phase cell cycle compartments, respectively. Values shown are averaged from two independent measurements.

highest dose of 10 Gy (Fig. 5). These data support a role for Trp53 in regulating the radiation response of neural precursor cells *in vivo*.

X Irradiation Leads to Increased ROS in Primary Rat Neural Precursor Cells

Neural precursor cells *in vitro* showed a significant increase in ROS after exposure to X rays, and compared to controls, the levels of ROS were elevated at each dose and postirradiation time (Fig. 6). ROS levels exhibited statistically significant ($P < 0.05$) fluctuations, increasing in a dose-dependent manner over the first 12 h before dropping at 18 h and rising again at 24 h. Mean fluorescence values obtained by integration of FACS histograms indicated that ROS levels reached relative maximums at 12 h after 5 Gy (35% over controls) and 24 h after 1 Gy (31% over controls). The ROS data also showed an important correlation between apoptosis and ROS, where peak levels of each end point were found to coincide temporally (i.e. at 12 and 24 h after irradiation).

Radiation Exposure Leads to Persistent Increases in ROS and Apoptosis

Having demonstrated that apoptosis and ROS increased in a temporally consistent manner after irradiation, we wanted to determine whether those changes were transient

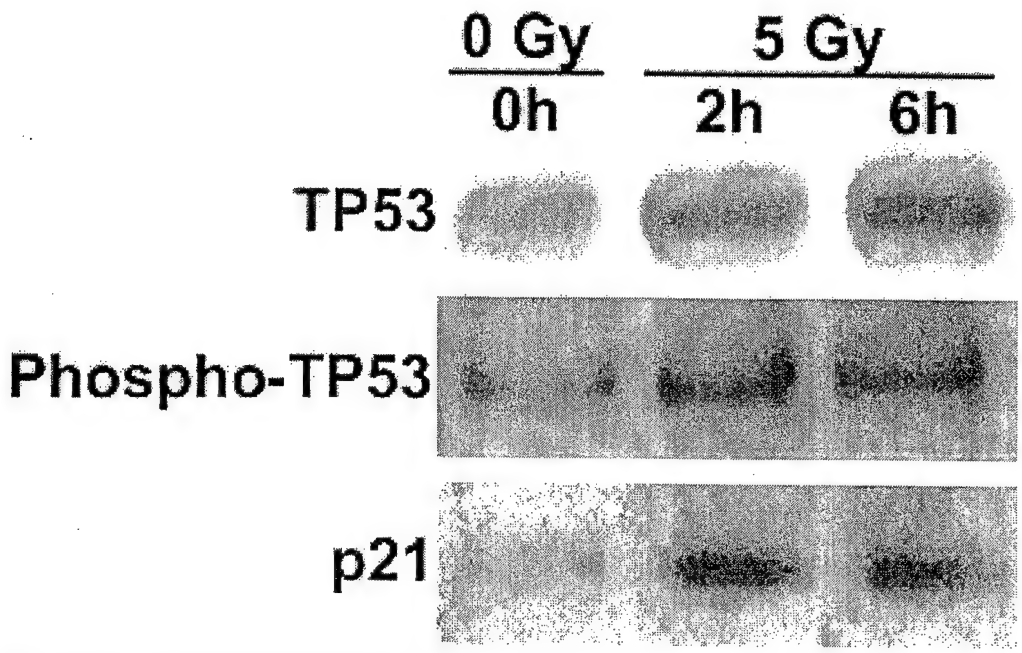

FIG. 4. X irradiation activates the Trp53 (TP53) pathway. Nuclear lysates were prepared from neural precursor cells 2 and 6 h after receiving 5 Gy of X rays. Compared to unirradiated controls, Trp53 protein levels are observed to increase ~two- and fourfold at 2 and 6 h after irradiation. Increases in Trp53 were also associated with an increase in ser15 phospho-Trp53 and Cdkn1a (p21) protein levels. All sample loading was normalized to protein content.

or permanent. Persistent and dose-dependent changes in apoptosis (Fig. 7) and ROS (Fig. 8) were observed 1 week after irradiation, especially after 5 Gy. Apoptosis and ROS levels measured 1 week after 5 Gy were increased by 45 and 180%, respectively, relative to unirradiated controls. Postirradiation levels of ROS were persistently elevated over a 3–4-week interval, reaching another relative peak (130% over controls) at day 25 before approaching background levels 8 days later. Apoptosis did not persist to the same extent, and after the 7-day maximum, it progressively declined to control levels by week 3.

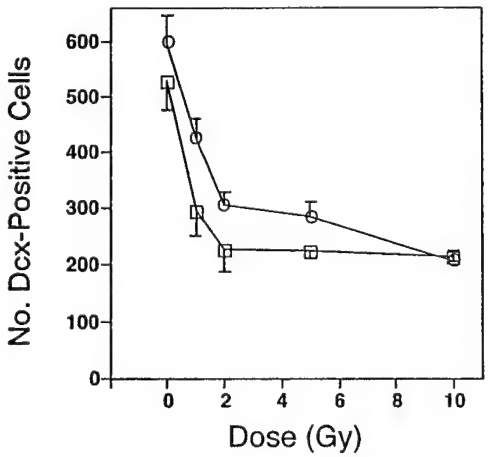

FIG. 5. Trp53 deficiency spares radiation-induced depletion of immature neurons in the dentate gyrus. Wild-type and Trp53 knockout mice were assessed quantitatively for numbers of Dcx-positive cells (immature neurons) 48 h after irradiation. Dose-dependent reductions in the numbers of immature neurons were observed in both types of mice. Compared to wild-type (squares) mice, Trp53 knockout (circles) mice showed a statistically significant ($P < 0.01$) elevation in the number of immature neurons after low doses. No difference was observed at the highest dose of 10 Gy.

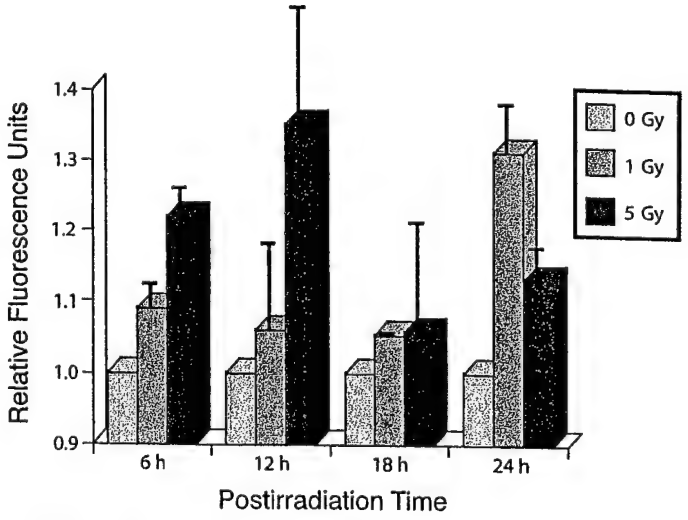

FIG. 6. Generation of reactive oxygen species in primary rat neural precursor cells after X irradiation. Exponentially growing cultures of rat neural precursor cells were X-irradiated and assayed for ROS at the indicated times by incubation (1 h) with the fluorogenic dye CM-H_2DCFDA (5 μM). FACS analysis of dye-loaded cells showed that relative to sham-irradiated cultures, precursor cells exposed to 1 or 5 Gy of X rays exhibit increased levels of ROS over 24 h that peak 12 h after irradiation. Bars represent the average of three to six independent measurements ± SD, and all values were normalized to controls (set to unity) run the same day.

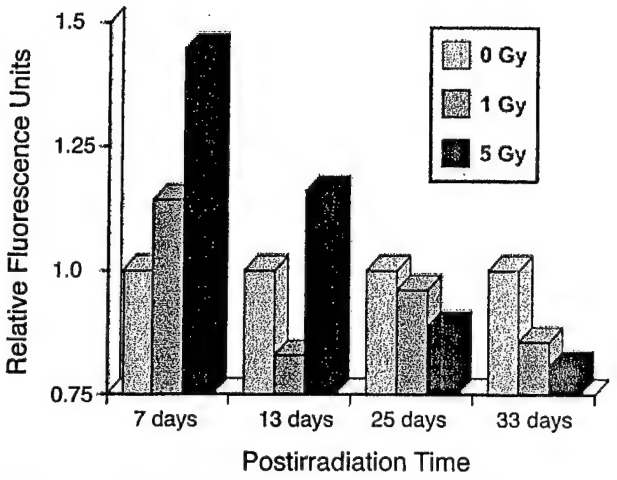

FIG. 7. Long-term induction of apoptosis after X irradiation of primary rat neural precursor cells. Exponentially growing cultures of rat neural precursor cells were X-irradiated and maintained over the course of 1 month. At the indicated times, cells were harvested for the assessment of apoptosis by annexin V binding. FACS analysis of cells showed that relative to sham-irradiated cultures, precursor cells exhibit a persistent increase in apoptosis, particularly 1 week after irradiation, before falling to background levels thereafter. Bars represent the average of two independent measurements ± SD, and all values were normalized to controls (set to unity) run the same day.

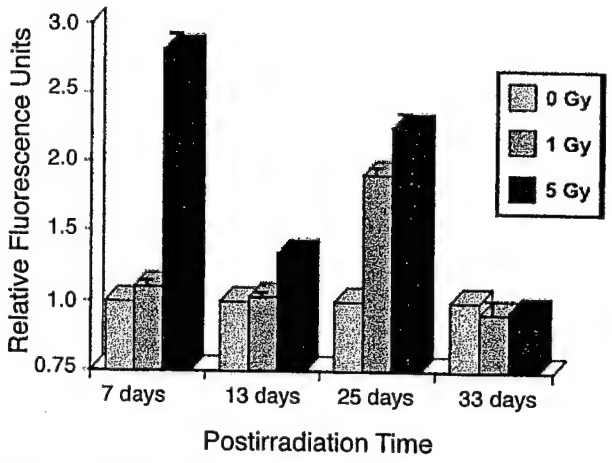

FIG. 8. Persistent elevation of ROS after X irradiation of primary rat neural precursor cells. Exponentially growing cultures of rat neural precursor cells were X-irradiated and maintained over the course of 1 month. At the indicated times, cells were harvested for the assessment of ROS using the fluorogenic dye CM-H_2DCFDA. FACS analysis of cells showed that relative to sham-irradiated cultures, precursor cells exhibit a persistent increase in ROS, with the relative maximum occurring 1 and 3 weeks after irradiation. Bars represent the average of two independent measurements ± SD, and all values were normalized to controls (set to unity) run the same day.

Radiation Exposure Leads to Increased Oxidative Stress In Vivo

To determine whether oxidative stress might modulate the radiation response of neural precursor cells *in vivo,* hippocampal precursor cells within the SGZ were analyzed for MDA, an end product of lipid peroxidation. Tissues from mice irradiated 24 h earlier with 10 Gy were stained with an antibody against MDA. MDA-positive cells were observed in the dentate gyrus and to a lesser extent in the hilar region (data not shown). Unirradiated controls showed no appreciable staining in the dentate gyrus (data not shown). To quantify MDA levels in irradiated brain, mice were given 10 Gy, and 1 week later hippocampi were dissected and homogenized. Compared to unirradiated controls, MDA levels increased significantly after irradiation (Fig. 9).

DISCUSSION

The main findings of the present study are: (1) the acute radiation response of neural precursor cells involves a dose-related increase in ROS and apoptosis; (2) significant dose-related elevations in ROS persist for 3–4 weeks postirradiation; (3) persistent apoptosis is observed, but only for 1 week after irradiation; (4) the radiation response of neural precursor cells is characterized by specific cell cycle blocks showing the presence of radioresponsive checkpoints; (5) functional cell cycle checkpoints are associated with an increase in Trp53, phospho-Trp53 and Cdkn1a protein levels; (6) Trp53 deficiency spares the radiation-induced depletion of SGZ proliferating cells and immature neurons; and (7) elevated lipid peroxidation can be found in the SGZ 1 week after irradiation. These data suggest that radiation-induced increases in ROS and apoptosis in neural precursor cells may be tied to Trp53-dependent regulation of cell cycle control and stress-activated pathways. The similarities between our *in vitro* data and recent studies of precursor cell radiation response *in vivo* (*14–16*) suggest that oxidative stress may play a contributory role in the inhibition of neurogenesis and perhaps in the development of cognitive impairment after exposure to radiation.

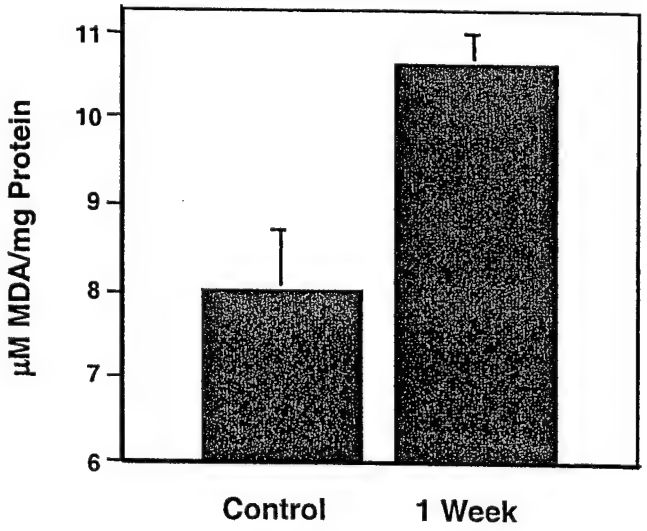

FIG. 9. Lipid peroxidation in the hippocampus of irradiated mice. Hippocampal tissue was dissected from irradiated (10 Gy) and unirradiated mice and processed for the determination of MDA. Compared to controls, tissue isolated 1 week after irradiation showed significant increases ($P < 0.05$) in MDA levels.

Irradiation of the CNS has been shown to cause a long-term and dose-dependent inhibition of hippocampal neurogenesis (*14–17*). Neurogenesis is characterized by a proliferation of precursor cells within the SGZ and a migration of cells that can differentiate into neurons and other cell types (*33–35*). Impaired neurogenesis induced by cranial irradiation is preceded by an acute apoptotic response in the SGZ and a long-lasting decrease in the numbers of proliferating SGZ precursor cells and new neurons (*14, 16*). While functional and cognitive deficits correlate with decreased neurogenesis[2] (*17*), the significance of neurogenesis in such findings is not yet clear. Relevant *in vitro* models of radiation effects on neural stem/precursor cells enable us to address specific mechanisms that may have an impact on the response of these cells to ionizing radiation and may clarify their role in cognitive changes induced by radiation.

In pilot studies, we used mouse neural precursor cells derived from the cerebellum and immortalized with *Myc* (*v-myc*) (*41, 42*). These cells were not found to be markedly sensitive to X rays and exhibited a typical survival curve having a shoulder with a D_0 of 1.25, which is in the range for most other mammalian cell lines (*43*). Cell lines retrovirally transduced with *Myc* often exhibit perturbations to basal stress response pathways (i.e. apoptosis; ref. *44*), and precursor cells from the cerebellum may exhibit different radiation responses compared to precursor cells from the forebrain. We found that these cells did not undergo significant apoptosis after irradiation (data not shown), which is in contrast to the situation observed *in vivo* (*14, 16*). Because of this and the potential problems associated with Myc-transformed cells, we focused on neural precursor cells whose radiation response was qualitatively similar to that seen in our *in vivo* models. In rat precursor cells, apoptosis occurred over a similar time frame (Fig. 2) as that seen in the SGZ and subependymal zone in the rat brain (*14, 45*) and the mouse SGZ (*16*). This similarity validates the utility of our cultured cell system for modeling radiation effects in the CNS.

Cell cycle analysis of irradiated precursor cells confirmed the presence of functional radiation-induced checkpoints, particularly in G_2/M (Fig. 3). The peak of G_2/M-phase arrest at 12 h coincided with maximal apoptosis, resulting in depletion of G_2/M cells and enrichment in the fraction of G_0/G_1 cells 6 h later. The activation of cell cycle checkpoints is consistent with the DNA damage response expected for cells containing a functional Trp53 protein (*47*). The Trp53 protein is a critical regulator of cell cycle events and exerts its influence through mechanisms involving transcriptional, translational and post-translational alterations in cell cycle regulatory proteins (*47, 48*). The checkpoint activation (Fig. 3) and increase in Trp53, phospho-Trp53 and Cdkn1a protein levels (Fig. 4) that we observed after irradiation of hippocampal precursor cells are consistent with the stabilization of a functional Trp53 in response to DNA damage.

Exogenous physical and chemical agents and endogenous agents such as oxidative stress continually threaten the integrity of DNA. To counteract these elements, cells rely upon Trp53 to regulate defense mechanisms to impede the proliferative expansion of damaged cells. The Trp53 protein plays multiple roles in regulating cell cycle events, apoptosis and DNA repair pathways and may be key in sensing and regulating ROS levels (*49*). Interactions of Trp53 with the $p66^{SHC}$ (*50, 51*) and Sir2 (*52, 53*) gene products have provided interesting links between Trp53 activity, oxidative stress, metabolism and life-span extension. As a transcription factor, Trp53 controls a number of redox-sensitive genes (*54, 55*) and may underlie the increased ROS observed in our system. Expression of dominant negative Trp53 constructs in our precursor cells will provide a rigorous assessment of this possibility.

While the data from our *in vitro* analyses clearly implicate the role of Trp53 in the radiation response of rat neural precursor cells, this information is of potential clinical importance only if the cell culture studies adequately represent what happens in the more complicated *in vivo* setting. We were able to address the role of Trp53 *in vivo* by taking advantage of the availability of mutant mice lacking both Trp53 alleles. Because proliferating precursor cells and their progeny, immature neurons, are found in the dentate SGZ, it is possible to quantify the radiation responses of these cells by counting their number in a standardized region of interest (*14, 16*). While the dose responses of these cells were qualitatively similar in wild-type and knockout mice, the mice lacking Trp53 showed less sensitivity, at least after doses below 5 Gy. One possible complication in our study is that our *in vivo* studies were carried out in mice, while the *in vitro* analyses relied upon cells derived from rat brain. While species differences can affect experimental results in some cases, we have considerable data showing remarkable similarities between mice and rats in terms of acute and chronic responses within the SGZ (*14–16*). We feel, therefore, that the responses seen *in vitro* adequately represent what happens *in vivo*, and that Trp53 plays a contributory role in the radiation response of neural precursor cells in culture and *in vivo*.

In addition to Trp53, the elevated ROS that are observed in X-irradiated hippocampal precursor cells are likely to be important. Radiation has been found to cause a delayed and/or persistent induction of ROS in other cell lines (*49, 56–58*). Elevated ROS have been found to potentiate apoptosis by inducing the release of cytochrome c from the mitochondria (*59*), and elevated apoptosis, ROS and mitochondrial dysfunction have been observed multiple generations (20–80 population doublings) after X irradiation in subclones exhibiting indications of genomic instability (*57, 58*). The persistence of ROS, and to a lesser extent the apoptosis that is observed weeks after irradiation in hippocampal precursor cells, may be indicative of some ge-

[2] Raber et al., manuscript submitted for publication.

nome-destabilizing event(s) and may well be relevant to other neurological end points in the CNS. Oxidative stress has recently been demonstrated in the irradiated hippocampus (*60*) and in the spinal cord (*3*), but unlike the present study, it was not determined whether this effect was dose responsive. Our qualitative and quantitative data showing elevated MDA levels *in vivo* suggest that after irradiation there is significant oxidative stress in the dentate gyrus. Given the prevalence of oxidative stress after other forms of CNS insult (*21–25*), it is reasonable to suspect that ROS may contribute to many of these radiation-induced end points. Thus it seems reasonable to suspect that the redox-related changes observed *in vitro* may also play a significant role in modulating the radiation response of the SGZ *in vivo*. ROS may mediate the interplay between damaged and undamaged cells and may be important in regulating the remodeling of the CNS microenvironment in response to irradiation.

Changes in the microenvironment can be triggered by radiation-induced signaling pathways that initiate the expression and secretion of cytokines that can regulate both acute and chronic inflammatory responses (*61*). The expression levels of certain cytokines have also been observed to fluctuate over many months after irradiation (*62, 63*) and may be linked to the long-term changes in ROS levels found weeks after irradiation of hippocampal precursor cells. Further changes in the microvasculature and recruitment of alternative cell types such as microglia can tailor the interplay between tissues adapting to radiation injury (*15, 16*). Alterations in the microenvironment are also sufficient to inhibit differentiation of unirradiated precursor cells transplanted into an irradiated hippocampus (*15*). While its tempting to speculate that the inhibition of hippocampal neurogenesis is related to the depletion of SGZ precursor cells and modifications to the microenvironment observed after radiation injury in the CNS, the underlying mechanisms remain to be elucidated. The persistent increase in ROS levels observed days to weeks after irradiation may, however, provide a clue, suggesting that oxidative stress may be a biochemical mechanism involved in the regulation of a wide number of radiation-induced sequelae in the CNS.

ACKNOWLEDGMENTS

This work was supported by ACS grant RPG-00-036-01-CNE (CLL), by DOD grant DAMD17-01-1-0820 (JRF, CLL), NIH grants R01 CA76141 and R21 NS40088 (JRF), and in part with Federal funds from the Department of Health and Human Services under Contract Number 22xs026a (JRF). The contents of this publication do not necessarily reflect the views or policies of the Department of Health and Human Services nor does mention of trade names, commercial products, or organization imply endorsement the U.S. Government.

Received: March 21, 2003; accepted: September 9, 2003

REFERENCES

1. G. E. Sheline, W. M. Wara and V. Smith, Therapeutic irradiation and brain injury. *Int. J. Radiat. Oncol. Biol. Phys.* **6**, 1215–1228 (1980).
2. H. Hodges, N. Katzung, P. Sowinski, J. W. Hopewell, J. H. Wilkinson, T. Bywaters and M. Rezvani, Late behavioural and neuropathological effects of local brain irradiation in the rat. *Behav. Brain Res.* **91**, 99–114 (1998).
3. P. J. Tofilon and J. R. Fike, The radioresponse of the central nervous system: A dynamic process. *Radiat. Res.* **153**, 357–370 (2000).
4. O. K. Abayomi, Pathogenesis of irradiation-induced cognitive dysfunction. *Acta Oncol.* **35**, 659–663 (1996).
5. J. R. Crossen, D. Garwood, E. Glatstein and E. A. Neuwelt, Neurobehavioral sequelae of cranial irradiation in adults: A review of radiation-induced encephalopathy. *J. Clin. Oncol.* **12**, 627–642 (1994).
6. J. H. Kramer, M. R. Crittenden, F. E. Halberg, W. M. Wara and M. J. Cowan, A prospective study of cognitive functioning following low-dose cranial radiation for bone marrow transplantation. *Pediatrics* **90**, 447–450 (1992).
7. D. D. Roman and P. W. Sperduto, Neuropsychological effects of cranial radiation: Current knowledge and future directions. *Int. J. Radiat. Oncol. Biol. Phys.* **31**, 983–998 (1995).
8. O. Surma-aho, M. Niemela, J. Vilkki, M. Kouri, A. Brander, O. Salonen, A. Paetau, M. Kallio, J. Pyykkonen and J. Jaaskelainen, Adverse long-term effects of brain radiotherapy in adult low-grade glioma patients. *Neurology* **56**, 1285–1290 (2001).
9. H. A. Cameron, C. S. Woolley, B. S. McEwen and E. Gould, Differentiation of newly born neurons and glia in the dentate gyrus of the adult rat. *Neuroscience* **56**, 337–344 (1993).
10. G. Kempermann, H. G. Kuhn and F. H. Gage, More hippocampal neurons in adult mice living in an enriched environment. *Nature* **386**, 493–495 (1997).
11. P. S. Eriksson, E. Perfilieva, T. Bjork-Eriksson, A. M. Alborn, C. Nordborg, D. A. Peterson and F. H. Gage, Neurogenesis in the adult human hippocampus. *Nat. Med.* **4**, 1313–1317 (1998).
12. E. Gould, A. Beylin, P. Tanapat, A. Reeves and T. J. Shors, Learning enhances adult neurogenesis in the hippocampal formation. *Nat. Neurosci.* **2**, 260–265 (1999).
13. G. Kempermann, D. Gast, G. Kronenberg, M. Yamaguchi and F. H. Gage, Early determination and long-term persistence of adult-generated new neurons in the hippocampus of mice. *Development* **130**, 391–399 (2003).
14. E. Tada, J. M. Parent, D. H. Lowenstein and J. R. Fike, X-irradiation causes a prolonged reduction in cell proliferation in the dentate gyrus of adult rats. *Neuroscience* **99**, 33–41 (2000).
15. M. L. Monje, S. Mizumatsu, J. R. Fike and T. D. Palmer, Irradiation induces neural precursor-cell dysfunction. *Nat. Med.* **8**, 955–962 (2002).
16. S. Mizumatsu, M. Monje, D. Morhardt, R. Rola, T. Palmer and J. Fike, Extreme sensitivity of adult neurogenesis to low doses of X-irradiation. *Cancer Res.* **63**, 4021–4027 (2003).
17. T. M. Madsen, P. E. Kristjansen, T. G. Bolwig and G. Wortwein, Arrested neuronal proliferation and impaired hippocampal function following fractionated brain irradiation in the adult rat. *Neuroscience* **119**, 635–642 (2003).
18. P. Dent, A. Yacoub, J. Contessa, R. Caron, G. Amorino, K. Valerie, M. P. Hagan, S. Grant and R. Schmidt-Ullrich, Stress and radiation-induced activation of multiple intracellular signaling pathways. *Radiat. Res.* **159**, 283–300 (2003).
19. L. Cartee, J. A. Vrana, Z. Wang, J. S. Park, M. Birrer, P. B. Fisher, S. Grant and P. Dent, Inhibition of the mitogen activated protein kinase pathway potentiates radiation-induced cell killing via cell cycle arrest at the G_2/M transition and independently of increased signaling by the JNK/c-Jun pathway. *Int. J. Oncol.* **16**, 413–422 (2000).
20. S. A. Amundson, M. Bittner, P. Meltzer, J. Trent and A. J. Fornace, Jr., Induction of gene expression as a monitor of exposure to ionizing radiation. *Radiat. Res.* **156**, 657–661 (2001).
21. P. H. Chan, Oxygen radicals in focal cerebral ischemia. *Brain Pathol.* **4**, 59–65 (1994).
22. S. Love, Oxidative stress in brain ischemia. *Brain Pathol.* **9**, 119–131 (1999).

23. A. Lewen, P. Matz and P. H. Chan, Free radical pathways in CNS injury. *J. Neurotrauma* **17**, 871–890 (2000).
24. G. W. Kim, A. Lewen, J. Copin, B. D. Watson and P. H. Chan, The cytosolic antioxidant, copper/zinc superoxide dismutase, attenuates blood–brain barrier disruption and oxidative cellular injury after photothrombotic cortical ischemia in mice. *Neuroscience* **105**, 1007–1018 (2001).
25. A. Lewen, T. Sugawara, Y. Gasche, M. Fujimura and P. H. Chan, Oxidative cellular damage and the reduction of APE/Ref-1 expression after experimental traumatic brain injury. *Neurobiol. Dis.* **8**, 380–390 (2001).
26. N. A. Simonian and J. T. Coyle, Oxidative stress in neurodegenerative diseases. *Annu. Rev. Pharmacol. Toxicol.* **36**, 83–106 (1996).
27. K. J. Smith, R. Kapoor and P. A. Felts, Demyelination: The role of reactive oxygen and nitrogen species. *Brain Pathol.* **9**, 69–92 (1999).
28. L. Packer, H. J. Tritschler and K. Wessel, Neuroprotection by the metabolic antioxidant alpha-lipoic acid. *Free Radic. Biol. Med.* **22**, 359–378 (1997).
29. A. Bast, G. R. Haenen and C. J. Doelman, Oxidants and antioxidants: state of the art. *Am. J. Med.* **91**, 2S–13S (1991).
30. S. Peuchen, J. P. Bolanos, S. J. Heales, A. Almeida, M. R. Duchen and J. B. Clark, Interrelationships between astrocyte function, oxidative stress and antioxidant status within the central nervous system. *Prog. Neurobiol.* **52**, 261–281 (1997).
31. J. Smith, E. Ladi, M. Mayer-Proschel and M. Noble, Redox state is a central modulator of the balance between self-renewal and differentiation in a dividing glial precursor cell. *Proc. Natl. Acad. Sci. USA* **97**, 10032–10037 (2000).
32. M. C. Raff, H. R. Miller and M. Noble, A glial progenitor cell that develops *in vitro* into an astrocyte or an oligodendrocyte depending upon culture medium. *Nature* **303**, 390–396 (1983).
33. T. D. Palmer, J. Takahashi and F. H. Gage, The adult rat hippocampus contains primordial neural stem cells. *Mol. Cell. Neurosci.* **8**, 389–404 (1997).
34. T. D. Palmer, E. A. Markakis, A. R. Willhoite, F. Safar and F. H. Gage, Fibroblast growth factor-2 activates a latent neurogenic program in neural stem cells from diverse regions of the adult CNS. *J. Neurosci.* **19**, 8487–8497 (1999).
35. R. M. Seaberg and D. van der Kooy, Adult rodent neurogenic regions: The ventricular subependyma contains neural stem cells, but the dentate gyrus contains restricted progenitors. *J. Neurosci.* **22**, 1784–1793 (2002).
36. J. D. Dignam, Preparation of extracts from higher eukaryotes. *Methods Enzymol.* **182**, 194–203 (1990).
37. B. J. Fisher, E. Naumova, C. C. Leighton, G. N. Naumov, N. Kerklviet, D. Fortin, D. R. Macdonald, J. G. Cairncross, G. S. Bauman and L. Stitt, Ki-67: A prognostic factor for low-grade glioma? *Int. J. Radiat. Oncol. Biol. Phys.* **52**, 996–1001 (2002).
38. N. Kee, S. Sivalingam, R. Boonstra and J. M. Wojtowicz, The utility of Ki-67 and BrdU as proliferative markers of adult neurogenesis. *J. Neurosci. Methods* **115**, 97–105 (2002).
39. J. Nacher, C. Crespo and B. S. McEwen, Doublecortin expression in the adult rat telencephalon. *Eur. J. Neurosci.* **14**, 629–644 (2001).
40. C. Shinohara, G. T. Gobbel, K. R. Lamborn, E. Tada and J. R. Fike, Apoptosis in the subependyma of young adult rats after single and fractionated doses of X-rays. *Cancer Res.* **57**, 2694–2702 (1997).
41. E. F. Ryder, E. Y. Snyder and C. L. Cepko, Establishment and characterization of multipotent neural cell lines using retrovirus vector-mediated oncogene transfer. *J. Neurobiol.* **21**, 356–375 (1990).
42. E. Y. Snyder, D. L. Deitcher, C. Walsh, S. Arnold-Aldea, E. A. Hartwieg and C. L. Cepko, Multipotent neural cell lines can engraft and participate in development of mouse cerebellum. *Cell* **68**, 33–51 (1992).
43. E. J. Hall, *Radiobiology for the Radiobiologist,* 4th ed. Lippincott Williams & Wilkins, Philadelphia, 2000.
44. S. Pelengaris, M. Khan and G. I. Evan, Suppression of Myc-induced apoptosis in beta cells exposes multiple oncogenic properties of Myc and triggers carcinogenic progression. *Cell* **109**, 321–334 (2002).
45. E. Tada, C. Yang, G. T. Gobbel, K. R. Lamborn and J. R. Fike, Long-term impairment of subependymal repopulation following damage by ionizing irradiation. *Exp. Neurol.* **160**, 66–77 (1999).
46. J. P. Murnane, Cell cycle regulation in response to DNA damage in mammalian cells: A historical perspective. *Cancer Metastasis Rev.* **14**, 17–29 (1995).
47. M. L. Agarwal, A. Agarwal, W. R. Taylor and G. R. Stark, p53 controls both the G_2/M and the G_1 cell cycle checkpoints and mediates reversible growth arrest in human fibroblasts. *Proc. Natl. Acad. Sci. USA* **92**, 8493–8497 (1995).
48. S. M. de Toledo, E. I. Azzam, P. Keng, S. Laffrenier and J. B. Little, Regulation by ionizing radiation of CDC2, cyclin A, cyclin B, thymidine kinase, topoisomerase IIα, and RAD51 expression in normal human diploid fibroblasts is dependent on p53/p21Waf1. *Cell Growth Differ.* **9**, 887–896 (1998).
49. R. E. Rugo, M. B. Secretan and R. H. Schiestl, X radiation causes a persistent induction of reactive oxygen species and a delayed reinduction of TP53 in normal human diploid fibroblasts. *Radiat. Res.* **158**, 210–219 (2002).
50. E. Migliaccio, M. Giorgio, S. Mele, G. Pelicci, P. Reboldi, P. P. Pandolfi, L. Lanfrancone and P. G. Pelicci, The p66shc adaptor protein controls oxidative stress response and life span in mammals. *Nature* **402**, 309–313 (1999).
51. S. Nemoto and T. Finkel, Redox regulation of forkhead proteins through a p66shc-dependent signaling pathway. *Science* **295**, 2450–2452 (2002).
52. J. Luo, A. Y. Nikolaev, S. Imai, D. Chen, F. Su, A. Shiloh, L. Guarente and W. Gu, Negative control of p53 by Sir2alpha promotes cell survival under stress. *Cell* **107**, 137–148 (2001).
53. E. Langley, M. Pearson, M. Faretta, U. M. Bauer, R. A. Frye, S. Minucci, P. G. Pelicci and T. Kouzarides, Human SIR2 deacetylates p53 and antagonizes PML/p53-induced cellular senescence. *EMBO J.* **21**, 2383–2396 (2002).
54. J. Lotem, M. Peled-Kamar, Y. Groner and L. Sachs, Cellular oxidative stress and the control of apoptosis by wild-type p53, cytotoxic compounds, and cytokines. *Proc. Natl. Acad. Sci. USA* **93**, 9166–9171 (1996).
55. P. Hainaut and K. Mann, Zinc binding and redox control of p53 structure and function. *Antioxid. Redox Signal.* **3**, 611–623 (2001).
56. S. M. Clutton, K. M. S. Townsend, C. Walker, J. D. Ansell and E. G. Wright, Radiation-induced genomic instability and persisting oxidative stress in primary bone marrow cultures. *Carcinogenesis* **17**, 1633–1639 (1996).
57. C. L. Limoli, A. Hartmann, L. Shephard, C. R. Yang, D. A. Boothman, J. Bartholomew and W. F. Morgan, Apoptosis, reproductive failure, and oxidative stress in Chinese hamster ovary cells with compromised genomic integrity. *Cancer Res.* **58**, 3712–3718 (1998).
58. C. Limoli, E. Giedzinski, W. Morgan, S. Swarts, G. Jones and W. Hyun, Persistent oxidative stress in chromosomally unstable cells. *Cancer Res.* **63**, 3107–3111 (2003).
59. S. Ueda, H. Masutani, H. Nakamura, T. Tanaka, M. Ueno and J. Yodoi, Redox control of cell death. *Antioxid. Redox Signal.* **4**, 405–414 (2002).
60. P. E. Lonergan, D. S. Martin, D. F. Horrobin and M. A. Lynch, Neuroprotective effect of eicosapentaenoic acid in hippocampus of rats exposed to gamma-irradiation. *J. Biol. Chem.* **277**, 20804–20811 (2002).
61. W. H. McBride, J. S. Economou, N. Kuber, J. H. Hong, C. S. Chiang, R. Syljuasen, S. T. Dougherty and G. J. Dougherty, Modification of tumor microenvironment by cytokine gene transfer. *Acta Oncol.* **34**, 447–451 (1995).
62. W. H. McBride, Cytokine cascades in late normal tissue radiation responses. *Int. J. Radiat. Oncol. Biol. Phys.* **33**, 233–234 (1995).
63. C. S. Chiang, J. H. Hong, A. Stalder, J. R. Sun, H. R. Withers and W. H. McBride, Delayed molecular responses to brain irradiation. *Int. J. Radiat. Biol.* **72**, 45–53 (1997).

Available online at www.sciencedirect.com

SCIENCE DIRECT

Experimental Neurology 188 (2004) 316–330

Experimental Neurology

www.elsevier.com/locate/yexnr

Radiation-induced impairment of hippocampal neurogenesis is associated with cognitive deficits in young mice

Radoslaw Rola,[a] Jacob Raber,[b,c,d] Angela Rizk,[b] Shinji Otsuka,[a] Scott R. VandenBerg,[a,e] Duncan R. Morhardt,[a] and John R. Fike[a,*]

[a] *Brain Tumor Research Center, Department of Neurological Surgery, University of California, San Francisco, San Francisco, CA 94143, USA*
[b] *Department of Behavioral Neuroscience, Oregon Health and Science University, Portland, OR 97239, USA*
[c] *Department of Neurology, Oregon Health and Science University, Portland, OR 97239, USA*
[d] *Division of Neuroscience ONPRC, Oregon Health and Science University, Portland, OR 97239, USA*
[e] *Department of Pathology, University of California, San Francisco, San Francisco, CA 94143, USA*

Received 12 February 2004; revised 30 April 2004; accepted 4 May 2004
Available online 15 June 2004

Abstract

Advances in the management of pediatric brain tumors have increased survival rates in children, but their quality of life is impaired due to cognitive deficits that arise from irradiation. The pathogenesis of these deficits remains unknown, but may involve reduced neurogenesis within the hippocampus. To determine the acute radiosensitivity of the dentate subgranular zone (SGZ), 21-day-old C57BL/J6 male mice received whole brain irradiation (2–10 Gy), and 48 h later, tissue was assessed using immunohistochemistry. Proliferating SGZ cells and their progeny, immature neurons, were decreased in a dose-dependent fashion. To determine if acute changes translated into long-term alterations in neurogenesis, mice were given a single dose of 5 Gy, and 1 or 3 months later, proliferating cells were labeled with 5-bromo-2′-deoxyuridine (BrdU). Confocal microscopy was used to determine the percentage of BrdU-labeled cells that showed mature cell phenotypes. X-rays significantly reduced the production of new neurons at both time points, while glial components showed no change or small increases. Measures of activated microglia and infiltrating, peripheral monocytes indicated that reduced neurogenesis was associated with a chronic inflammatory response. Three months after irradiation, changes in neurogenesis were associated with spatial memory retention deficits determined using the Morris water maze. Behavioral training and testing increased the numbers of immature neurons, most prominently in irradiated animals. These data provide evidence that irradiation of young animals induces a long-term impairment of SGZ neurogenesis that is associated with hippocampal-dependent memory deficits.

Keywords: Brain; Radiation; Precursor cells; Neurogenesis; Subgranular zone; Mice; Barnes maze; Water maze; Environmental enrichment

Introduction

Recent advances in multimodality treatment protocols have dramatically increased survival rates in children with both primary (Bailey et al., 1995; Packer et al., 1994; Rousseau et al., 1994) and secondary (ACS, 2003) brain tumors. These encouraging findings have resulted in an emergent interest in the delayed effects of these treatments that may impact the growing population of long-term brain tumor survivors (Riva et al., 2000). The identification, characterization, and minimization of specific side effects, especially those related to neuropsychological sequelae, can have a critical impact on the quality of life, particularly with respect to career and educational goals (Macedoni-Luksic et al., 2003). Among the various therapeutic modalities used in the management of intracranial brain tumors, ionizing irradiation has been recognized as one of the major causes of long-term cognitive impairments, particularly in children (Christie et al., 1995; Fletcher and Copeland, 1988; Grill et al., 1999; Meadows et al., 1981; Roman and Sperduto, 1995). Moreover, reported irradiation-related cognitive deficits seem to be irreversible, and progressive (Duffner et al., 1983; Ellenberg et al., 1987). Consequently, understanding how irradiation affects normal brain tissue is of crucial importance in developing potential

* Corresponding author. Brain Tumor Research Center, Department of Neurological Surgery, University of California, San Francisco, Box 0520, San Francisco, CA 94143. Fax: +1-415-502-0613.
E-mail address: jfike@itsa.ucsf.edu (J.R. Fike).

0014-4886/$ - see front matter © 2004 Elsevier Inc. All rights reserved.
doi:10.1016/j.expneurol.2004.05.005

approaches/strategies to reduce cognitive impairments after cranial irradiation.

Radiation-induced cognitive changes are often manifested as deficits in hippocampal-dependent functions of learning and memory, including spatial information processing (Abayomi, 1996; Crossen et al., 1994; Lee et al., 1989; Roman and Sperduto, 1995; Surma-aho et al., 2001). The underlying mechanisms for these effects have remained elusive, although recently it was suggested that changes in neuronal precursor cells in the dentate subgranular zone (SGZ) of the hippocampus may be involved (Madsen et al., 2003; Mizumatsu et al., 2003; Monje et al., 2002). Neurogenesis occurs in the SGZ throughout life (Eriksson et al., 1998; Kuhn et al., 1996), resulting in cells that are capable of migrating into the granule cell layer (GCL) of the dentate gyrus (Kuhn et al., 1996). There, they develop granule cell morphology and neuronal markers (Cameron et al., 1993) and connect to their target area, CA3 (Markakis and Gage, 1999; Stanfield and Trice, 1988). These newborn cells subsequently become functionally integrated into local circuitry, and have passive membrane properties, action potentials, and functional synaptic inputs similar to those found in mature dentate granule cells (van Praag et al., 2002). Such data imply that newly born cells may play a significant role in synaptic plasticity (van Praag et al., 1999). Recent studies show that various insults result in a loss of neural precursor cells from the dentate SGZ and lead to a reduction in the number of newly generated neurons; such reductions are associated with learning impairments (Shors et al., 2001) and with inhibition of long-term potentiation (Snyder et al., 2001). These data support the hypothesis that radiation-induced impairment of SGZ neurogenesis may play an important role in the pathogenesis of cognitive dysfunction after irradiation.

Previous studies from our lab (Mizumatsu et al., 2003; Monje et al., 2002; Parent et al., 1999; Tada et al., 2000), as well as others (Nagai et al., 2000; Peissner et al., 1999; Sasaki et al., 2000), have addressed the radiation response of cells in the dentate gyrus. In rodents, proliferating SGZ precursor cells and their progeny undergo apoptosis after irradiation (Mizumatsu et al., 2003; Parent et al., 1999; Tada et al., 2000), and consequential reductions in the generation of new neurons are still observed months after exposure (Mizumatsu et al., 2003; Tada et al., 2000). In addition to these studies in adult animals, considerable data are available regarding hippocampal structure and function after irradiation in prenatal or neonatal rodents (Czurko et al., 1997; Mickley et al., 1989; Moreira et al., 1997; Sienkiewicz et al., 1992, 1994, 1999). However, to the best of our knowledge, no data exist with respect to the radiation response of young animals, those roughly equivalent in age to young children (i.e., <5 years old). This is important because the incidence of brain tumors in young children is higher than that seen in adults (ACS, 2003), and because irradiation is a primary treatment modality in those patients. In the current study, we addressed the effects of irradiation on neurogenesis and cognitive function in mice irradiated at a young age. Our results show that neural precursor cells in the dentate SGZ of young mice are extremely sensitive to X-irradiation, and that changes in neurogenesis are associated with specific cognitive impairments.

Methods

Twenty-one-day-old male C57BL/J6 mice (Jackson Laboratories, Bar Harbor, ME), which are roughly equivalent of toddler humans (Yager and Thornhill, 1997), were used in all experiments. All studies were done in accordance with federal and institutional guidelines. Animals were kept in a temperature and light-controlled environment with a 12/12 h light/dark cycle, and provided food and water ad libitum. For all irradiation and perfusion procedures, animals were anesthetized with an intraperitoneal (i.p.) injection of ketamine hydrochloride (60 mg/kg, Abbott Laboratories, North Chicago, IL) and medetomidine hydrochloride (0.25 mg/kg, Orion Corp., Espoo, Finland). Sham irradiated mice (controls) were treated accordingly.

Mice were irradiated using a Phillips orthovoltage X-ray system as described previously (Mizumatsu et al., 2003). Dosimetry was performed using a Keithley electrometer ionization chamber calibrated using lithium fluoride thermal luminescent dosimeters. The corrected dose rate was approximately 1.75 Gy/min at a source-to-skin distance of 21 cm.

Acute radiation response

To determine the radiation dose response of proliferating SGZ cells and their progeny, whole brain doses of 2, 5, and 10 Gy were given to groups of mice ($n = 4$), and tissue was collected 48 h after irradiation; control mice ($n = 4$) were killed at the same time.

For tissue collection, anesthetized animals were perfused with 50 ml of a 10% buffered formalin solution into the ascending aorta using a mechanical pump (Masterflex Model 7014; Cole Parmer, Chicago, IL) over a 5-min period. Subsequently, mice were decapitated, and the brains were removed and immersed in a 10% buffered formalin solution for 3 days. Tissue was gross sectioned and stored in 70% ethanol until paraffin embedding as described previously (Tada et al., 2000). A rotary microtome was used to cut 6-μm-thick transverse sections that were placed on SuperFrost Plus (Fisher Scientific, Pittsburgh, PA) glass microscope slides.

After brain sections were deparaffinized, endogenous peroxidase activity was quenched as described (Mizumatsu et al., 2003). Sections were then soaked in 10 mM sodium citrate buffer (pH = 6.0), boiled for 10 min using a microwave oven, and incubated with blocking serum for 30 min. To determine radiation-induced changes in the cellular composition of the SGZ, proliferating cells and immature neurons were labeled with antibodies against

Ki-67 (DakoCytomation, Caprinteria, CA, diluted 1:100 in PBS with 2% normal rabbit serum) and Doublecortin (DCx, Santa Cruz Biotechnology, Santa Cruz, CA, diluted 1:500 in PBS with 5% normal horse serum), respectively (Mizumatsu et al., 2003). Briefly, sections were incubated overnight at 4°C with primary antibodies and subsequently for 30 min at room temperature with biotinylated secondary antibodies (rabbit anti-rat IgG, Vector, Burlingame, CA, diluted 1:200 in PBS with 2% normal rabbit serum for Ki-67 and horse anti-goat IgG, Vector, diluted 1:500 in 5% normal horse serum for DCx). Binding of secondary antibodies was detected using an avidin-biotinylated peroxidase complex system (ABC; Vector) and developed with 0.025% 3,3′-diaminobenzidine (DAB, Zymed, South San Francisco, CA) dissolved in double distilled water containing 0.005% H_2O_2. Sections were then counterstained with Gill's hematoxylin, dehydrated, and mounted.

Cell numbers were scored blind using a histomorphometric approach (Mizumatsu et al., 2003; Parent et al., 1999; Shinohara et al., 1997; Tada et al., 2000). Because some brain sections were used in other related studies (not shown), we were unable to do a rigorous stereological analysis. However, the methods used here are well standardized and have been used effectively to determine dose and time responses for cells in the dentate SGZ after radiation treatment of adult mice and rats (Mizumatsu et al., 2003; Parent et al., 1999; Tada et al., 1999). Our analysis involved a standardized counting area based on 6-μm-thick coronal sections from three different brain levels representing the rostral/mid hippocampus (Parent et al., 1999; Tada et al., 2000). The brain levels were approximately 50 μm apart and the most rostral brain level corresponded to the F −1.1 section in a stereotaxic mouse brain atlas (Slotnick and Leonard, 1975). For each mouse, three non-overlapping sections were analyzed, one each from the three regions of the hippocampus. All positively labeled cells within the SGZ of the suprapyrimidal and infrapyrimidal blades of the dentate gyrus were counted. The total number of positively labeled cells was determined by summing the values from both hemispheres in all three tissue sections.

Neurogenesis/inflammation

To determine the effects of irradiation on the production of new cells in the SGZ (i.e., neurogenesis), groups of mice ($n = 4$) received a whole brain dose of 5 Gy and were allowed to recover from anesthesia. One or 3 months following irradiation, mice received a single i.p. injection (50 mg/kg) of 5-bromo-2′-deoxyuridine (BrdU, Sigma, St. Louis, MO) daily for 7 days. Three weeks after the last BrdU injection, mice were anesthetized and perfused with ice-cold saline followed by ice-cold 4% paraformaldehyde made up that day. The brain was removed and post-fixed in paraformaldehyde overnight and then equilibrated in phosphate-buffered 30% sucrose. Free-floating 50-μm-thick sections were then cut on a freezing microtome and stored in cryoprotectant. Four randomly chosen sections from rostral/mid hippocampus [located between F −1.1 and F −2.0 sections in a stereotaxic mouse brain atlas (Slotnick and Leonard, 1975)] were subsequently immunostained as described (Monje et al., 2002; Palmer et al., 2000) using the following primary antibodies and working concentrations: rat anti-BrdU (1:10; Oxford Biotechnology, Kidlington, Oxford, UK), mouse anti-NeuN (1:200; Chemicon, Temecula, CA), rabbit anti-NG2 (1:200; Chemicon), goat anti-GFAP (1:100; Santa Cruz Biotechnology), and rat anti-CD68 (1:20; Serotec, Inc., Raleigh, NC). To qualitatively determine the expression of the inflammatory marker CCR2, we randomly selected sections of the hippocampus (F −1.1—F −2.0, stereotaxic atlas) and immunostained using anti-CCR2 primary antibody (1:100; Santa Cruz Biotechnology) and anti-goat secondary antibody conjugated with Alexa 633 fluorophore (1:200; Molecular Probes, Eugene, OR). Nuclei were counterstained with DAPI (Molecular Probes).

Confocal microscopy was performed using a Zeiss 510 confocal microscope (Thornwood, New York), using techniques previously described (Monje et al., 2002; Palmer et al., 2000). Appropriate gain and black-level settings were obtained on control tissues stained with secondary antibodies alone. Upper and lower thresholds were always set using a range indicator function to minimize data loss due to saturation. The primary confocal endpoints were total number of BrdU-positive cells and the proportion of BrdU-positive cells that co-expressed each lineage-specific phenotype. Cell counts were limited to the dentate GCL and a 50-μm border along the hilar margin that included the SGZ. When possible, at least 100 BrdU-positive cells were scored for each marker per animal. Each cell was manually examined in its full 'z' dimension with use of split panel analysis, and only those cells for which the BrdU-positive nucleus was unambiguously associated with the lineage-specific marker were scored as positive.

Behavioral testing

To determine behavioral effects after irradiation, mice received either sham irradiation ($n = 12$) or a single dose of 5 Gy ($n = 12$) and were group housed until 1 week before training and testing. To minimize the effects of social influences on behavior during testing, all mice were then housed singly before the initiation of training and continuing throughout the 30 days of testing. The sequence of behavioral testing was such that tests were administered in the order of increasing stress level (Raber et al., 1998); the tests used included open field, elevated plus maze, elevated zero maze, novel location and novel object recognition, rotorod test, Morris water maze, Barnes maze, and passive avoidance learning. The experimenter was blinded to the treatment of the mice. The open field, elevated plus maze, and passive avoidance were performed exactly as described previously (Raber et al., 1998, 2000a,b, 2002).

Elevated zero maze

The elevated zero maze (Hamilton-Kinder, Poway, CA) is a circular maze that consists of two enclosed areas and two open areas and has a diameter of 53.3 cm. The open and closed areas were identical in length to the open and closed arms in the elevated plus maze. Mice were placed in the closed part of the maze and allowed free access for 10 min. A Noldus EthoVision (Leesburg, VA) video tracking system was used to calculate the time spent into the open areas.

Novel location and novel object recognition

On three consecutive days, mice were habituated individually to an open field (Hamilton-Kinder, Poway, CA) for 5 min. On the fourth day, the mice were trained in three consecutive trials and then tested in two consecutive trials with a 5-min inter-trial interval. For both the training and testing sessions, three plastic toy objects were placed in the open field, and each mouse was allowed to explore for 10 min. All objects were only used once and replicas were used in subsequent trials. Five minutes after the training trials, each animal was tested in a trial where one of the familiar objects was moved to a novel location in the arena. Five minutes after the novel location test, each mouse was tested in a trial where one of the familiar objects was replaced by a novel object. For each trial, the experimenter recorded the time spent exploring each object; the percentage of time spent exploring each object in all trials was calculated.

Water maze

In the water maze test, mice were first trained to locate a visible platform (days 1 and 2) and then a submerged hidden platform (days 3–5) in two daily sessions 3.5 h apart, each consisting of three 60-s trials (at 10 min intervals). Mice that failed to find the hidden platform within 60 s were put onto it for 15 s. During the visible platform training, the platform was moved to a different quadrant for each session. During the hidden platform training, the platform was placed in the center of the target quadrant and was kept constant for each mouse. The starting point at which the mouse was placed into the water was changed for each trial. Time to reach the platform (latency), path length, and swim speed were recorded with a Noldus EthoVision video tracking system set to analyze two samples per second. A 60-s probe trial (platform removed) was performed 1 h after the last hidden-platform session on days 3–5. For probe trial data analysis, the pool was divided into four quadrants.

Barnes maze

The Barnes circular maze for mice has been described in detail (Bach et al., 1995; Barnes et al., 1994). The maze is 122 cm in diameter and elevated 80 cm above the floor; 40 holes, 5 cm in diameter, are located 2.5 cm from the perimeter, and a metal escape tunnel (10 × 6 × 43 cm in size) was placed under one of the holes (Bach et al., 1995). At the beginning of a trial, each mouse was placed in a white cylinder (10 cm high, 12 cm diameter) for 10 s and a white noise generator (108 dB) and a bright fluorescent light (2100 lm) were activated to motivate escape behavior. Each trial ended when the mouse entered the escape tunnel or after 5 min.

The Barnes maze test consisted of three versions: a spatial hippocampal-dependent version, a random version to determine if non-spatial cues were used, and a cued version where the escape tunnel was visible. Mice were first trained to locate a hidden escape tunnel (spatial version; four trials per day) always located underneath the same hole; the position of the escape tunnel was randomly determined for each mouse. Subsequently, to determine if mice used non-spatial (e.g., olfaction) rather than spatial cues to locate the tunnel, two probe trials were used where the tunnel was relocated under different holes by moving it 180° (first trial) or 270° (second trial) from its original position. Finally, in the visible sessions (four trials per day), a colored tube was placed directly behind the hole containing the escape tunnel. The position of the escape tunnel in the visible sessions varied from session to session. For all trials, path length and velocity were recorded with a Noldus EthoVision video tracking system set to analyze two samples per second. The following parameters were analyzed by reviewing the video: (a) errors, defined as searches of any hole not containing the escape tunnel; (b) distance from the escape tunnel, defined as the number of holes between the first hole explored in a trial and the hole containing the escape tunnel; and (c) search strategies. Three search strategies were distinguished. Serial strategy was systematic consecutive hole searching in a clockwise or counterclockwise manner. Spatial strategy was finding the escape tunnel with errors and number of holes between the first hole explored in a trial and the hole containing the escape tunnel smaller than or equal to 3. The random search strategy was defined as exploring holes in an unsystematic fashion with many center maze crossings.

Behavioral training effects on indicators of neurogenesis

To determine if the behavioral training and testing affected quantitative measures relating to neurogenesis, that is, cell proliferation and immature neurons, groups of control ($n = 4$) mice and mice irradiated with a single dose of 5 Gy ($n = 4$) were perfused with 10% buffered formalin 3 months after irradiation, at the time the behavioral training was started. Mice that underwent behavioral training ($n = 12$ for controls and irradiated) were perfused with formalin at the end of testing. The perfusion technique and the immunohistochemical analyses for numbers of Ki-67-positive and DCx-positive cells were identical to those described above. In addition, for a qualitative appraisal of potential effects of irradiation on myelin levels in and around the hippocampus, tissue sections from these mice were stained with Luxol fast blue using standard histologic methods.

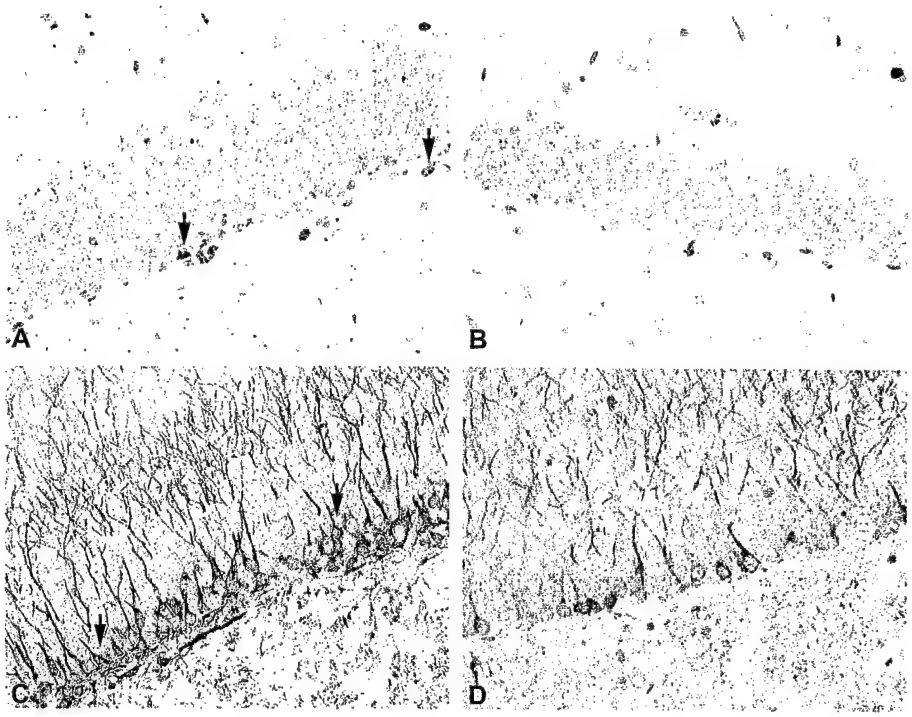

Fig. 1. Photomicrographs depicting specific cellular responses in mouse dentate gyrus before irradiation (A, C) and 48 h after 5 Gy (B, D). Panels include proliferating cells (Ki-67, A, B) and immature neurons (Doublecortin, C, D). Proliferating Ki-67-positive cells (arrows, A) are spread out within the SGZ in tissues from unirradiated animals; only an occasional Ki-67-positive cell was found after 5 Gy (B). Dcx-positive cells are highly concentrated in the SGZ and lower regions of the GCL of unirradiated mice (arrows, B). After 5 Gy, there are substantially fewer Dcx-positive cells (D). All micrographs are at 400× magnification.

Statistics

For each histologic endpoint, values for all animals in a given treatment group were averaged and standard errors of the mean (SEM) were calculated. A two-sided Jonckhere–Terpstra test was used to determine whether cellular changes in acute radiation response were monotonic, that is, either increasing or decreasing with increasing treatment dose. For long-term studies of neurogenesis, to compare distribution of cellular markers in response to radiation, the Wilcoxon–Mann–Whitney test was used.

For behavioral studies, differences among means were evaluated by ANOVA, followed by Tukey–Kramer post hoc tests if indicated. Learning curves were compared by repeated-measures ANOVA using contrasts to assess differences between specific groups of mice. To compare the distribution of search strategies in the Barnes maze, the Wilcoxon–Mann–Whitney test was used. For all analyses, the null hypothesis was rejected at the 0.05 level.

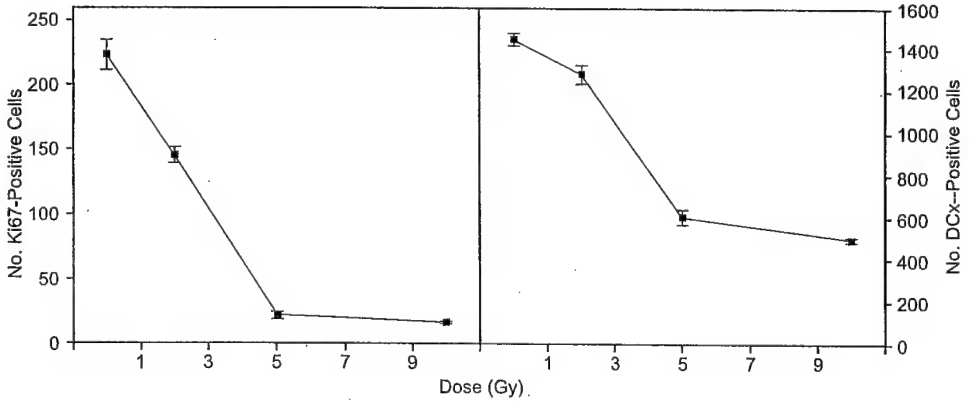

Fig. 2. Numbers of proliferating cells (left panel) and immature neurons (right panel) in the dentate subgranular zone are significantly decreased 48 h after irradiation. Antibodies against Ki-67 and Doublecortin were used to detect proliferating cells and immature neurons, respectively. All doses substantially reduced the numbers of proliferating cells and the dose response from 2 to 10 Gy was significant ($P < 0.001$). Immature neurons were also reduced in a dose-dependent fashion ($P < 0.001$). Each datum point represents an average of four animals and error bars are SEM.

Results

Radiation exposure results in an acute reduction of proliferating cells and their progeny in the dentate subgranular zone

Cell proliferation was visualized using an antibody against Ki-67, a nuclear antigen that is expressed during all stages of the cell cycle except G_0 (Fisher et al., 2002; Kee et al., 2002). Significant numbers of proliferating cells were detected in the SGZ along both blades of the dentate gyrus (Fig. 1A), occasionally in the hilus and only rarely in the GCL near the SGZ. The number of Ki-67-positive cells averaged 223 ± 11.7 in control mice. Forty-eight hours after exposure, there was a substantial reduction in the number of proliferating cells (Fig. 2) that ranged from a 35% reduction after 2 Gy to a 93% reduction after 10 Gy. The decrease in proliferating cells as a function of radiation dose was highly

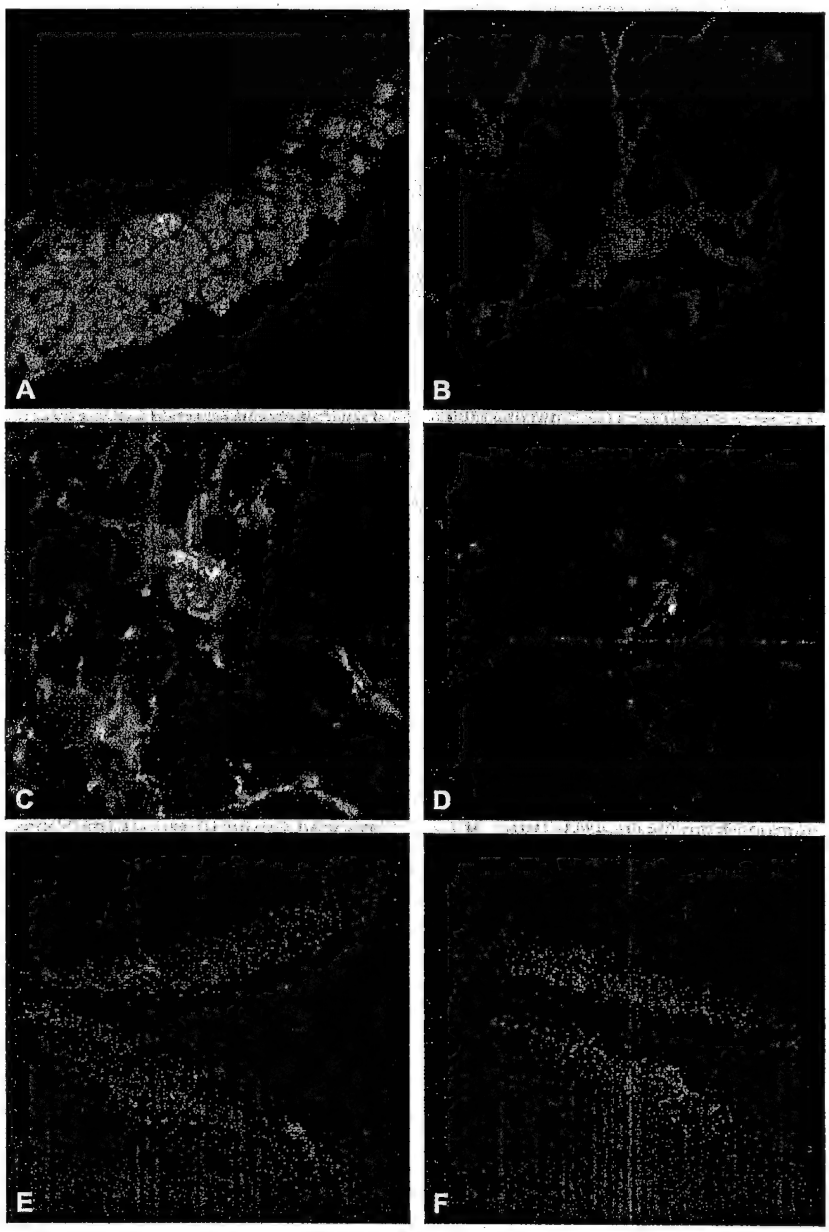

Fig. 3. Confocal images were used to quantify the percentage of BrdU-positive cells that co-expressed mature cell markers (A–D) and to show a qualitative difference in the expression of the CCR2 receptor (E and F). Proliferating cells were labeled with BrdU (red/orange in confocal images A–D), and 3 weeks later, the relative proportion of cells adopting a recognized cell fate was determined. Neurons (green cells in A), astrocytes (blue cells in B), oligodendrocytes (green cells in C), and activated microglia (blue cells in D) were labeled with antibodies against NeuN, GFAP, NG2, and CD68, respectively; each of the confocal images A–D shows a double-labeled cell. CCR2 staining (red in E and F) shows a substantial qualitative difference in the level of expression of this receptor between control (E) and irradiated (F) animals 2 months after irradiation.

significant ($P < 0.001$). DCx, a microtubule-associated protein that is expressed in migrating neuroblasts (Englund et al., 2002; Mizuguchi et al., 1999; Nacher et al., 2001), is commonly used to detect and quantify numbers of immature neurons in the dentate SGZ (Jessberger and Kempermann, 2003; Kempermann et al., 2003). DCx-positive cells were observed in large numbers in the SGZ and in the GCL immediately adjacent to SGZ (Fig. 1C). For our standardized counting area, the average number of DCx-positive cells in sham irradiated animals was 1448.0 ± 30.2. Forty-eight hours after irradiation, there was a substantial reduction in the number of immature neurons (Fig. 2), ranging from 12% after 2 Gy to 75% after 10 Gy. The dose-related decrease in the numbers of DCx-positive cells was highly significant ($P < 0.001$).

Radiation exposure results in a persistent decrease in SGZ neurogenesis

While our acute studies showed that there was a substantial loss of proliferating cells and their progeny (Fig. 2), even after the highest dose (10 Gy) about 10% of the proliferating cells appeared to be viable. To determine the fate of cells produced by surviving precursor cells, either 1 or 3 months after a single dose of 5 Gy, we administered BrdU (Mizumatsu et al., 2003; Monje et al., 2002) and used cell-specific antibodies to assess the phenotype of BrdU-positive cells. Irradiation reduced overall BrdU labeling by approximately 70% at both time points. The cumulative numbers of BrdU-positive cells from four non-overlapping confocal sections were 883.5 ± 179.1 for controls and 269.9 ± 91.6 for irradiated animals 1 month after irradiation and 438.7 ± 88.9 (controls) and 121.5 ± 46.7 (irradiated) 3 months after irradiation.

One month after sham treatment, most of the newly born cells (~80%) differentiated into neurons (Fig. 3A), while significantly fewer cells differentiated into astrocytes (Fig. 3B) (<10%) or oligodendrocytes (<4%) (Fig. 3C, Table 1). In contrast to what has been reported in adult mice (Mizumatsu et al., 2003), activated microglia (Fig. 3D) were also observed in the dentate SGZ in young control mice (Table 1). One month after irradiation, there was a significant decrease in the percentage of BrdU-positive cells co-expressing NeuN (Table 1), no change in BrdU-positive cells co-expressing GFAP, and a small but significant increase in BrdU-positive cells co-expressing NG2 (Table 1). With respect to radiation-induced inflammatory responses, there was a 2.5-fold increase in number of BrdU-positive cells co-expressing CD68 (activated microglia) and over a 5-fold increase in BrdU-positive cells co-expressing CD68 + NG2 (peripheral monocytes) (Table 1). Given the strong microglial/monocytic presence after irradiation, along with recent studies reporting the role of monocyte chemoattractant protein (MCP-1) and its receptor CCR2 in neuroinflammation (Banisadr et al., 2002; Gerard and Rollins, 2001), we made a qualitative appraisal of CCR2 immunoreactivity. A marked difference in CCR2 immunofluorescence within the dentate gyrus was seen between controls (Fig. 3E) and irradiated tissues (Fig. 3F).

Generally, the trends in the fate of newly born cells seen 3 months after irradiation were similar to those seen at 1 month, although the percentage values varied somewhat (Table 1). Irradiation significantly decreased neuronal differentiation and the trend toward increased astrocyte production became significant, albeit at levels similar to those observed 2 months earlier. While there appeared to be a slight increase in the production of new oligodendrocytes, that increase was insignificant. Regarding the inflammatory response, there still was a significant increase in activated microglia at 3 months, but the peripheral component (CD68 + NG2) was not statistically significant (Table 1).

In addition to neurogenesis measurements 3 months after treatment, tissues from separate groups of control and irradiated mice were also analyzed using thin section immunohistochemistry. In our standardized counting region, we saw that the number of proliferating cells was decreased by about 90% while the number of immature neurons was decreased by 77% (Fig. 6). At this time, which corresponded to the time that the behavioral tests were initiated, Luxol fast blue staining did not show differences in myelination or gross vascular abnormalities in or around the hippocampus (not shown).

Table 1
The fate of newly born cells produced by surviving precursor cells assessed by BrdU labeling with subsequent use of cell-specific antibodies

Cell line marker	Percentage of double-labeled cells (mean ± SEM)					
	1 month after irradiation			3 months after irradiation		
	Control	Irradiated	*P*	Control	Irradiated	*P*
NeuN	78.52 ± 4.69	43.41 ± 2.46	0.02	60.39 ± 1.55	37.38 ± 1.77	0.03
GFAP	8.97 ± 0.60	12.01 ± 1.70	ns	5.04 ± 0.75	10.34 ± 0.48	0.03
NG2	3.52 ± 0.46	8.76 ± 1.23	0.03	7.04 ± 3.65	9.22 ± 3.33	ns
CD68	17.45 ± 1.16	43.82 ± 3.59	0.03	14.15 ± 1.44	35.56 ± 3.88	0.03
CD68/NG2	0.6 ± 0.32	6.2 ± 1.65	0.03	1.34 ± 0.49	4.39 ± 1.48	ns

Overall BrdU-positive cells number was reduced by ~70% after 5 Gy.
NeuN—neuron-specific nuclear protein, GFAP—glial fibrillary acidic protein, NG2—chondroitin sulfate proteoglycan, CD68—macrosialin, CD68/NG2.

Changes in neurogenesis were associated with cognitive impairments

To determine if the reduced neurogenesis seen at 3 months was associated with cognitive deficits, we used the standard Morris water maze (Morris, 1984). Control and irradiated mice had similar swim speeds during the visible sessions (control: 11.92 ± 0.36 cm/s; irradiated: 11.52 ± 0.35 cm/s). All mice significantly improved their performance during the visible and hidden platform sessions ($P < 0.01$). However, there was a group difference when the total and visible learning curves were compared ($P < 0.05$, Tukey–Kramer) while there was no group difference when the hidden sessions alone were compared ($P = 0.16$) (Fig. 4A). In the second and third probe trials, the control and irradiated groups showed memory retention and spent significantly more time in the target quadrant than in any other quadrant (control: $P < 0.01$, target vs. any other quadrant; irradiated: $P < 0.05$, target vs. any other quadrant). However, when time spent in the target quadrant only was compared, control mice spent significantly more time in the target quadrant than irradiated mice on days 2 ($P = 0.037$) and 3 ($P = 0.049$) (Fig. 4B). These data show reduced memory retention in mice irradiated at 3 weeks of age.

Given our water maze results, we questioned if similar deficits could be detected using the Barnes maze. Mice from both groups learned to locate the hidden tunnel location ($P < 0.01$). During the hidden sessions, despite apparent trends toward impaired performance for irradiated animals, there was no group difference in the distance the mice moved to

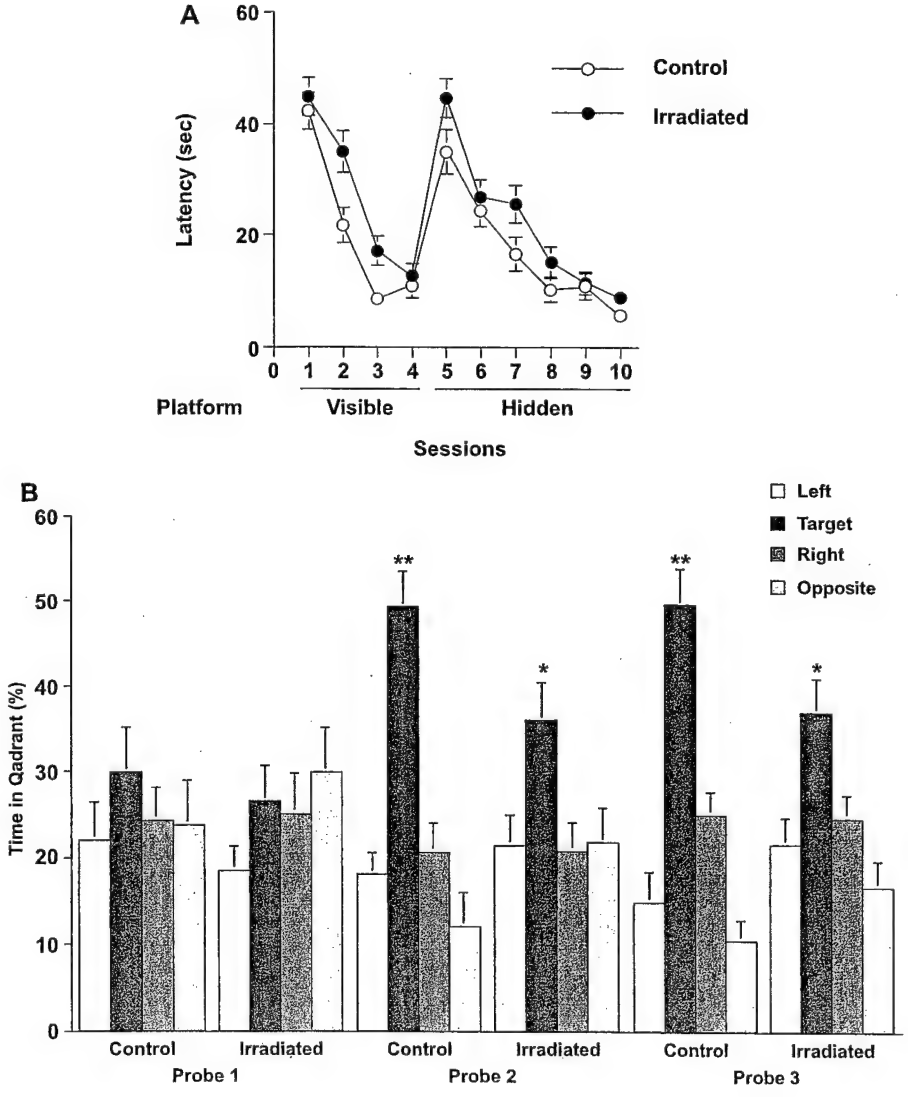

Fig. 4. Water maze performance showed significant group differences in the total and visible water maze learning curves (A) and in memory retention in the second and third probe trials (B). Mice were first trained to locate a visible platform (days 1 and 2) and then a submerged hidden platform (days 3–5). As there were no group differences in swim speeds during the visible trials, time to reach the platform location (Latency) was used to quantify performance (A). A 60-s probe trial (platform removed) was performed 1 h after the last hidden-platform session on days 3–5 (B). *$P < 0.05$ vs. any other quadrant; **$P < 0.01$ vs. any other quadrant. Each datum point or bar represents the mean value for irradiated ($n = 12$) and non-irradiated ($n = 12$) mice, and error bars are SEM.

locate the tunnel ($P = 0.24$) (Fig. 5A), the number of errors made ($P = 0.32$) (Fig. 5B), or in the percentage spatial or serial search strategies used. Probe trial results showed that all mice learned to locate the hidden escape tunnel using search strategies not involving olfaction or proximal cues.

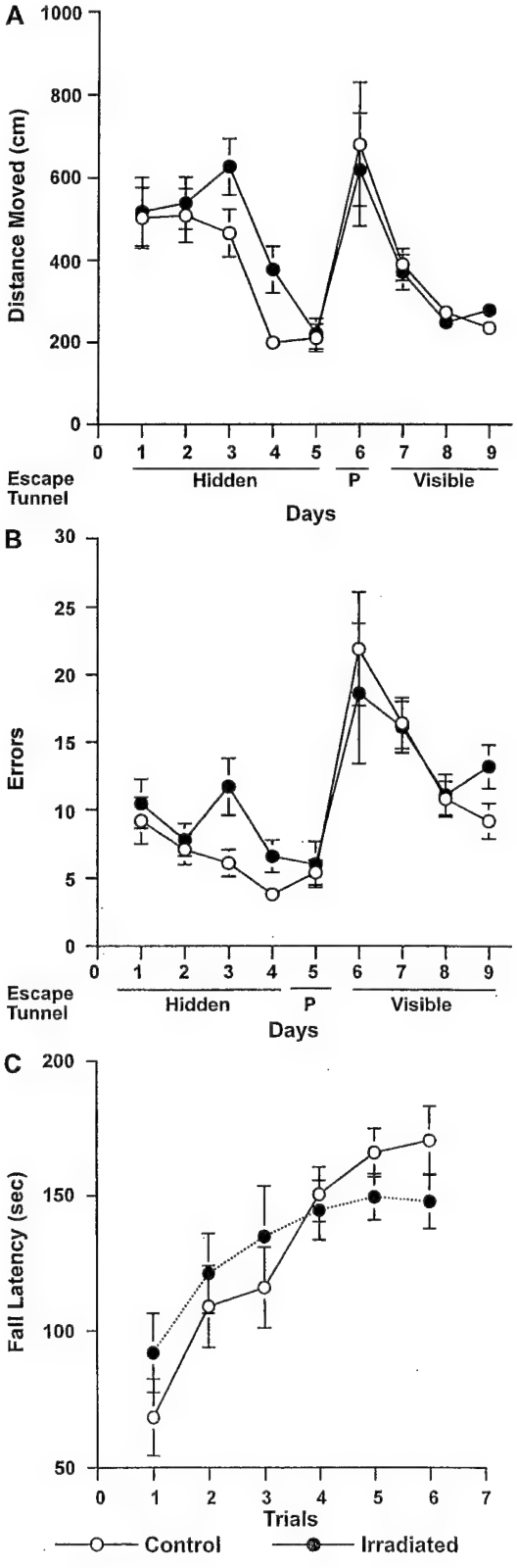

Table 2
Open field activity and elevated plus maze performance of irradiated and control mice

Open field	Zone/ Arms	Distance (cm)	Active time (s)	Rest time (s)	Entries (events)
Control	Periphery	3620 ± 101	406 ± 8	153 ± 7	29 ± 4
Irradiated		3966 ± 168	405 ± 11	146 ± 9	32 ± 5
Control	Center	543 ± 66	37 ± 4	4 ± 1	32 ± 5
Irradiated		605 ± 82	42 ± 6	7 ± 3	29 ± 4
Plus maze	**Zone/ Arms**	**Distance (cm)**	**Total time (s)**	**Rest time (s)**	**Entries (events)**
Control	Open	351 ± 39	50 ± 8	20 ± 5	7.8 ± 1.0
Irradiated		340 ± 47	58 ± 11	26 ± 8	7.9 ± 0.7
Control	Closed	2367 ± 106	522 ± 11	300 ± 13	23 ± 3
Irradiated		2272 ± 164	511 ± 10	284 ± 9	22 ± 2

Finally, both groups of mice were equally adept at learning to locate the visible escape tunnel, a function that is not hippocampal dependent.

Novel location and novel object recognition tests were used to evaluate hippocampus- and cortex-dependent non-spatial learning and memory (Malleret et al., 2001). In response to a change in location of a familiar object, both groups of mice spent more time exploring the object in the novel location; there was no significant difference between groups (controls: 47 ± 4%, irradiated: 44 ± 4%). Five minutes after the novel location trial, mice were tested for novel object recognition. All mice spent more time exploring novel objects than familiar objects, but there was no group difference (controls: 67 ± 5%, irradiated: 67 ± 3%).

Alterations in exploratory activity in a novel environment, anxiety levels, or sensorimotor function could conceivably influence performance in the water maze. However, our data (Table 2, Fig. 5C) indicated that there were no differences in exploratory activity, measures of anxiety or rotorod performance, which could have contributed to the differences in water maze performance. In the elevated plus maze, the mouse needs to turn around in the open arms to return to the closed arms. This turn is highly anxiogenic and might constitute a non-natural behavior for a mouse. Therefore, we also assessed anxiety levels in the elevated zero maze, which is a circular design and does not therefore require a change in direction. Consistent with the

Fig. 5. Behavioral testing of irradiated and non-irradiated mice shows comparable Barnes maze (A, B) and rotorod (C) performance. Endpoints shown include distance moved to find the escape tunnel (A), and number of errors made (B) in the Barnes maze. On days 1–5, mice were trained to locate a hidden escape tunnel, and on day 6, two probe trials were used with the tunnel placed under different holes. On days 7–10, mice were trained to locate a visible escape tunnel. While there were no significant group differences in the Barnes maze, there appeared to be a trend toward impaired performance in the irradiated mice. All mice significantly improved their rotorod performance with training (C) ($P < 0.01$), but there was no group difference ($P = 0.9$). Each datum point or bar represents the mean value for irradiated (n=12) and non-irradiated ($n = 12$) mice, and error bars are SEM.

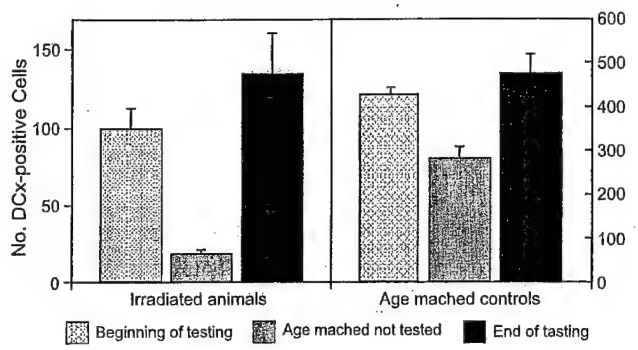

Fig. 6. Behavioral testing significantly ($P < 0.01$) increased numbers of immature neurons (DCx), apparently negating the age-dependent decline in cell number relative to age-matched animals. This effect was much more pronounced in irradiated animals. Each datum point represents the mean value of three to four mice; error bars are SEM.

elevated plus maze data, there were no group differences in times spent in the open areas of the zero maze (controls: 102 ± 14 s; irradiated: 82 ± 9 s). Finally, we tested whether irradiation had effects on emotional learning and memory using the passive avoidance test. While both groups showed emotional learning and memory, there were no group differences ($P = 0.18$; not shown).

After the behavioral testing was completed, we perfused the mice with formalin and analyzed numbers of proliferating SGZ cells and immature neurons in our standardized counting region. Given previous reports about beneficial effects of environmental enrichment (Kempermann et al., 1998a,b) and physical activity (van Praag et al., 1999) on hippocampal neurogenesis, we were interested if behavioral testing by itself might have any effects on the proliferating and/or immature neuron populations. There was no apparent change in number of proliferating (Ki67-positive) cells due to behavioral training/testing (not shown). However, behavioral testing resulted in significantly ($P < 0.01$) increased numbers of immature neurons (DCx), apparently negating the age-dependent decline in cell number (Fig. 6). Interestingly, this effect was much more pronounced in irradiated animals (Fig. 6).

Discussion

In the present study, we have shown that: (1) radiosensitive cells in the dentate SGZ of young mice include proliferating cells and immature neurons; (2) acute changes after irradiation qualitatively correlate with a persistent decrease in the production of new neurons; (3) after irradiation, a chronic inflammatory reaction occurs in conjunction with reduced neurogenesis; (4) reduced SGZ neurogenesis correlates in time with deficits in hippocampal-dependent memory retention; and (5) behavioral testing increases numbers of immature neurons relative to naive age-matched animals, an effect that is much more pronounced in irradiated animals.

The prevailing feeling among clinicians who treat patients with cranial irradiation is that radiation-induced changes, including cognitive impairments, are generally more severe in the developing or young brain (Peissner et al., 1999; Roman and Sperduto, 1995). The pathogenesis of cognitive dysfunction is not yet understood, although we (Mizumatsu et al., 2003; Monje et al., 2002; Tada et al., 2000), and others (Nagai et al., 2000; Peissner et al., 1999; Sasaki et al., 2000), have suggested that damage to the hippocampus may be involved. Previous studies from our laboratory (Mizumatsu et al., 2003; Monje et al., 2002; Parent et al., 1999; Tada et al., 2000) have addressed the radiation response of neural precursor cells in the adult rodent hippocampus and have shown that cells associated with neurogenesis are particularly sensitive. Interestingly, in the present study, we found that the acute (48 h) response of SGZ precursor cells in young mice was qualitatively similar to that observed in adults (Mizumatsu et al., 2003), showing clear dose–response relationships for both proliferating cells and immature neurons (Fig. 2). While the percentage decreases in proliferating cells and immature neurons after a given dose were roughly the same in young and adult mice (e.g., ~58% in DCx after 5 Gy in young mice vs. ~53% after 5 Gy in adults; Mizumatsu et al., 2003), the absolute numbers of cells lost were substantially different. For instance in controls, there were roughly twice as many proliferating cells and ~2.5 times more DCx cells in young mice than in adults. Thus, while the inherent radiation sensitivity of precursor cells appears to be independent of age, the impact of a given dose in terms of absolute cell numbers is more significant in the younger animals. Determining how such a significant loss of cell input into the dentate gyrus, as well as loss of cells committed to a neuronal lineage, affect neurogenesis and cognitive function was the objective of this study.

Our previous studies in adult mice showed that the dose–response relationships seen 48 h after irradiation qualitatively tracked the dose-response curve for neurogenesis determined 1 month later (Mizumatsu et al., 2003). Given that most radiation-induced brain injury, including cognitive impairment, evolve over time, we were interested in not only determining how the acute response related to later developing changes in neurogenesis in young mice, but also to determine if relatively early occurring effects on neurogenesis (i.e., 1 month post-treatment) were transient or if they persisted or became more severe. BrdU labeling revealed that relative to controls, irradiated mice had about 70% and 72% reductions in cell proliferation at 1 and 3 months post-irradiation, respectively. This indicated that little, if any, recovery was seen with respect to cell proliferation after treatment. In contrast, in adult mice, the same dose as used in the current study resulted in about a 40% reduction in BrdU labeling (Mizumatsu et al., 2003). Given that the mechanism(s) behind the acute (48 h) radiation response of the SGZ appear to be similar across age, the differences in BrdU labeling seen 1–3 months later suggest

that other factors besides inherent radiosensitivity impact the long-term survival of the precursor population.

While measurement of cell proliferation, either by BrdU incorporation or Ki-67 labeling, is a critical parameter of neurogenesis, it is not a suitable measure of new cell survival by itself, given that many newly born cells die shortly after they leave the cell cycle (Biebl et al., 2000). Using BrdU plus cell-specific markers allowed us to determine the survival and fate of the new cells. Furthermore, given that our measurements were made a month following the beginning of BrdU administration, we could be reasonably sure that our cell counts represented a valid estimate of long-term survival (Kempermann et al., 2003). Most of the surviving newly born cells in unirradiated animals differentiated into neurons and a single dose of 5 Gy significantly reduced those numbers (Table 1). This result is similar to what was seen in adult mice 1 month after treatment (Mizumatsu et al., 2003). While the percentage reductions were roughly the same, regardless of age, given the substantial difference in numbers of newly born cells (i.e., BrdU-positive) in younger animals, the net loss in NeuN-positive cells was higher in young than adult mice.

Recently it has been hypothesized that the function of adult neurogenesis is to enable the brain to accommodate novelty, and that new cell formation may represent a long-term adjustment of hippocampal circuitry to an experienced level of higher complexity (Kempermann, 2002). If true, neurogenesis would thus provide cells that could refine the way the hippocampus processes data, and this could explain why the learning ability does not deteriorate in older animals despite an age-related decrease in neurogenesis (Kempermann, 2002; Kuhn et al., 1996). Conversely, young animals that do not yet have the experience of older animals may need more neurogenesis to deal with an increasingly complex environment. Thus, a relatively modest decrease in the extent of neurogenesis, such as that induced by a low dose of X-rays may have a more profound effect in young animals than in older, more experienced animals. While this idea cannot be proved by our study, our data suggest that in young animals, the various elements associated with neurogenesis may in fact be more sensitive to irradiation than those seen in adults.

In contrast to the production of new neurons, gliogenesis in irradiated young mice was not reduced, and was, in fact, increased modestly, depending upon time after irradiation (Table 1). The significance of such changes is not yet clear, but our results suggest that within the SGZ, the production of new glia is somewhat more radioresistant than the production of new neurons, a finding also seen in adult rodents (Mizumatsu et al., 2003; Monje and Palmer, 2003). While differences in inherent radiosensitivity may play a role, it is also possible that radiation affects the mechanisms that are responsible for fate decisions in SGZ (Mizumatsu et al., 2003; Monje and Palmer, 2003; Monje et al., 2002). Furthermore, given that GFAP-expressing cells in the SGZ have been shown to have stem cell functions (Doetsch et al., 1999), it also may be that the increases in GFAP-expressing cells seen at 3 months reflect a regenerative response. On the other hand, the observed changes in GFAP-positive cells may be the initial steps in the well-described astrogliosis seen after X-irradiation (Calvo et al., 1988). Regarding oligodendrocytes, it is well known that myelination continues postnatally in mice (Rogister et al., 1999), but in the present study, the fraction of newly born oligodendrocytes in control mice was not different from that seen in unirradiated adults (Mizumatsu et al., 2003). Our data suggest that at least after the dose used here, irradiation did not adversely affect the production of new oligodendrocytes (Table 1), and this was confirmed qualitatively by Luxol fast blue histochemistry, which showed no radiation-induced changes in myelin patterns in or near the hippocampus.

While our data imply a common mechanism with respect to the acute (48 h) inherent radioreponsiveness of precursor cells as a function of age, the persistent impairment of neurogenesis after irradiation appears to reflect more than just acute cell loss. One possible explanation is that the more persistent changes result from radiation-dependent depletion or dysfunction of specific, neuronal lineage-restricted precursor cells. However, this seems unlikely based on the data from Monje et al. (2002) who recently showed that neuronal precursor cells from irradiated adult rats could grow and differentiate into neurons in vitro. It may be more likely that the longer term effects of radiation on neurogenesis depend upon an altered neurogenic environment (Luskin, 1998; Palmer et al., 2000; Song et al., 2002; Suhonen et al., 1996). In young mice, as in older animals (Mizumatsu et al., 2003; Monje et al., 2002), we found a robust inflammatory response 1 month after irradiation that persisted over the time frame examined (Table 1). Given recent findings that neuroinflammation inhibits hippocampal neurogenesis (Ekdahl et al., 2003; Monje et al., 2003), this observation may help explain our findings. It also opens a potential therapeutic avenue since Monje et al. (2003) have also shown that treatment with an anti-inflammatory agent may at least partially restore neurogenesis. What is not resolved, however, is the mechanism by which inflammation affects neurogenesis, the differential roles played by activated endogenous microglia and peripheral monocytes, and what molecules/pathways (e.g., MCP-1/CCR2) may be involved. It is of interest that in contrast to adults, in young mice, there was a significant population of proliferating and activated microglia in controls (Table 1). While the presence of such cells has been associated with myelination in young mice (Streit, 2001), if/how the presence of such cells affects subsequent radiation effects is unknown.

The functional role of hippocampal neurogenesis still remains undefined and studies exist showing an activity-dependent regulation of neurogenesis (Gould et al., 1999; Kempermann et al., 1997; Nilsson et al., 1999; van Praag et al., 1999). Conversely, there are studies showing that reduced neurogenesis from treatment with an antimitotic agent leads to impaired performance in a hippocampal-dependent conditioning task (Shors et al., 2001). These

observations raise questions regarding the functional consequences of radiation-related changes in neurogenesis described above. Because we were specifically addressing hippocampal function in the current study, we used an extensive battery of tests to assess both hippocampal-dependent spatial tasks (i.e., Morris water maze, Barnes maze) as well as hippocampal-dependent nonspatial tasks (i.e., novel location/novel object recognition). Additionally, because several non-hippocampal-dependent factors, for example, anxiety or sensorimotor function, can potentially affect performance in the maze tests, we also assessed those factors. Our behavioral studies showed no differences between control and irradiated mice in the non-hippocampal tests. However, performance in the probe trials in the water maze test was significantly impaired 3 months after irradiation, supporting the contention that hippocampal-dependent spatial memory retention was affected by irradiation. To our knowledge, this is the first time radiation-induced cognitive impairment has been seen in young mice after such a low dose and short time after irradiation. Interestingly, data from Alzheimer disease-related models (Raber et al., 1998, 2000a,b) showed that similar deficits in hippocampal-dependent spatial memory were an initial sign of a progressive cognitive decline. It may be that the cognitive impairments we saw here are only the very beginning of cognitive deficits that will progress and become far more significant; this remains to be proven.

Previous laboratory studies of radiation-induced cognitive dysfunction have largely been focused on two general populations of animals: fetal/neonates or adults. In most adult studies, cognitive deficits were generally detected after much higher doses and longer follow-up times (Akiyama et al., 2001; Hodges et al., 1998; Lamproglou et al., 1995), and in no case was the process of neurogenesis assessed. However, Madsen et al. (2003) recently reported cognitive deficits in adult rats at 3 weeks but not 7 weeks after a fractionated treatment of 40 Gy, and associated those changes with arrested proliferation in the dentate gyrus. Given that full maturation of newly born neurons may take many weeks or months (van Praag et al., 2002), there is uncertainty as to how the cognitive effects seen only 3 weeks after irradiation by Madsen et al. relate to altered neurogenesis, or if they represent some form of the transient 'early delayed reaction' reported by Sheline et al. (1980). Nevertheless, Madsen et al. (2003) provide valuable information supporting our contention that impaired neurogenesis might play a role in radiation-induced cognitive deficits.

In our study, mice were subjected to an extensive battery of cognitive tests; the amount of time each animal was exposed to training and testing averaged about 210 min. That, along with individual housing, which in male mice reduces stress, might be considered as an enriched environment (Rosenzweig and Bennett, 1996) when compared to regular laboratory conditions. Existing data show that enriched environment leads to an increase in hippocampal neurogenesis in adult rodents (Gould et al., 1999; Kempermann et al., 1997; Nilsson et al., 1999; van Praag et al., 1999), and we were interested in determining if cell proliferation and/or the number of immature neurons was affected by the behavioral training and testing. Our results clearly show that while no changes in proliferating cells were detected, numbers of immature neurons were significantly higher in cognitively trained and tested mice relative to age-matched non-tested naive animals. This effect apparently negated the age-related decline in number of immature neurons and was most prominent in the irradiated mice (Fig. 6). It is likely that these changes result from hippocampus-dependent, learning-enhanced survival of newly born cells (Gould et al., 1999) rather than strictly from physical activity which has been shown to affect proliferation of precursor cells (Rhodes et al., 2003). This conclusion is in agreement with previous studies done on elderly animals (Kempermann et al., 1998a,b). While there are no data if such enhanced survival of immature neurons leads to improved cognitive function, an appealing but not yet tested hypothesis is that environmental enrichment may have a possible therapeutic application in previously irradiated subjects. It remains to be determined if a longer term or more intensive enrichment paradigm might further enhance the effect observed here.

Our study shows a strong association, but not a proof of causality, with respect to altered neurogenesis and cognitive impairments after irradiation. But we also recognize that with the exception of the cerebellum, the entire brain was irradiated. An overall neuropathological examination of brain sections from irradiated animals immediately before and after testing using Luxol fast blue histochemistry did not reveal any obvious gross morphologic changes or alterations in white matter tracts in and around the hippocampus. However, we cannot definitively exclude other hippocampal/cortical areas as contributing to our observed behavioral changes. Furthermore, given recent reports in humans (Teunissen et al., 2003; Yaffe et al., 2003) and animal models (Heyser et al., 1997) relating cognitive decline to inflammation, our data showing a significant inflammatory response within the dentate gyrus at the time of cognitive testing, poses the possibility that cognitive deficits seen may result from inflammation-related impairments in hippocampal circuitry (Wilson et al., 2002). At this time, however, we cannot definitely distinguish if these cognitive deficits are related to decreased neurogenesis, inflammation or both. Studies of mutant mice deficient in specific inflammatory mediators should be useful in distinguishing the relative roles of these processes in the development of radiation-induced cognitive impairments. In summary, our results reinforce the contention that radiation-induced changes in the dentate SGZ may play a contributory if not causative role in the pathogenesis underlying cognitive impairments. Our present data and those from our studies in adult rodents (Mizumatsu et al., 2003; Monje et al., 2002; Tada et al., 2000) create a basis for further studies which may ultimately aid in the development

of strategies/approaches to ameliorate or treat radiation-induced cognitive impairments.

Acknowledgments

We want to thank Dr. Kathleen Lamborn, from the Brain Tumor Research Center, Department of Neurological Surgery, UCSF, for assisting in the statistical analyses of the immunohistochemistry data; Dr. Kenneth James, Oregon Health and Science University, for his help with the nonparametric statistical analysis of the Barnes maze strategies; and Anthony LeFevour for technical assistance. This work was supported by NIH grants R21 NS40088 (J.R.F.), RO1 CA76141 (J.R.F.), R01 AG20904 (J.R.), EMF grant AG-NS-0201 (J.R.), and DOD grant DAMD17-01-1-0820 (J.R.F.).

References

Abayomi, O.K., 1996. Pathogenesis of irradiation-induced cognitive dysfunction. Acta Oncol. 35, 659–663.

ACS, 2003. Cancer Facts and Figures. URL: http://www.cancer.org.

Akiyama, K., Tanaka, R., Sato, M., et al., 2001. Cognitive dysfunction and histological findings in adult rats one year after whole brain irradiation. Neurol. Med. Chir. (Tokyo) 41, 590–598.

Bach, M.E., Hawkins, R.D., Osman, M., et al., 1995. Impairment of spatial but not contextual memory in CaMKII mutant mice with a selective loss of hippocampal LTP in the range of the theta frequency. Cell 81, 905–915.

Bailey, C.C., Gnekow, A., Wellek, S., et al., 1995. Prospective randomised trial of chemotherapy given before radiotherapy in childhood medulloblastoma. International Society of Paediatric Oncology (SIOP) and the (German) Society of Paediatric Oncology (GPO): SIOP II. Med. Pediatr. Oncol. 25, 166–178.

Banisadr, G., Queraud-Lesaux, F., Boutterin, M.C., et al., 2002. Distribution, cellular localization and functional role of CCR2 chemokine receptors in adult rat brain. J. Neurochem. 81, 257–269.

Barnes, C.A., Jung, M.W., McNaughton, B.L., et al., 1994. LTP saturation and spatial learning disruption: effects of task variables and saturation levels. J. Neurosci. 14, 5793–5806.

Biebl, M., Cooper, C.M., Winkler, J., et al., 2000. Analysis of neurogenesis and programmed cell death reveals a self-renewing capacity in the adult rat brain. Neurosci. Lett. 291, 17–20.

Calvo, W., Hopewell, J.W., Reinhold, H.S., et al., 1988. Time- and dose-related changes in the white matter of the rat brain after single doses of X rays. Br. J. Radiol. 61, 1043–1052.

Cameron, H.A., Woolley, C.S., McEwen, B.S., et al., 1993. Differentiation of newly born neurons and glia in the dentate gyrus of the adult rat. Neuroscience 56, 337–344.

Christie, D., Leiper, A.D., Chessells, J.M., et al., 1995. Intellectual performance after presymptomatic cranial radiotherapy for leukaemia: effects of age and sex. Arch. Dis. Child. 73, 136–140.

Crossen, J.R., Garwood, D., Glatstein, E., et al., 1994. Neurobehavioral sequelae of cranial irradiation in adults: a review of radiation-induced encephalopathy. J. Clin. Oncol. 12, 627–642.

Czurko, A., Czeh, B., Seress, L., et al., 1997. Severe spatial navigation deficit in the Morris water maze after single high dose of neonatal x-ray irradiation in the rat. Proc. Natl. Acad. Sci. U. S. A. 94, 2766–2771.

Doetsch, F., Caille, I., Lim, D.A., et al., 1999. Subventricular zone astrocytes are neural stem cells in the adult mammalian brain. Cell 97, 703–716.

Duffner, P.K., Cohen, M.E., Thomas, P., 1983. Late effects of treatment on the intelligence of children with posterior fossa tumors. Cancer 51, 233–237.

Ekdahl, C.T., Claasen, J.H., Bonde, S., et al., 2003. Inflammation is detrimental for neurogenesis in adult brain. Proc. Natl. Acad. Sci. U. S. A. 100, 13632–13637.

Ellenberg, L., McComb, J.G., Siegel, S.E., 1987. Factors affecting intellectual outcome in pediatric brain tumor patients. Neurosurgery 21, 638–644.

Englund, U., Bjorklund, A., Wictorin, K., 2002. Migration patterns and phenotypic differentiation of long-term expanded human neural progenitor cells after transplantation into the adult rat brain. Brain Res. Dev. Brain Res. 134, 123–141.

Eriksson, P.S., Perfilieva, E., Bjork-Eriksson, T., et al., 1998. Neurogenesis in the adult human hippocampus. Nat. Med. 4, 1313–1317.

Fisher, B.J., Naumova, E., Leighton, C.C., et al., 2002. Ki-67: a prognostic factor for low-grade glioma? Int. J. Radiat. Oncol. Biol. Phys. 52, 996–1001.

Fletcher, J.M., Copeland, D.R., 1988. Neurobehavioral effects of central nervous system prophylactic treatment of cancer in children. J. Clin. Exp. Neuropsychol. 10, 495–537.

Gerard, C., Rollins, B.J., 2001. Chemokines and disease. Nat. Immunol. 2, 108–115.

Gould, E., Beylin, A., Tanapat, P., et al., 1999. Learning enhances adult neurogenesis in the hippocampal formation. Nat. Neurosci. 2, 260–265.

Grill, J., Renaux, V.K., Bulteau, C., et al., 1999. Long-term intellectual outcome in children with posterior fossa tumors according to radiation doses and volumes. Int. J. Radiat. Oncol. Biol. Phys. 45, 137–145.

Heyser, C.J., Masliah, E., Samimi, A., et al., 1997. Progressive decline in avoidance learning paralleled by inflammatory neurodegeneration in transgenic mice expressing interleukin 6 in the brain. Proc. Natl. Acad. Sci. U. S. A. 94, 1500–1505.

Hodges, H., Katzung, N., Sowinski, P., et al., 1998. Late behavioural and neuropathological effects of local brain irradiation in the rat. Behav. Brain. Res. 91, 99–114.

Jessberger, S., Kempermann, G., 2003. Adult-born hippocampal neurons mature into activity-dependent responsiveness. Eur. J. Neurosci. 18, 2707–2712.

Kee, N., Sivalingam, S., Boonstra, R., 2002. The utility of Ki-67 and BrdU as proliferative markers of adult neurogenesis. J. Neurosci. Methods 115, 97–105.

Kempermann, G., 2002. Why new neurons? Possible functions for adult hippocampal neurogenesis. J. Neurosci. 22, 635–638.

Kempermann, G., Kuhn, H.G., Gage, F.H., 1997. More hippocampal neurons in adult mice living in an enriched environment. Nature 386, 493–495.

Kempermann, G., Brandon, E.P., Gage, F.H., 1998a. Environmental stimulation of 129/SvJ mice causes increased cell proliferation and neurogenesis in the adult dentate gyrus. Curr. Biol. 8, 939–942.

Kempermann, G., Kuhn, H.G., Gage, F.H., 1998b. Experience-induced neurogenesis in the senescent dentate gyrus. J. Neurosci. 18, 3206–3212.

Kempermann, G., Gast, D., Kronenberg, G., et al., 2003. Early determination and long-term persistence of adult-generated new neurons in the hippocampus of mice. Development 130, 391–399.

Kuhn, H.G., Dickinson-Anson, H., Gage, F.H., 1996. Neurogenesis in the dentate gyrus of the adult rat: age-related decrease of neuronal progenitor proliferation. J. Neurosci. 16, 2027–2033.

Lamproglou, I., Chen, Q.M., Boisserie, G., et al., 1995. Radiation-induced cognitive dysfunction: an experimental model in the old rat. Int. J. Radiat. Oncol. Biol. Phys. 31, 65–70.

Lee, P.W., Hung, B.K., Woo, E.K., et al., 1989. Effects of radiation therapy on neuropsychological functioning in patients with nasopharyngeal carcinoma. J. Neurol. Neurosurg. Psychiatry 52, 488–492.

Luskin, M., 1998. Neuroblasts of the postnatal mammalian forebrain: their phenotype and fate. J. Neurobiol. 36, 221–233.

Macedoni-Luksić, M., Jereb, B., Todorovski, L., 2003. Long-term sequelae in children treated for brain tumors: impairments, disability, and handicap. Pediatr. Hematol. Oncol. 20, 89–101.

Madsen, T.M., Kristjansen, P.E., Bolwig, T.G., et al., 2003. Arrested neuronal proliferation and impaired hippocampal function following fractionated brain irradiation in the adult rat. Neuroscience 119, 635–642.

Malleret, G., Haditsch, U., Genoux, D., et al., 2001. Inducible and reversible enhancement of learning, memory, and long-term potentiation by genetic inhibition of calcineurin. Cell 104, 675–686.

Markakis, E.A., Gage, F.H., 1999. Adult-generated neurons in the dentate gyrus send axonal projections to field CA3 and are surrounded by synaptic vesicles. J. Comp. Neurol. 406, 449–460.

Meadows, A.T., Gordon, J., Massari, D.J., et al., 1981. Declines in IQ scores and cognitive dysfunctions in children with acute lymphocytic leukaemia treated with cranial irradiation. Lancet 2, 1015–1018.

Mickley, G.A., Ferguson, J.L., Mulvihill, M.A., et al., 1989. Progressive behavioral changes during the maturation of rats with early radiation-induced hypoplasia of fascia dentata granule cells. Neurotoxicol. Teratol. 11, 385–393.

Mizuguchi, M., Qin, J., Yamada, M., et al., 1999. High expression of doublecortin and KIAA0369 protein in fetal brain suggests their specific role in neuronal migration. Am. J. Pathol. 155, 1713–1721.

Mizumatsu, S., Monje, M.L., Morhardt, D.R., et al., 2003. Extreme sensitivity of adult neurogenesis to low doses of X-irradiation. Cancer Res. 63, 4021–4027.

Monje, M.L., Palmer, T., 2003. Radiation injury and neurogenesis. Curr. Opin. Neurol. 16, 129–134.

Monje, M.L., Mizumatsu, S., Fike, J.R., et al., 2002. Irradiation induces neural precursor-cell dysfunction. Nat. Med. 8, 955–962.

Monje, M.L., Toda, H., Palmer, T.D., 2003. Inflammatory blockade restores adult hippocampal neurogenesis. Science 302, 1760–1765.

Moreira, R.C.M., Moreira, M.V., Bueno, J.L.O., et al., 1997. Hippocampal lesions induced by ionizing radiation: a parametric study. J. Neurosci. Methods 75, 41–47.

Morris, R., 1984. Developments of a water-maze procedure for studying spatial learning in the rat. J. Neurosci. Methods 11, 47–60.

Nacher, J., Crespo, C., McEwen, B.S., 2001. Doublecortin expression in the adult rat telencephalon. Eur. J. Neurosci. 14, 629–644.

Nagai, R., Tsunoda, S., Hori, Y., et al., 2000. Selective vulnerability to radiation in the hippocampal dentate granule cells. Surg. Neurol. 53, 503–506 (discussion 506–507).

Nilsson, M., Perfilieva, E., Johansson, U., et al., 1999. Enriched environment increases neurogenesis in the adult rat dentate gyrus and improves spatial memory. J. Neurobiol. 39, 569–578.

Packer, R.J., Sutton, L.N., Elterman, R., et al., 1994. Outcome for children with medulloblastoma treated with radiation and cisplatin, CCNU, and vincristine chemotherapy. J. Neurosurg. 81, 690–698.

Palmer, T.D., Willhoite, A.R., Gage, F.H., 2000. Vascular niche for adult hippocampal neurogenesis. J. Comp. Neurol. 425, 479–494.

Parent, J.M., Tada, E., Fike, J.R., et al., 1999. Inhibition of dentate granule cell neurogenesis with brain irradiation does not prevent seizure-induced mossy fiber synaptic reorganization in the rat. J. Neurosci. 19, 4508–4519.

Peissner, W., Kocher, M., Treuer, H., et al., 1999. Ionizing radiation-induced apoptosis of proliferating stem cells in the dentate gyrus of the adult rat hippocampus. Brain Res. Mol. Brain Res. 71, 61–68.

Raber, J., Wong, D., Buttini, M., et al., 1998. Isoform-specific effects of human apolipoprotein E on brain function revealed in ApoE knockout mice: increased susceptibility of females. Proc. Natl. Acad. Sci. U. S. A. 95, 10914–10919.

Raber, J., Akana, S.F., Bhatnagar, S., et al., 2000a. Hypothalamic–pituitary–adrenal dysfunction in Apoe(−/−) mice: possible role in behavioral and metabolic alterations. J. Neurosci. 20, 2064–2071.

Raber, J., Wong, D., Yu, G.Q., et al., 2000b. Apolipoprotein E and cognitive performance. Nature 404, 352–354.

Raber, J., Bongers, G., LeFevour, A., et al., 2002. Androgens protect against apolipoprotein E4-induced cognitive deficits. J. Neurosci. 22, 5204–5209.

Rhodes, J.S., van Praag, H., Jeffrey, S., 2003. Exercise increases hippocampal neurogenesis to high levels but does not improve spatial learning in mice bred for increased voluntary wheel running. Behav. Neurosci. 117, 1006–1016.

Riva, D., Bova, S.M., Bruzzone, M.G., 2000. Neuropsychological testing may predict early progression of asymptomatic adrenoleukodystrophy. Neurology 54, 1651–1655.

Rogister, B., Ben-Hur, T., Dubois-Dalcq, M., 1999. From neural stem cells to myelinating oligodendrocytes. Mol. Cell. Neurosci. 14, 287–300.

Roman, D.D., Sperduto, P.W., 1995. Neuropsychological effects of cranial radiation: current knowledge and future directions. Int. J. Radiat. Oncol. Biol. Phys. 31, 983–998.

Rosenzweig, M.R., Bennett, E.L., 1996. Psychobiology of plasticity: effects of training and experience on brain and behavior. Behav. Brain Res. 78, 57–65.

Rousseau, P., Habrand, J.L., Sarrazin, D., et al., 1994. Treatment of intracranial ependymomas of children: review of a 15-year experience. Int. J. Radiat. Oncol. Biol. Phys. 28, 381–386.

Sasaki, R., Matsumoto, A., Itoh, K., et al., 2000. Target cells of apoptosis in the adult murine dentate gyrus and O4 immunoreactivity after ionizing radiation. Neurosci. Lett. 279, 57–60.

Sheline, G.E., Wara, W.M., Smith, V., 1980. Therapeutic irradiation and brain injury. Int. J. Radiat. Oncol. Biol. Phys. 6, 1215–1228.

Shinohara, C., Gobbel, G.T., Lamborn, K.R., et al., 1997. Apoptosis in the subependyma of young adult rats after single and fractionated doses of X-rays. Cancer Res. 57, 2694–2702.

Shors, T.J., Miesegaes, G., Beylin, A., et al., 2001. Neurogenesis in the adult is involved in the formation of trace memories. Nature 410, 372–376.

Sienkiewicz, Z.J., Saunders, R.D., Butland, B.K., 1992. Prenatal irradiation and spatial memory in mice: investigation of critical period. Int. J. Radiat. Biol. 62, 211–219.

Sienkiewicz, Z.J., Haylock, R.G., Saunders, R.D., 1994. Prenatal irradiation and spatial memory in mice: investigation of dose–response relationship. Int. J. Radiat. Biol. 65, 611–618.

Sienkiewicz, Z.J., Haylock, R.G., Saunders, R.D., 1999. Differential learning impairments produced by prenatal exposure to ionizing radiation in mice. Int. J. Radiat. Biol. 75, 121–127.

Slotnick, B.M., Leonard, C.M., 1975. A Stereotaxic Atlas of the Albino Mouse Forebrain. U.S. Dept. of Health Education and Welfare Public Health Service Alcohol Drug Abuse and Mental Health Administration., Rockville, MD.

Snyder, J.S., Kee, N., Wojtowicz, J.M., 2001. Effects of adult neurogenesis on synaptic plasticity in the rat dentate gyrus. J. Neurophysiol. 85, 2423–2431.

Song, H., Stevens, C.F., Gage, F.H., 2002. Astroglia induce neurogenesis from adult neural stem cells. Nature 417, 39–44.

Stanfield, B.B., Trice, J.E., 1988. Evidence that granule cells generated in the dentate gyrus of adult rats extend axonal projections. Exp. Brain Res. 73, 399–406.

Streit, W.J., 2001. Microglia and macrophages in the developing CNS. Neurotoxicology 22, 619–624.

Suhonen, J.O., Peterson, D.A., Ray, J., et al., 1996. Differentiation of adult hippocampus-derived progenitors into olfactory neurons in vivo. Nature 383, 624–627.

Surma-aho, O., Niemela, M., Vilkki, J., et al., 2001. Adverse long-term effects of brain radiotherapy in adult low-grade glioma patients. Neurology 56, 1285–1290.

Tada, E., Yang, C., Gobbel, G.T., et al., 1999. Long-term impairment of subependymal repopulation following damage by ionizing irradiation. Exp. Neurol. 160, 66–77.

Tada, E., Parent, J.M., Lowenstein, D.H., et al., 2000. X-irradiation causes a prolonged reduction in cell proliferation in the dentate gyrus of adult rats. Neuroscience 99, 33–41.

Teunissen, C.E., van Boxtel, M.P., Bosma, H., et al., 2003. Inflammation markers in relation to cognition in a healthy aging population. J. Neuroimmunol. 134, 142–150.

van Praag, H., Christie, B.R., Sejnowski, T.J., 1999. Running enhances neurogenesis, learning, and long-term potentiation in mice. Proc. Natl. Acad. Sci. U. S. A. 96, 13427–13431.

van Praag, H., Schinder, A.F., Christie, B.R., et al., 2002. Functional neurogenesis in the adult hippocampus. Nature 415, 1030–1034.

Wilson, C.J., Finch, C.E., Cohen, H.J., et al., 2002. Cytokines and cognition—the case for a head-to-toe inflammatory paradigm. J. Am. Geriatr. Soc. 50, 2041–2056.

Yaffe, K., Lindquist, K., Penninx, B.W., et al., 2003. Inflammatory markers and cognition in well-functioning African-American and white elders. Neurology 61, 76–80.

Yager, J.Y., Thornhill, J.A., 1997. The effect of age on susceptibility to hypoxic–ischemic brain damage. Neurosci. Biobehav. Rev. 21, 167–174.

RADIATION RESEARCH 162, 39–47 (2004)
0033-7587/04 $15.00

Radiation-Induced Cognitive Impairments are Associated with Changes in Indicators of Hippocampal Neurogenesis

Jacob Raber,[a,b,c] Radoslaw Rola,[d] Anthony LeFevour,[a] Duncan Morhardt,[d] Justine Curley,[a] Shinichiro Mizumatsu,[d] Scott R. VandenBerg[d,f] and John R. Fike[d,e,1]

Departments of [a] Behavioral Neuroscience and [b] Neurology, [c] Division of Neuroscience, ONPRC, Oregon Health & Science University, Portland, Oregon, 97239; and [d] Brain Tumor Research Center, Department of Neurological Surgery, and Departments of [e] Radiation Oncology and [f] Pathology, University of California, San Francisco, California 94143

Raber, J., Rola, R., LeFevour, A., Morhardt, D., Curley, J., Mizumatsu, S., VandenBerg, S. R. and Fike, J. R. Radiation-Induced Cognitive Impairments are Associated with Changes in Indicators of Hippocampal Neurogenesis. *Radiat. Res.* 162, 39–47 (2004).

During treatment of brain tumors, some head and neck tumors, and other diseases, like arteriovenous malformations, the normal brain is exposed to ionizing radiation. While high radiation doses can cause severe tissue destruction, lower doses can induce cognitive impairments without signs of overt tissue damage. The underlying pathogenesis of these impairments is not well understood but may involve the neural precursor cells in the dentate gyrus of the hippocampus. To assess the effects of radiation on cognitive function, 2-month-old mice received either sham treatment (controls) or localized X irradiation (10 Gy) to the hippocampus/cortex and were tested behaviorally 3 months later. Compared to controls, X-irradiated mice showed hippocampal-dependent spatial learning and memory impairments in the Barnes maze but not the Morris water maze. No nonspatial learning and memory impairments were detected. The cognitive impairments were associated with reductions in proliferating Ki-67-positive cells and Doublecortin-positive immature neurons in the subgranular zone (SGZ) of the dentate gyrus. This study shows significant cognitive impairments after a modest dose of radiation and demonstrates that the Barnes maze is particularly sensitive for the detection of radiation-induced cognitive deficits in young adult mice. The significant loss of proliferating SGZ cells and their progeny suggests a contributory role of reduced neurogenesis in the pathogenesis of radiation-induced cognitive impairments. © 2004 by Radiation Research Society

INTRODUCTION

The brain is exposed to ionizing radiation in a number of clinical situations, and although radiotherapy can be very effective, the dose that can be administered safely is limited by the potential injury to normal brain tissues. While changes involving macroscopic tissue destruction generally occur after high doses of radiation (*1*), less severe morphological injury can occur after relatively low doses, resulting in variable degrees of cognitive dysfunction in both pediatric and adult patients (*2–9*). This cognitive dysfunction often manifests as deficits in hippocampal-dependent learning and memory, including spatial information processing (*2, 8–11*), and it has been suggested that the severity of cognitive impairments depends upon the dose delivered to the medial temporal lobes (*2*), the site of the hippocampus.

In the mammalian forebrain, the hippocampus is one of two sites of active neurogenesis (*12*). In humans and animals, active cell proliferation occurs in the subgranular zone (SGZ) of the hippocampal dentate gyrus (*13–16*), and the newly born cells migrate into the dentate granule cell layer (GCL) (*17*), develop granule cell morphology and neuronal markers (*14*), and connect with CA3, their normal target area (*18, 19*). Ultimately, the newly born neurons become functionally integrated into the dentate gyrus and have passive membrane properties, action potentials and functional synaptic inputs (*20*). While there still is uncertainty as to the functionality of these newly born neurons, it has been shown that long-term potentiation (LTP) at the level of field potentials, a proposed electrophysiological measure of learning and memory, is increased in mice with enhanced neurogenesis (*21*). Furthermore, the toxin methylazoxymethanol acetate, which reduces the number of newly born neurons in the hippocampus, impairs learning (*22*). Since cells involved in neurogenesis are extremely sensitive to low and moderate doses of ionizing radiation (*23–28*), reduced production of new neurons in the dentate gyrus might play a role in radiation-induced cognitive impairments.

Studies involving hippocampal lesioning have confirmed that in mice, as in rats, the hippocampus is involved in performance during specific cognitive tasks (*29*). For instance, ibotenic acid lesions in the mouse hippocampus result in profound spatial learning impairments in the Morris water maze (*29–31*). Furthermore, mice with cytotoxic le-

[1] Address for correspondence: Brain Tumor Research Center, Box 0520, University of California, San Francisco, San Francisco, CA 94143-0520; e-mail: jfike@itsa.ucsf.edu.

sions of the hippocampus show impaired learning in locating an escape tunnel in a paddling pool (*32*), which has combined elements of the Morris water maze and the Barnes maze (*33*). Importantly, it has been shown that when damage is localized to the hippocampal formation, the induced deficits are significant only in the spatial version of the Morris water maze; there are no deficits in the visible version (*31*). However, when lesions are variable in size, extending beyond the hippocampal formation into the entorinal cortex, amygdala and thalamus, impairments are then detected in the visible version of the Morris water maze (*30*). Based on these data, the Morris water maze and Barnes maze tests can be used effectively to assess radiation effects on cognition, particularly functions associated with the hippocampus in mice.

In the present study, we assessed the effects of a single, moderate dose (10 Gy) of X rays on cognitive function in mice and on specific cellular markers associated with neurogenesis (*25*). Our data demonstrate that irradiated mice show cognitive impairments related to the hippocampus and that those impairments are associated with reductions in proliferating neural precursor cells and their progeny, immature neurons.

METHODS

Animals

Twenty-eight young adult (2-month-old) male C57BL/6J mice were purchased from The Jackson Laboratory (Bar Harbor, ME) and housed and cared for in accordance with the United States Department of Health and Human Services Guide for the Care and Use of Laboratory Animals; all protocols were approved by institutional animal welfare committees. Mice were maintained in a temperature and light-controlled environment with a 12/12-h light/dark cycle and provided food (PicoLab Rodent Diet 20, #5053, PMI Nutrition International, St. Louis, MO) and water *ad libitum*. To minimize the effects of social influences on behavior, mice were housed singly starting 1 week before behavioral training and continuing for the entire 6 weeks of testing.

Irradiation

For irradiation and perfusion procedures, mice were anesthetized with a mixture of ketamine (60 mg/kg) and medetomidine (0.25 mg/kg) injected intraperitoneally; sham-irradiated mice (controls) were only anesthetized. A single dose of 10 Gy was given to 16 mice; the other 12 mice acted as controls. Irradiation was performed using a Philips orthovoltage X-ray system as described previously (*25*). Treatment was restricted to the bilateral hippocampus/cortex using lead shielding over the body, neck, cerebellum, eyes and nose. The corrected dose rate was approximately 1.75 Gy/min at a source-to-skin distance of 21 cm.

Cognitive Testing

An extensive battery of behavioral tests was performed to assess hippocampal-dependent and hippocampal-independent tasks. The sequence of behavioral testing was such that tests were administered in the order of increasing stress level (*34*). The order of testing was open field, elevated plus maze, novel object recognition, rotorod, Morris water maze, Barnes maze, and passive avoidance. After training/testing of open-field activity, elevated plus maze, novel object recognition, rotorod, Barnes maze, and passive avoidance, all equipment was cleaned with 1 m*M* acetic acid to remove residual odors that could affect testing performance. During testing, the experimenter was blinded to the treatment given to the mice.

Open field. Different levels of anxiety can affect motivation and performance in learning and memory tests. Therefore, we assessed measures of anxiety using two tests, the open field (*34*) and the elevated plus maze (below). For the open field, mice were placed singly in brightly lit, automated infrared photocell activity arenas (40.64 × 40.64 cm with 16 × 16 photocells for measuring horizontal movements, 8 photocells for measuring rearing) that interfaced with a computer (Hamilton-Kinder, Poway, CA). The open field was divided into a center zone (20.32 × 20.32 cm) and a peripheral zone. Increases in time spent in the center zone are thought to reflect decreased measures of anxiety (*35*). The following parameters were calculated for both zones: active times (defined as time, within 1 s, in which a new light beam was broken), distance moved, rearing events, corner entries, center entries, and percentage of time spent in the center zone. Ten minutes of open-field activity was recorded after a 1-min adaptation period.

Elevated plus maze. We previously described the specifics of the elevated plus maze (*36*), which was used to assess anxiety. The elevated, plus-shaped maze consisted of two open arms and two closed arms equipped with rows of infrared photocells interfaced with a computer (Hamilton-Kinder, Poway, CA). Increases in time spent in, and entries into, the open arms are thought to reflect decreased anxiety (*35*). Mice were placed individually in the center of the maze and allowed free access for 10 min. They were able to spend time either in a closed, safe area (closed arms), in an open area (open arms), or in the middle, intermediate zone. Recorded beam breaks were used to calculate the time spent and the distance moved in the open and closed arms and the number of times the mice reached over the edges of the open arms.

Novel location and novel object recognition. Novel location and novel object recognition were used to evaluate hippocampus- and cortex-dependent nonspatial learning and memory (*37*). On 3 consecutive days, mice were habituated to an open field for 5 min. On the fourth day, the mice were trained in three consecutive trials and then tested in two consecutive trials with a 5-min intertrial interval. For the training and testing sessions, three different plastic toys were placed in the open field, and each animal was allowed to explore for 10 min. All objects were used only once, and replicas of the objects were used in subsequent trials to eliminate potential confounds of residual odors when the objects were cleaned after a trial, or potential scratching marks on particular objects. In the first test trial, one of the familiar objects was moved to a novel location. In the second test trial, one of the familiar objects was replaced by a novel object. For all trials, the experimenter recorded the time spent exploring each object and calculated the percentage of time spent exploring each object.

Rotorod. Rotorod balancing requires a variety of proprioceptive, vestibular and fine-tuned motor abilities. The task requires the mouse to balance on a rotating rod and is used to screen for motor deficits that might influence performance in other learning and memory tests (*38*). The rod has a diameter of 7 cm and is placed 64 cm high (Hamilton-Kinder, Poway, CA). After a 1-min adaptation period on the rod at rest, the rod was accelerated by 5 rpm over 3 s every 15 s, and the length of time the mice remained on the rod (fall latency) was recorded. The mice had three consecutive trials on the first day of training and one trial per day on each of 2 subsequent days.

Water maze learning. The standard Morris water maze (*39*) is commonly used to assess the acquisition and retention of spatial memory. The water maze test assesses the ability of a mouse to locate a hidden submerged platform in a pool (diameter 122 cm) filled with warm (24°C) opaque water. To find the platform, mice have to relate their position in the pool to constant extramaze cues and then quickly store, retrieve and use that information to determine where the platform is located. Mice were first trained to locate a visible platform (days 1 and 2) and then a submerged hidden platform (days 3–5) in two daily sessions 3.5 h apart; each session consisted of three 60-s trials (at 10-min intervals). Mice that failed to find the hidden platform within 60 s were manually placed on

it for 15 s. For data analysis, the pool was divided into four quadrants. During the visible platform training, the platform was moved to a different quadrant for each session. During the hidden platform training, the platform location was kept constant for each mouse (in the center of the target quadrant). The starting point at which the mouse was placed into the water was changed for each trial. Time to reach the platform (latency), path length, and swim speed were recorded with the Noldus Ethovision video tracking system (Wageningen, The Netherlands) set to analyze two samples per second. A 60-s probe trial (platform removed) was performed 1 h after the last hidden-platform session.

Barnes maze. The Barnes maze for mice has been described in detail (*33, 40*); it is a challenging measure of the acquisition and retention of spatial memory. The maze is 122 cm in diameter and is elevated 80 cm above the floor; 40 holes, 5 cm in diameter, are located 2.5 cm from the perimeter, and a metal escape tunnel (10 × 6 × 43 cm in size) is placed under one of the holes (*40*). At the beginning of a trial, each mouse was placed in a white cylinder (10 cm high, 12 cm diameter) for 10 s and a white noise generator (108 dB) and a bright fluorescent light (2100 lumens) were activated to motivate escape behavior. Each trial ended when the mouse entered the escape tunnel or after 5 min. The Barnes maze test consisted of three types of test: (a) a spatial hippocampal-dependent version (days 1–5); (b) a random version to determine if nonspatial cues were used for escape (day 6); and (c) a cued version where the escape tunnel was visible (days 7–10). Mice were first trained to locate a hidden escape tunnel (spatial version), which was always located underneath the same hole; the position of the escape tunnel was determined randomly for each mouse. The mice were trained in two daily sessions with two trials/session (intersession interval 3.5 h). Subsequently, to determine if mice used nonspatial (e.g. olfaction) rather than spatial cues to locate the tunnel, two probe trials (intertrial interval 30 min) were used where the tunnel was relocated under different holes by moving it 180° (first trial) or 270° (second trial) from its original position. Finally, in the visible sessions, a colored tube was placed directly behind the hole containing the escape tunnel. The position of the escape tunnel in the visible sessions varied from session to session. The mice were trained in two daily sessions (intersession interval 3.5 h) with one trial per session on day 7 and two trials per session on days 8–10. For all trials, path length and average speed of movement were recorded with a Noldus EthoVision video tracking system set to analyze two samples per second. The following parameters were analyzed by reviewing the video: (a) errors, defined as searches of any hole not containing the escape tunnel; (b) distance from the escape tunnel, defined as the number of holes between the first hole explored in a trial and the hole containing the escape tunnel; and (c) search strategies. Three search strategies were distinguished. Serial strategy was systematic consecutive hole searching in a clockwise or counterclockwise manner. Spatial strategy was finding the escape tunnel with errors and number of holes between the first hole explored in a trial and the hole containing the escape tunnel smaller than or equal to 3. The random search strategy was defined as exploring holes in an unsystematic fashion with many center maze crossings.

Passive avoidance learning. To evaluate emotional learning and memory, passive avoidance learning was used with a step-through box consisting of a brightly lit compartment and a dark compartment connected by a sliding door (Hamilton-Kinder, Poway, CA). Each mouse was placed in the lighted compartment, and when it entered the dark compartment, the sliding door was closed, and the mouse received a slight foot shock (0.3 mA, 1 s). Twenty-four hours later, the mice were again placed into the lighted compartment, and the time to enter the dark compartment (latency) was recorded up to 300 s.

Immunohistochemistry

Mice were anesthetized as described above and perfused with a 10% buffered formalin solution. Brain tissue was processed for paraffin embedding as reported previously (*23, 25*). Representative sections from each animal were stained using luxol fast blue to qualitatively assess myelin integrity in white matter tracts in and around the hippocampus. Proliferating cells were labeled with an antibody against Ki-67, a nuclear antigen that is expressed during all proliferative stages of the cell cycle except G_0 (*41*). Immature neurons were detected using an antibody against Doublecortin (Dcx), a protein expressed by migrating neuroblasts (*42*). All immunostaining and morphometric analyses were done as described previously (*25*).

Statistical Analysis

Most data were expressed as means ± SEM. Behavioral and immunohistochemical data were evaluated by multi-measure ANOVA, followed by Tukey-Kramer posthoc tests when appropriate, as described (*34, 36*). *F* values, measures of the probability that the compared experimental groups are different, were included. To compare the distribution of search strategies in the Barnes maze, the Wilcoxon-Mann-Whitney test was used. For all analyses, the null hypothesis was rejected at the 0.05 level.

RESULTS

Radiation treatment was well tolerated and did not cause any detectable physical (e.g. lightning of the hair) or neurological changes. Three months after irradiation, tissues from irradiated ($n = 4$) and control ($n = 4$) mice were collected and assessed for numbers of proliferating cells and immature neurons in the SGZ, as described previously (*25*). The remaining animals from each treatment group underwent behavioral testing. After behavioral testing, proliferating cells and immature neurons were quantified in tissues from representative animals.

Cell proliferation and numbers of immature neurons were decreased by about 90% relative to controls 3 months after irradiation (Fig. 1). At that time we also initiated behavioral testing to determine whether reductions in the indicators of neurogenesis were associated with cognitive impairments. We first looked for radiation-induced alterations in exploratory activity in a novel environment, anxiety levels, or sensorimotor function, measures that could conceivably influence performance in later tests of hippocampal-dependent learning and memory. Data from these tests (Table 1, Fig. 2) indicated that there were no radiation-induced alterations in these measures that could contribute to potential differences in tests of hippocampal-dependent learning and memory.

Next we used the novel location and novel object recognition test to assess hippocampus- and cortex-dependent learning and memory. In response to a change in location of a familiar object, both groups of mice spent more time exploring the object in the novel location (control, 47 ± 4%; irradiated, 44 ± 4%). Five minutes after the novel location trial, mice were tested for novel object recognition. All mice spent more time exploring the novel object than the familiar objects, but there was no difference between groups (control, 67 ± 5%; irradiated 67 ± 3%).

To determine whether the observed cellular changes (Fig. 1) were associated with alterations in hippocampal-dependent spatial memory, we used the Morris water maze and the Barnes maze. In the Morris water maze, mice were first trained to locate a visible platform and then a hidden platform. The hidden platform was then removed (probe trial)

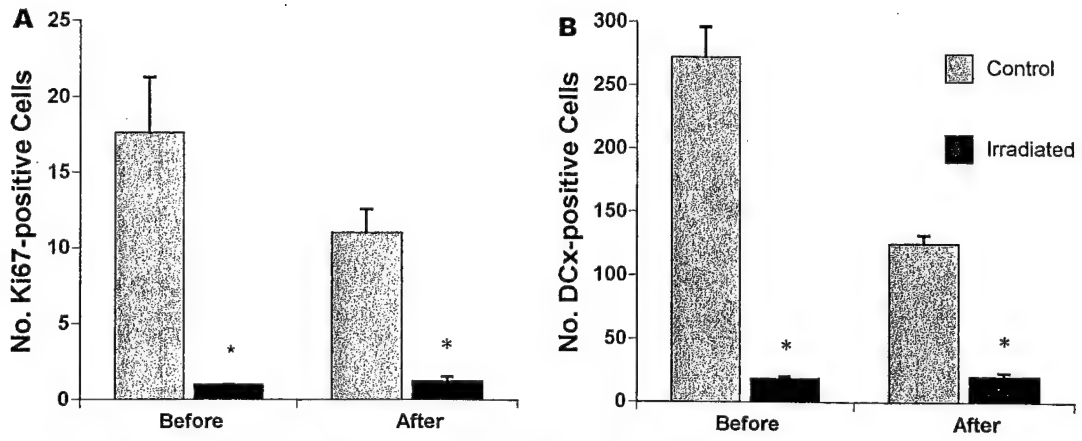

FIG. 1. Changes in numbers of proliferating cells (Ki-67, panel A) and immature neurons (Dcx, panel B) in the dentate gyrus after 10 Gy of X rays. Measurements were obtained from tissues collected just before the onset of cognitive testing, i.e. 3 months after irradiation, or from tissues collected immediately after the completion of cognitive testing, i.e. 4 months after irradiation. Before and after testing, radiation reduced proliferation and production of immature neurons in the dentate gyrus (*$P < 0.001$). Each bar represents an average of three to five mice; error bars are SEM.

to measure retention of spatial memory. The performance of irradiated and control mice during the visible (days 1–4) and hidden (days 5–10) sessions was compared. All mice significantly improved their performance during the visible and hidden platform sessions (effect of session, $P < 0.01$). There was no group difference during the visible platform sessions [$F(1,18) = 1.183$, $P = 0.2910$]. While there appeared to be a subtle difference between the treatment groups in performance during the hidden platform sessions, it did not reach statistical significance [$F(1,18) = 1.032$, $P = 0.3231$, Fig. 3A]. All mice swam continuously at similar speeds and in similar patterns (not shown), and there were no significant periods of passive floating. In the probe trial, both groups showed comparable memory retention and spent significantly more time in the target quadrant than in any other quadrant [effect of quadrant, $F(3,21) = 31.943$, $P < 0.001$] (Fig. 3B), but there was no difference between groups in time spent in the target quadrant [$F(1,18) = 1.464$, $P = 0.2420$].

Given our water maze results, we questioned whether we could detect significant effects of radiation on performance in the Barnes maze. While mice from both treatment groups learned to locate the hidden tunnel (effect of day, $P < 0.01$), they did so at different rates (Fig. 4A, B). In locating the escape tunnel, irradiated mice traveled greater distances [$F(1,18) = 4.645$, $P = 0.0449$] (Fig. 4A) and made significantly more errors than controls [$F(1,18) = 4.712$, $P = 0.0436$] (Fig. 4B). Furthermore, during training, irradiated mice used more random (Fig. 4C) and fewer spatial (Fig. 4D) search strategies than controls. During the hidden escape tunnel trials, the distribution of spatial and random search strategies was significantly different between the treatment groups ($P = 0.0001$). There were no differences between groups in the use of serial strategies (not shown).

TABLE 1
Open-Field Activity and Elevated Plus Maze Performance of Irradiated and Control Mice

	Zone/arms	Distance (cm)	Time (s)	Rest time (s)	Entries (events)
Open field					
Control	Periphery	3674 ± 150	544 ± 8	147 ± 8	32.9 ± 3.9
Irradiated		3754 ± 132	549 ± 5	149 ± 5	31.6 ± 3.0
Control	Center	667 ± 84	56 ± 8	7 ± 1	32.4 ± 4.0
Irradiated		601 ± 57	51 ± 5	8 ± 1	31.0 ± 3.1
Plus maze					
Control	Open	437 ± 77	58 ± 12	19 ± 5	13.0 ± 3.3
Irradiated		613 ± 79	76 ± 8	22 ± 3	17.2 ± 2.0
Control	Closed	3352 ± 114	509 ± 16	192 ± 12	35.0 ± 2.7
Irradiated		3194 ± 133	491 ± 10	192 ± 11	37.6 ± 1.4

Notes. In open field and the plus maze, there were no differences between treatment groups in any of the end points measured. While plus-maze values appeared to be different, statistical analyses showed that there were no significant differences in distance moved [$F(1,18) = 2.286$, $P = 0.1479$], time spent in the open or closed arms [$F(1,18) = 1.619$, $P = 0.2195$], or entries into arms [$F(1,18) = 1.335$, $P = 0.2630$].

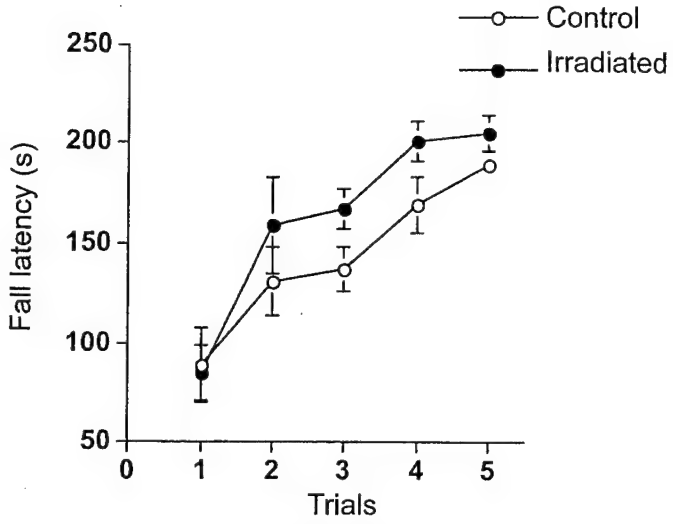

FIG. 2. Testing of sensorimotor function using the rotorod. All mice significantly improved their performance with training ($P < 0.01$), but there was no difference between group [$F(1,18) = 2.794$, $P = 0.1119$]. Each data point represents the mean value ± SEM per trial for irradiated ($n = 12$) and nonirradiated ($n = 8$) mice.

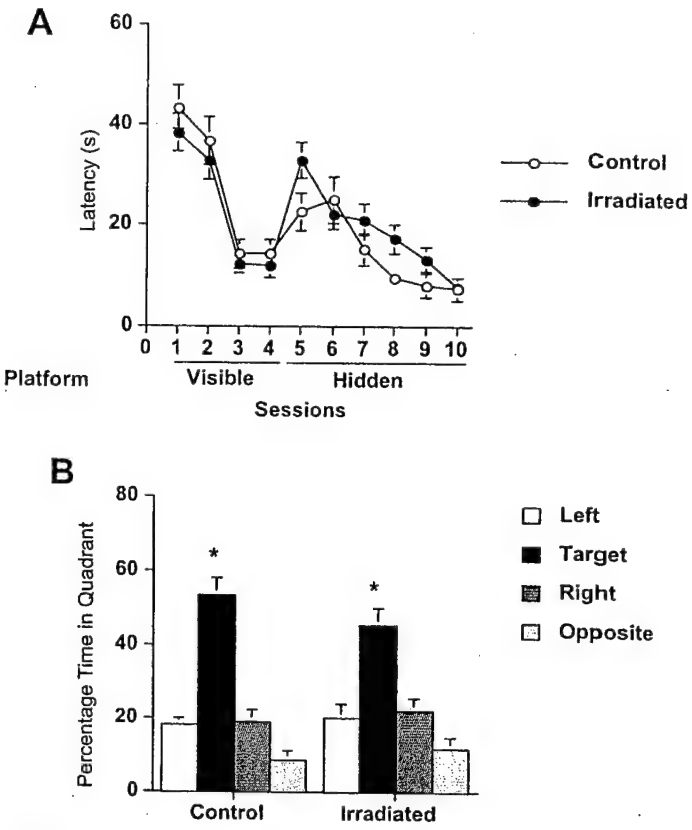

FIG. 3. Cognitive testing of irradiated and nonirradiated mice shows no differences between groups in the Morris water maze. There were no differences in the times to locate either the visible or hidden platform (latency) (panel A) or in the probe trial (panel B). In the probe trial, both groups showed retention of spatial memory ($P < 0.01$), spending most of the time in the target quadrant. Each data point (panel A) or column (panel B) represents the mean value ± SEM for irradiated ($n = 12$) and nonirradiated ($n = 8$) mice.

Probe trial results showed that all mice learned to locate the hidden escape tunnel using search strategies not involving olfaction or proximal cues. Finally, both groups of mice were equally adept at learning to locate the visible escape tunnel (Fig. 4A, B), a function that is not hippocampal-dependent.

Radiation did not affect passive avoidance learning and memory. There were no differences between groups in latency to enter the dark compartment on either day 1 or day 2 (data not shown).

Finally, we assessed myelin staining, cell proliferation, and the production of immature neurons in the subgranular zone of behaviorally tested animals. There was no qualitative difference between controls and irradiated mice in luxol fast blue staining in white matter tracts, hippocampus or fimbria (not shown). Consistent with an age-related decrease in neurogenesis (*17*), Dcx labeling decreased in sham-irradiated mice relative to that seen a month earlier [Fig. 1, $F(1,7) = 18.747$, $P = 0.0034$]. Ki-67 did not decrease significantly [$F(1,7) = 0.995$, $P = 0.3611$]. In irradiated mice there were significantly fewer Ki-67- and Dcx-labeled cells, but there was no further decrease from what was seen prior to training.

DISCUSSION

Our study shows that a modest dose of X rays induces significant hippocampal-dependent cognitive impairments, which are associated with reduced cell proliferation and reduced numbers of immature neurons in the dentate SGZ. Given the extreme sensitivity of neurogenesis to low to moderate doses of X rays (*24, 25*), and the persistent reductions in specific cellular elements associated with neurogenesis at the time of cognitive testing (Fig. 1), our data suggest that altered production of new neurons in the dentate gyrus might play a contributory role in the development of cognitive impairments after irradiation. Radiation-induced changes in numbers of Ki-67-positive proliferating cells and Dcx-positive immature neurons occur early after irradiation, and the dose–response characteristics of these cells seen shortly after irradiation are similar to later-developing changes in production of mature neurons (*25*). In our previous study, we showed that 1–2 months after a single dose of 10 Gy the production of new hippocampal neurons was reduced by over 80% relative to nonirradiated controls (*25*). In the present study, at the time of cognitive testing (3 months after treatment), we saw that the numbers of Ki-67-positive and Dcx-positive cells were decreased by about 90% (Fig. 1), suggesting that neurogenesis was significantly affected.

In this study we hypothesized that radiation-induced changes in the dentate SGZ would be associated with hippocampal-dependent cognitive impairments. We chose a radiation dose that we knew would significantly affect neurogenesis (*23–25*) but would not induce the tissue changes seen in other studies of radiation-induced cognitive impair-

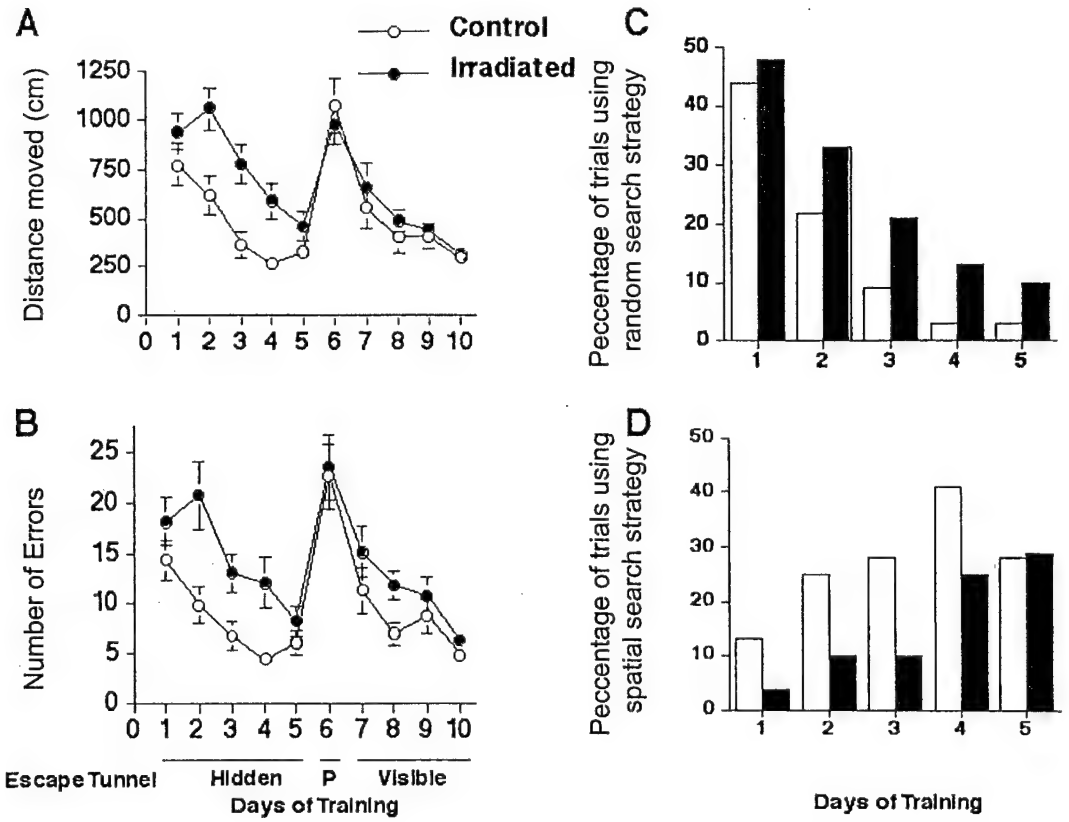

FIG. 4. Cognitive testing of irradiated and nonirradiated mice reveals significant impairments of irradiated mice in Barnes maze performance. End points shown are distance moved to find the escape tunnel (panel A), number of errors made (panel B), and random (panel C) and spatial (panel D) search strategies. On days 1–5, mice were trained to locate a hidden escape tunnel, and on day 6, two probe trials (P) were used with the tunnel placed under different holes. On days 7–10, mice were trained to locate a visible escape tunnel. For distance moved (panel A) and number of errors (panel B), each data point represents the daily mean value ± SEM. For the search strategies (panels C, D), the bars represent the daily percentage of trials in which a particular search strategy was used. The white bars represent the control mice and the black bars the irradiated mice (n = 12 irradiated and n = 8 nonirradiated mice). For distance moved and number of errors made, the daily averages per mouse were used for statistical analysis. In the analysis of search strategies, the percentages of trials/day a particular search strategy was used in each treatment group were compared statistically.

ment using higher radiation doses (*43–45*). Using the linear-quadratic relationship (*46*) and a range of α/β ratios for proliferating precursor cells in the CNS (4.9–7.3 Gy) (*47*), we could predict that a single dose of 10 Gy was equivalent to about ten 2-Gy fractions, well below the threshold for inducing obvious tissue breakdown. Qualitative evaluation of overall morphology and myelin in and around the hippocampus using luxol fast blue staining showed no obvious changes. In addition, no structural alterations were observed in the fimbria, a region closely associated physically and functionally with the dentate gyrus, and that has been shown to be particularly sensitive to radiation (*48*).

Given that we were specifically addressing hippocampal function, we chose behavioral tests that have been associated with hippocampal function (Morris water maze, Barnes maze, novel location, and novel object recognition). Furthermore, because a variety of non-hippocampal-dependent factors can potentially affect maze performance (e.g. anxiety levels, exploratory activity, sensorimotor function, and vision), we also incorporated a number of control tests to rule out those factors as affecting maze performance. To our knowledge, this is the first time radiation-induced cognitive impairments have been investigated using such a comprehensive battery of behavioral assessments. In contrast to hippocampal lesion studies (*29–31*), we did not see significant impairment of hippocampal-dependent object recognition and water maze performance. It may be that more extensive tissue destruction within the hippocampus is required to detect impairments in those tests.

To our knowledge there are no other studies available that have used the Barnes maze to assess radiation injury. In our study, we detected radiation-induced changes in the spatial component (hidden escape tunnel) of the Barnes maze test; there were no changes in the visible component (visible escape tunnel) (Fig. 4). In light of hippocampal lesion studies that have corroborated the role of the hippocampus in spatial learning (*29–31*), our data suggest that specific hippocampal-dependent spatial learning and mem-

ory were impaired 3 months after 10 Gy. The majority of other studies of cognition after irradiation have involved rats and have relied upon the commonly used Morris water maze as the principal assessment of cognitive function (*43–45*). However, in those studies deficits in water maze performance were detected only after substantially higher single doses (21–25 Gy) and longer follow-up times (6–12 months) than used here (*43–45*). In a recent study by Madsen *et al.* (*49*), rats received eight fractions of 3 Gy over 11 days, and water maze performance was assessed 2 weeks later, but no cognitive deficits were seen. While no effects were seen in the Morris water maze, at roughly the same time, impaired hippocampal function was seen using a place recognition test; that impairment was not detectable at 7 weeks after treatment. That study is of particular interest because it reported arrested neuronal proliferation in the dentate gyrus acutely after fractionated irradiation, a finding previously reported by us after single X-ray doses (*24, 25*). Madsen *et al.* (*49*) went on to associate their observed changes in neuronal proliferation with the early and transient cognitive deficits. Given that the full maturation of newly born neurons may take many weeks or months (*20*), there is some question whether the early cognitive effects seen in that study relate to altered neurogenesis or whether they represent some form of the "early delayed reaction" previously described by Sheline (*1*).

While our cognitive measurements were done at a later time than those of Madsen *et al.* (*49*), we too saw no significant difference in Morris water maze performance between irradiated and control animals at the time when Barnes maze performance was significantly affected. This suggests that under conditions of this study, the Barnes maze is more sensitive than the water maze for detecting relatively early radiation changes in young adult mice. Interestingly, the Barnes maze is also more sensitive than the Morris water maze in detecting spatial learning disruption after LTP saturation in the dentate gyrus (*33*). While the Barnes maze and Morris water maze are both tests of spatial learning and memory, the former is based on the natural preference of rodents for a dark environment and requires less physical energy because it does not involve swimming (*50*). In addition, the Barnes maze might be more sensitive than the water maze to potential confounds of altered exploratory activity and anxiety levels (*51*). The stressors used in both tests, swim stress in the Morris water maze and white noise and bright light used to motivate escape behavior in the Barnes maze, are very different, and they might differentially influence test performance under baseline conditions or after irradiation. However, we cannot exclude the possibility that a more challenging version of the Morris water maze test, where the hidden platform location is changed daily (*34*), or inclusion of additional probe trials during hidden platform training would also have elucidated early radiation-induced cognitive changes.

Memory functions are complicated and not wholly associated with a single brain structure, nor are all memory functions spatial in nature. While spatial learning and memory is tightly associated with the hippocampus, there are also hippocampal and cortex-dependent nonspatial learning and memory functions. To assess whether radiation affects nonspatial learning and memory, we used the novel location and novel object recognition test (*37*). In response to a change in location of a familiar object, both groups of mice spent more time exploring the object in the novel location. Similarly, all mice spent more time exploring the novel object than the familiar ones, but there was no group difference. There was also no group difference in passive avoidance learning. This suggests that nonspatial learning and memory is less sensitive than spatial learning and memory to the effects of radiation.

Another factor that can affect motivation and maze performance is anxiety, which is mediated, at least in part, through the amygdala. Open field (*34*) and the elevated plus maze (*36*) tests were used to assess potential differences in anxiety levels, and our results showed that radiation had no significant effect on measures of anxiety in either of these tests (Table 1). Based on these data, we can conclude that altered anxiety levels after irradiation could not account for the impaired performance in the Barnes maze. Furthermore, there were no differences in sensorimotor function (Fig. 2) between treatment groups that could have contributed to the observed differences in the Barnes maze.

At least in the context of the tests used in this study, radiation appears to affect specific cognitive functions associated with the hippocampus. The hippocampus is unique inasmuch as it is a site of active neurogenesis, and recent studies have shown that the cells associated with this process are extremely sensitive to radiation (*23–25*). While the precise function(s) of the newly born neurons has not yet been clearly demonstrated, there is good correlative evidence that functional stimuli promote survival of new hippocampal neurons and that this survival is associated with improved hippocampal learning (*15, 52, 53*). Conversely, animals treated with a chemical agent to reduce hippocampal neurogenesis performed poorly in a hippocampal-dependent conditioning task (*22*). Even though many newly born neurons die shortly after their birth (*54*), a significant number are integrated into the hippocampal circuitry and persist for a long time (*55*). Therefore, it has been suggested that even a few new hippocampal neurons, if strategically localized within a network, could significantly increase the complexity and thereby the processing capacity of that network (*56*). Whether radiation affects cognitive function simply by reducing the numbers of newly born cells that can be incorporated into the hippocampal networks and/or by other mechanisms need to be elucidated.

Studies of the effects of ionizing radiation on hippocampal structure have been carried out in rats (*23, 24, 27, 49*), and mice (*25, 26, 28*), and recent studies have shown that the effects of radiation on hippocampal neurogenesis are similar in these two species (*24, 25*). In contrast, until now most studies of cognitive function after irradiation have

been carried out using rats (*43–45, 49*). While studies exist showing similar cognitive performance in these species after hippocampal lesioning (*29*), other studies show differences in performance on hippocampus-dependent cognitive tasks (*57*). Such differences can be related to differential ability in performing a specific task, particularly a water maze, or ability to cope with the stress of test (*58, 59*). In fact, it has been reported that for optimal place learning in mice, satisfactory performance is more likely to be obtained in "dry-land" tasks, such as the Barnes maze than in swimming pool tasks (*59*). This increased sensitivity of non-water-based tests to detect cognitive impairments in mice may be why we were able to detect changes after a relatively short time and modest radiation dose in the Barnes maze and not the Morris water maze.

We focused our study on the dentate gyrus because it has been reported that hippocampal neurogenesis seems to play a specific role in only hippocampal-dependent learning (*60, 61*). However, other mechanisms besides neurogenesis can also be involved in memory formation (*62, 63*), and because other hippocampal/cortical areas were also irradiated, we cannot definitively exclude effects of radiation on these areas as contributing to our findings. Recognizing this caveat, however, our data support the notion that radiation-induced changes in the dentate SGZ may play an important role in the pathogenesis underlying cognitive impairments. Given the potentially devastating consequences of cranial irradiation, such information is essential for the development of strategies/approaches to ameliorate or treat radiation-induced cognitive injury.

ACKNOWLEDGMENTS

We thank Kenneth James for his help with the nonparametric statistical analysis. This work was supported by the NIH Grants R21 NS40088 (to JRF), R01 AG20904 (to JR), EMF grant AG-NS-0201-02 (to JR) and DOD grant DAMD17-01-1-0820 (to JRF).

Received: January 5, 2004; accepted: April 2, 2004

REFERENCES

1. G. E. Sheline, W. M. Wara and V. Smith, Therapeutic irradiation and brain injury. *Int. J. Radiat. Oncol. Biol. Phys.* **6**, 1215–1228 (1980).
2. O. K. Abayomi, Pathogenesis of irradiation-induced cognitive dysfunction. *Acta Oncol.* **35**, 659–663 (1996).
3. R. W. Butler, J. M. Hill, P. G. Steinherz, P. A. Meyers and J. L. Finlay, Neuropsychologic effects of cranial irradiation, intrathecal methotrexate and systemic methotrexate in childhood cancer. *J. Clin. Oncol.* **12**, 2621–2629 (1994).
4. M. Dennis, B. J. Spiegler, M. C. Obonsawin, B. L. Maria, C. Cowell, H. J. Hoffman, E. B. Hendrick, R. P. Humphreys, J. D. Bailey and R. M. Ehrlich, Brain tumors in children and adolescents—III. Effects of radiation and hormone status on intelligence and on working, associative and serial-order memory. *Neuropsychologia* **30**, 257–275 (1992).
5. J. H. Kramer, M. R. Crittenden, F. E. Halberg, W. M. Wara and M. J. Cowan, A prospective study of cognitive functioning following low-dose cranial radiation for bone marrow transplantation. *Pediatrics* **90**, 447–450 (1992).
6. J. Grill, V. K. Renaux, C. Bulteau, D. Viguier, C. Levy-Piebois, C. Sainte-Rose, G. Dellatolas, M. A. Raquin, I. Jambaque and C. Kalifa, Long-term intellectual outcome in children with posterior fossa tumors according to radiation doses and volumes. *Int. J. Radiat. Oncol. Biol. Phys.* **45**, 137–145 (1999).
7. C. A. Meyers, F. Geara, P. F. Wong and W. H. Morrison, Neurocognitive effects of therapeutic irradiation for base of skull tumors. *Int. J. Radiat. Oncol. Biol. Phys.* **46**, 51–55 (2000).
8. J. R. Crossen, D. Garwood, E. Glatstein and E. A. Neuwelt, Neurobehavioral sequelae of cranial irradiation in adults: A review of radiation-induced encephalopathy. *J. Clin. Oncol.* **12**, 627–642 (1994).
9. D. D. Roman and P. W. Sperduto, Neuropsychological effects of cranial radiation: Current knowledge and future directions. *Int. J. Radiat. Oncol. Biol. Phys.* **31**, 983–998 (1995).
10. P. W. Lee, B. K. Hung, E. K. Woo, P. T. Tai and D. T. Choi, Effects of radiation therapy on neuropsychological functioning in patients with nasopharyngeal carcinoma. *J. Neurol. Neurosurg. Psychiatry* **52**, 488–492 (1989).
11. O. Surma-aho, M. Niemela, J. Vilkki, M. Kouri, A. Brander, O. Salonen, A. Paetau, M. Kallio, J. Pyykkonen and J. Jaaskelainen, Adverse long-term effects of brain radiotherapy in adult low-grade glioma patients. *Neurology* **56**, 1285–1290 (2001).
12. F. H. Gage, G. Kempermann, T. D. Palmer, D. A. Peterson and J. Ray, Multipotent progenitor cells in the adult dentate gyrus. *J. Neurobiol.* **36**, 249–266 (1998).
13. S. A. Bayer and J. Altman, The effects of X-irradiation on the postnatally-forming granule cell populations in the olfactory bulb, hippocampus, and cerebellum of the rat. *Exp. Neurol.* **48**, 167–174 (1975).
14. H. A. Cameron, C. S. Woolley, B. S. McEwen and E. Gould, Differentiation of newly born neurons and glia in the dentate gyrus of the adult rat. *Neuroscience* **56**, 337–344 (1993).
15. G. Kempermann, H. G. Kuhn and F. H. Gage, More hippocampal neurons in adult mice living in an enriched environment. *Nature* **386**, 493–495 (1997).
16. P. S. Eriksson, E. Perfilieva, T. Bjork-Eriksson, A. M. Alborn, C. Nordborg, D. A. Peterson and F. H. Gage, Neurogenesis in the adult human hippocampus. *Nat. Med.* **4**, 1313–1317 (1998).
17. H. G. Kuhn, H. Dickinson-Anson and F. H. Gage, Neurogenesis in the dentate gyrus of the adult rat: Age-related decrease of neuronal progenitor proliferation. *J. Neurosci.* **16**, 2027–2033 (1996).
18. E. A. Markakis and F. H. Gage, Adult-generated neurons in the dentate gyrus send axonal projections to field CA3 and are surrounded by synaptic vesicles. *J. Comp. Neurol.* **406**, 449–460 (1999).
19. B. B. Stanfield and J. E. Trice, Evidence that granule cells generated in the dentate gyrus of adult rats extend axonal projections. *Exp. Brain Res.* **73**, 399–406 (1988).
20. H. van Praag, A. F. Schinder, B. R. Christie, N. Toni, T. D. Palmer and F. H. Gage, Functional neurogenesis in the adult hippocampus. *Nature* **415**, 1030–1034 (2002).
21. H. van Praag, G. Kempermann and F. H. Gage, Running increases cell proliferation and neurogenesis in the adult mouse dentate gyrus. *Nat. Neurosci.* **2**, 266–270 (1999).
22. T. J. Shors, G. Miesegaes, A. Beylin, M. Zhao, T. Rydel and E. Gould, Neurogenesis in the adult is involved in the formation of trace memories. *Nature* **410**, 372–376 (2001).
23. E. Tada, J. M. Parent, D. H. Lowenstein and J. R. Fike, X-irradiation causes a prolonged reduction in cell proliferation in the dentate gyrus of adult rats. *Neuroscience* **99**, 33–41 (2000).
24. M. L. Monje, S. Mizumatsu, J. R. Fike and T. D. Palmer, Irradiation induces neural precursor-cell dysfunction. *Nat. Med.* **8**, 955–962 (2002).
25. S. Mizumatsu, M. L. Monje, D. R. Morhardt, R. Rola, T. D. Palmer and J. R. Fike, Extreme sensitivity of adult neurogenesis to low doses of x-irradiation. *Cancer Res.* **63**, 4021–4027 (2003).
26. R. Nagai, S. Tsunoda, Y. Hori and H. Asada, Selective vulnerability to radiation in the hippocampal dentate granule cells. *Surg. Neurol.* **53**, 503–506 (2000).

27. W. Peissner, M. Kocher, H. Treuer and F. Gillardon, Ionizing radiation-induced apoptosis of proliferating stem cells in the dentate gyrus of the adult rat hippocampus. *Brain Res. Mol. Brain Res.* **71**, 61–68 (1999).
28. R. Sasaki, A. Matsumoto, K. Itoh, T. Kawabe, Y. Ota, K. Yamada, T. Maruta, T. Soejima and K. Sugimura, Target cells of apoptosis in the adult murine dentate gyrus and O4 immunoreactivity after ionizing radiation. *Neurosci. Lett.* **279**, 57–60 (2000).
29. Y. H. Cho, E. Friedman and A. J. Silva, Ibotenate lesions of the hippocampus impair spatial learning but not contextual fear conditioning in mice. *Behav. Brain Res.* **98**, 77–87 (1999).
30. S. F. Logue, R. Paylor and J. M. Wehner, Hippocampal lesions cause learning deficits in inbred mice in the Morris water maze and conditioned-fear task. *Behav. Neurosci.* **111**, 104–113 (1997).
31. R. T. Gerlai, A. McNamara, S. Williams and H. S. Phillips, Hippocampal dysfunction and behavioral deficit in the water maze in mice: An unresolved issue? *Brain Res. Bull.* **57**, 3–9 (2002).
32. R. M. Deacon and J. N. Rawlins, Learning impairments of hippocampal-lesioned mice in a paddling pool. *Behav. Neurosci.* **116**, 472–478 (2002).
33. C. A. Barnes, M. W. Jung, B. L. McNaughton, D. L. Korol, K. Andreasson and P. F. Worley, LTP saturation and spatial learning disruption: effects of task variables and saturation levels. *J. Neurosci.* **14**, 5793–5806 (1994).
34. J. Raber, D. Wong, M. Buttini, M. Orth, S. Bellosta, E. R. Pitas, R. W. Mahley and L. Mucke, Isoform-specific effects of human apolipoprotein E on brain function revealed in ApoE knockout mice: Increased susceptibility of females. *Proc. Natl. Acad. Sci. USA* **95**, 10914–10919 (1998).
35. R. G. Lister, Ethologically-based animal models of anxiety disorders. *Pharmacol. Ther.* **46**, 321–340 (1990).
36. J. Raber, S. F. Akana, S. Bhatnagar, M. F. Dallman, D. Wong and L. Mucke, Hypothalamic-pituitary-adrenal dysfunction in Apoe$^{-/-}$ mice: Possible role in behavioral and metabolic alterations. *J. Neurosci.* **20**, 2064–2071 (2000).
37. G. Malleret, U. Haditsch, D. Genoux, M. W. Jones, T. V. Bliss, A. M. Vanhoose, C. Weitlauf, E. R. Kandel, D. G. Winder and I. M. Mansuy, Inducible and reversible enhancement of learning, memory, and long-term potentiation by genetic inhibition of calcineurin. *Cell* **104**, 675–686 (2001).
38. N. R. Rustay, D. Wahlsten and J. C. Crabbe, Influence of task parameters on rotarod performance and sensitivity to ethanol in mice. *Behav. Brain Res.* **141**, 237–249 (2003).
39. R. J. Morris, Developments of a water-maze procedure for studying spatial learning in the rat. *J. Neurosci. Methods* **11**, 47–60 (1984).
40. M. E. Bach, R. D. Hawkins, M. Osman, E. R. Kandel and M. Mayford, Impairment of spatial but not contextual memory in CaMKII mutant mice with a selective loss of hippocampal LTP in the range of the theta frequency. *Cell* **81**, 905–915 (1995).
41. N. Kee, S. Sivalingam, R. Boonstra and J. M. Wojtowicz, The utility of Ki-67 and BrdU as proliferative markers of adult neurogenesis. *J. Neurosci. Methods* **115**, 97–105 (2002).
42. J. Nacher, C. Crespo and B. S. McEwen, Doublecortin expression in the adult rat telencephalon. *Eur. J. Neurosci.* **14**, 629–644 (2001).
43. J. Hodges, N. Katzung, P. Sowinski, J. W. Hopewell, J. H. Wilkinson, T. Bywaters and M. Rezvani, Late behavioral and neuropathological effects of local brain irradiation in the rat. *Behav. Brain Res.* **91**, 99–114 (1998).
44. I. Lamproglou, Q. M. Chen, G. Boisserie, J-J. Mazeron, M. Poisson, F. Baillet, M. Le Poncin and J-V. Delattre, Radiation-induced cognitive dysfunction: an experimental model in the old rat. *Int. J. Radiat. Oncol. Biol. Phys.* **31**, 65–70 (1995).
45. K. Akiyama, R. Tanaka, M. Sato and N. Taked, Cognitive dysfunction and histological findings in adult rats one year after whole brain irradiation. *Neurol. Med. Chir. (Tokyo)* **41**, 590–598 (2001).
46. J. F. Fowler, The linear-quadratic formula and progress in fractionated radiotherapy. *Br. J. Radiol.* **62**, 679–694 (1989).
47. R. W. M. van der Maazen, B. J. Kleiboer, I. Verhagen and A. J. van der Kogel, Repair capacity of adult rat glial progenitor cells determined by an *in vitro* clonogenic assay after *in vitro* or *in vivo* fractionated irradiation. *Int. J. Radiat. Biol.* **63**, 661–666 (1993).
48. W. Calvo, J. W. Hopewell, H. S. Reinhold and T. K. Yeung, Time- and dose-related changes in the white matter of the rat brain after single doses of X rays. *Br. J. Radiol.* **61**, 1043–1052 (1988).
49. T. M. Madsen, P. E. Kristjansen, T. G. Bolwig and G. Wortwein, Arrested neuronal proliferation and impaired hippocampal function following fractionated brain irradiation in the adult rat. *Neuroscience* **119**, 635–642 (2003).
50. P. N. Pompl, M. J. Mullan, K. Bjugstad and G. W. Arendash, Adaptation of the circular platform spatial memory task for mice: Use in detecting cognitive impairment in the APP(SW) transgenic mouse model for Alzheimer's disease. *J. Neurosci. Methods* **87**, 87–95 (1999).
51. A. Holmes, C. C. Wrenn, A. P. Harris, K. E. Thayer and J. N. Crawley, Behavioral profiles of inbred strains on novel olfactory, spatial and emotional tests for reference memory in mice. *Genes Brain Behav.* **1**, 55–69 (2002).
52. E. Gould, A. Beylin, P. Tanapat, A. Reeves and T. J. Shors, Learning enhances adult neurogenesis in the hippocampal formation. *Nat. Neurosci.* **2**, 260–265 (1999).
53. M. Nilsson, E. Perfilieva, U. Johansson, O. Orwar and P. S. Eriksson, Enriched environment increases neurogenesis in the adult rat dentate gyrus and improves spatial memory. *J. Neurobiol.* **39**, 569–578 (1999).
54. M. Biebl, C. M. Cooper, J. Winkler and H. G. Kuhn, Analysis of neurogenesis and programmed cell death reveals a self-renewing capacity in the adult rat brain. *Neurosci. Lett.* **291**, 17–20 (2000).
55. G. Kempermann, D. Gast, G. Kronenberg, M. Yamaguchi and F. H. Gage, Early determination and long-term persistence of adult-generated new neurons in the hippocampus of mice. *Development* **130**, 391–399 (2003).
56. G. Kempermann, Why new neurons? Possible functions for adult hippocampal neurogenesis. *J. Neurosci.* **22**, 635–638 (2002).
57. K. M. Frick, E. T. Stillner and J. Berger-Sweeney, Mice are not little rats: Species differences in a one-day water maze task. *Neuroreport* **11**, 3461–3465 (2000).
58. D. C. Rogers, D. N. Jones, P. R. Nelson, C. M. Jones, C. A. Quilter, T. L. Robinson and J. J. Hagan, Use of SHIRPA and discriminant analysis to characterise marked differences in the behavioural phenotype of six inbred mouse strains. *Behav. Brain Res.* **105**, 207–217 (1999).
59. I. Q. Whishaw and J. A. Tomie, Of mice and mazes: Similarities between mice and rats on dry land but not water mazes. *Physiol. Behav.* **60**, 1191–1197 (1996).
60. E. Gould and P. Tanapat, Stress and hippocampal neurogenesis. *Biol. Psychiatr.* **46**, 1472–1479 (1999).
61. J. Prickaerts, G. Koopmans, A. Blokland and A. Scheepens, Learning and adult neurogenesis: Survival with or without proliferation? *Neurobiol. Learn. Mem.* **81**, 1–11 (2004).
62. V. Ramirez-Amaya, I. Balderas, J. Sandoval, M. L. Escobar and F. Bermudez-Rattoni, Spatial long-term memory is related to mossy fiber synaptogenesis. *J. Neurosci.* **21**, 7340–7348 (2001).
63. B. Leuner, J. Falduto and T. J. Shors, Associative memory formation increases the observation of dendritic spines in the hippocampus. *J. Neurosci.* **23**, 659–665 (2003).

Irradiation Attenuates Neurogenesis and Exacerbates Ischemia-Induced Deficits

Jacob Raber, PhD,[1] Yang Fan, MS,[2,3] Yasuhiko Matsumori, MD,[2,3] Zhengyan Liu, MD,[2,3] Philip R. Weinstein, MD,[2,3] John R. Fike, PhD,[2] and Jialing Liu, PhD[2,3]

Increased neurogenesis after cerebral ischemia suggests that functional recovery after stroke may be attributed, in part, to neural regeneration. In this study, we investigated the role of neurogenesis in the behavioral performance of gerbils after cerebral global ischemia. We used ionizing radiation to decrease neural regeneration, and 2 weeks later cerebral global ischemia was induced by bilateral common carotid artery occlusion. One month after the occlusion, the animals were behaviorally tested. Irradiation alone reduced neurogenesis but did not change vascular or dendritic morphology at the time of behavioral testing. Neither did irradiation, ischemia, or combined treatment impair rotor-rod performance or alter open-field activity. Gerbils subjected to both irradiation and ischemia demonstrated impaired performance in the water-maze task, compared with those that received only ischemia, radiation, or no treatment. These impairments after cerebral global ischemia under conditions of reduced neurogenesis support a role for the production of new cells in mediating functional recovery.

Ann Neurol 2004;55:381–389

Although a myriad of consequences associated with cerebral ischemia have been well documented,[1–3] a thorough understanding of the factors leading to structural/functional recovery is not well established.[4–7] Early recovery (ie, days) may be attributed to the resolution of edema, diaschisis, or reperfusion of the ischemic penumbra, whereas later recovery (1–2 weeks) likely reflects brain plasticity.[8–12] Clearly, the brain is able to repair itself,[13–16] reorganizing structural and electrophysiological connections,[4, 17] but it is not yet clear if that reorganization is a function solely of the plasticity of surviving cells or if it involves the contribution of newly born cells, that is, neurogenesis. Ischemia increases neurogenesis in the subgranular zone of the dentate gyrus (SGZ) and the striatum,[18–22] and, given the experimental studies showing clear structural repair in these sites, it is likely that the production of new cells plays an important role in this recovery. It is not yet known if neurogenesis participates in the functional repair seen after ischemia.

Neurogenesis occurs in the SGZ of all mammals including humans, and recent data show that newly born cells become functionally integrated into the dentate gyrus and have passive membrane properties, action potentials, and functional synaptic inputs similar to those found in mature dentate granule cells.[23] Most importantly, newly generated neurons play a significant role in synaptic plasticity,[23] and a reduction in the number of these cells impairs spatial learning.[24] Thus, inhibition of neurogenesis might play a role in the development of later developing cognitive impairments (J. Raber, R. Rola, A. LeFevour, D. Morhardt, J. Curley, S. Mizumatsu, S.R. Vandenburg, and J.R. Fike, unpublished data). However, there is no direct evidence linking neurogenesis to functional recovery in either humans or animal models of cerebral ischemia. This might be because of the lack of suitable experimental approaches to assess such effects. One way to address this would be to disrupt neurogenesis and determine if such disruption impedes functional recovery. This has been done recently using a model of radiation injury, in which a clear dose-related depression of neurogenesis was observed after whole-brain x-irradiation.[25–27] To determine if disruption of neurogenesis has a negative impact on structural and functional recovery after cerebral ischemia, we used x-ray irradiation to reduce SGZ neurogenesis before bilateral common carotid artery occlusion (BCCAO). Our results show that the irradiation has adverse effects on the performance in spatial learning and memory tests after ischemia and supports the combined use of radiation and

From the [1]Departments of Behavioral Neuroscience and Neurology, Oregon Health and Science University, Portland, OR; [2]Department of Neurological Surgery, University of California at San Francisco; and [3]San Francisco Veterans Affairs Medical Center, San Francisco, CA.

Received Jun 20, 2003; and in revised form Sep 3. Accepted for publication Oct 23, 2003.

Address correspondence to Dr J. Liu, Department of Neurological Surgery (112C), University of California at San Francisco and Department of Veterans Affairs Medical Center, 4150 Clement Street, San Francisco, CA 94121. E-mail: miro@itsa.ucsf.edu

Published by Wiley-Liss, Inc., through Wiley Subscription Services

BCCAO as a model system to assess the role of cellular regeneration in functional recovery.

Materials and Methods

Animals and Housing

Two-month-old male Mongolian gerbils (Harlan, San Diego, CA) were housed and cared for according to federal and institutional guidelines. To minimize the effects of social influences on behavior, we housed the gerbils singly during behavioral testing. All gerbils were anesthetized for irradiation and perfusion procedures; anesthesia consisted of an intraperitoneal injection of ketamine (80mg/kg; Parke-Davis, Morris Plains, NJ) and xylzine (15mg/kg; Butler, Columbus, OH).

Irradiation Treatment

Anesthetized gerbils were placed in sternal recumbency and irradiated as previously described with their eyes, cerebellum, and body shielded with lead.[25,26] Radiation was delivered as a split-dose paradigm involving two 5Gy doses separated by 7 days. Sham-irradiated animals (referred as controls) received the same treatment except for the exposure to irradiation.

Transient Global Ischemia

Two weeks after irradiation or sham irradiation, gerbils were subjected to 5 minutes of transient bilateral common carotid artery occlusion (BCCAO) as described.[18] Sham operation was not included because our previous data demonstrated that surgery and anesthesia did not induce neurogenesis.[18]

BrdU Labeling

The thymidine analog 5-bromo-2′-deoxyuridine-5′-monophosphate (BrdU) was administered intraperitoneally (50mg/kg; Sigma, St. Louis, MO). For investigation of the phenotype and survival of newborn cells, Gerbils received twice-daily injections of BrdU for 4 consecutive days, during the peak of cell proliferation, 9 to 12 days after ischemia[18] and were killed 2 to 3 weeks later.

Immunohistochemistry and Immunofluorescence Staining

Fifty-micrometer free-floating coronal sections were immunostained as described[18] using the following reagents: mouse anti-BrdU (0.25μg/ml; Roche, Indianapolis, IN); rat anti-BrdU (2μg/ml; Accurate Chemicals, Westbury, NY); mouse anti-NeuN (recognizing nuclear antigen in mature neurons, 1μg/ml; Chemicon, Temecula, CA); mouse anti–Tuj-1 (recognizing β-tubulin in immature neurons, 1μg/ml; BABCO, Berkeley, CA); or mouse anti–glial fibrillary acidic protein (GFAP) (recognizing intermediate filament protein in astrocytes, 1μg/ml; Chemicon); biotinylated sheep anti–mouse and anti–rat secondary antibodies (5μg/ml; Amersham, Cleveland, OH); ABC solution (Vector Laboratories, Burlingame, CA); streptavidine Alexa Fluor 488 and Alexa Fluor 594 goat anti–mouse immunoglobulin G conjugate (5μg/ml; Molecular Probes, Eugene, OR). Hoechst 33342 (50μg/ml; Molecular Probes) staining was used for the unbiased stereological counting of granule cells.

Confocal Microscopy

Fluorescence signals were detected using a Leica confocal imaging system (Leica, Wetzlar, Germany) with a sequential scanning mode for Alexa 488 and 594. Stacks of images (1,024 × 1,024 pixels) from consecutive 1μm-thick slices were obtained by averaging four scans per slice and processed with Adobe Photoshop (Adobe Systems, Mountain View, CA).

Cell Counting

The number of granule cells was determined in every sixth coronal section spanning the entire hippocampus using unbiased stereology[28] (Stereo Investigator, MicroBrightField). Counting frames (15 × 15 × 20μm) were placed at the intersection of a 200 × 200μm matrix randomly superimposed onto the region of interest by the program. Cells were counted using a ×63 oil objective. NeuN-stained cornu ammonis 1 region of the hippocampus (CA1) neurons were counted using the same method in the septal hippocampus where consistent ischemic injury was observed. BrdU-immunoreactive cells were counted in the SGZ and granule cell layer (GCL) and divided by the volume (mm^3) of these two regions determined using the Cavalieri's principal.[29] The number of BrdU/Tuj-1 or BrdU/GFAP double-labeled cells was estimated by multiplying the percentages of colocalization (determined by confocal microscopy) to the total number of BrdU-labeled cells (determined by Zeiss Axioskope 2 plus epifluorescent microscope; Zeiss, Thornwood, NY).[18]

Golgi-Cox Staining and Analysis

Golgi-Cox staining was performed on 100μm sections as described.[30] Fifteen neurons each from the dentate gyrus granule cell layer and layer II parietal cortex were selected from each animal (see insets in Fig 1D & E) at ×100 magnification. Dendritic arbors including the cell body, and dendrites were reconstructed using the Neurolucida neuron tracing program (MicroBrightField, Colchester, VT) at ×630 magnification. Apical and basilar dendritic arbors were quantified with Sholl concentric sphere analysis, and total dendritic length was estimated using the NeuroExplorer program (MicroBrightField). For Sholl analysis, the concentric rings with 20μm intervals were overlaid on each Neurolucida traced image, and the numbers of dendritic branch intersections were counted within each circle.

Behavioral Testing

One month after ischemia, gerbils underwent behavioral testing. To minimize the potential effects of stress related to previous testing on behavioral performance, we tested gerbils first in the open field, then on the rotor rod, and last in the water maze as previously described.[31,32] Because gerbils are not natural swimmers, they were given 5 days of swimming lessons before the water-maze test. This consisted of four 5-minute sessions per day with a 1-hour intersession interval.

Statistical Analysis

Data were expressed as mean ± standard error of the mean. Data were evaluated by analysis of variance, followed by Tukey–Kramer post hoc tests when appropriate. p values less than 0.05 were considered significant.

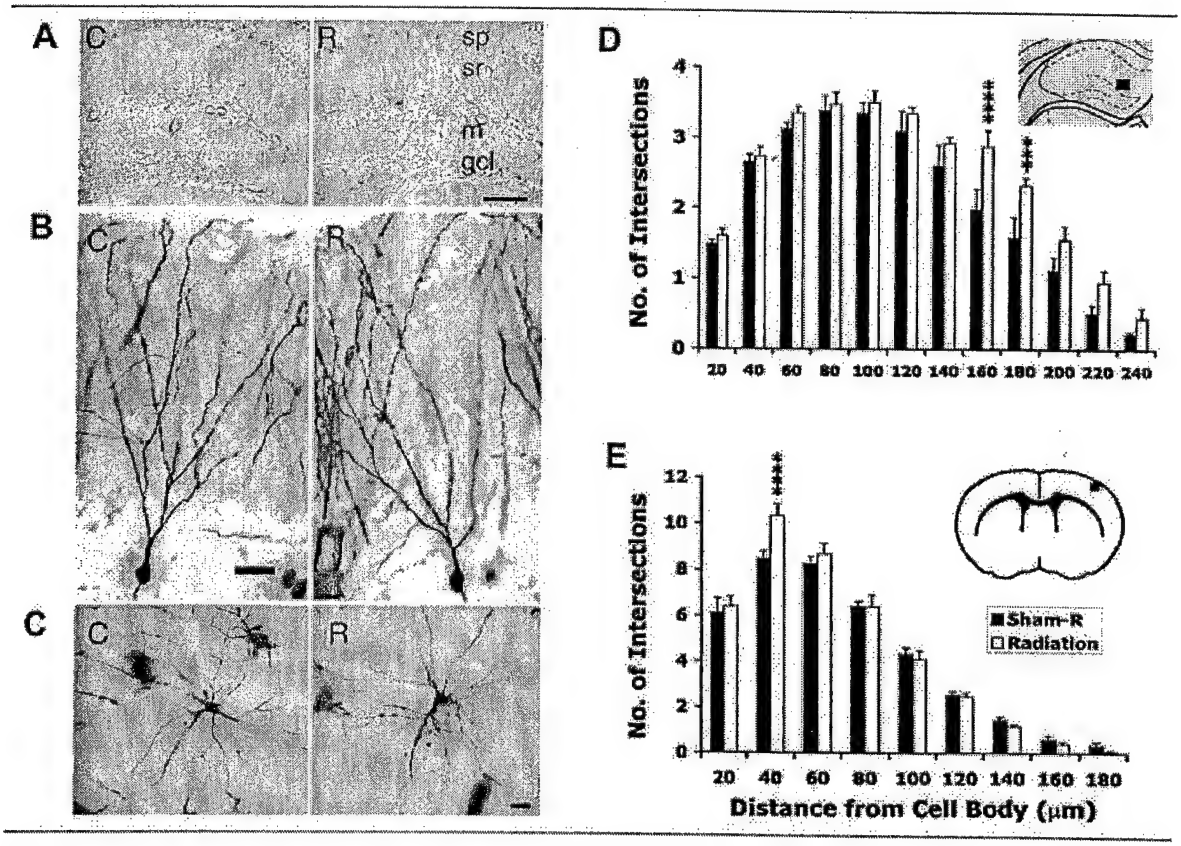

*Fig 1. Irradiation does not affect microvascular morphology or dendritic profiles. (A) Laminin staining of capillary vessels in the hippocampus of sham-irradiated control (C) and irradiation-treated gerbils (R). Irradiation does not have an effect on the general morphology of blood vessels in the hippocampus. Layers of hippocampus are illustrated as sp for stratum pyramidale, sr for stratum radiatum, m for molecular layer, gcl for granule cell layer. Scale bar-250μm. (B, C) Representative Golgi-Cox–stained granule neurons of the dentate gyrus (B) and layer II parietal cortex (C) in control (C) and irradiation-treated (R) gerbils. Scale bar-25μm. (D, E) Sholl concentric sphere analysis shows no overall differences in apical dendritic branching pattern of the dentate granule neurons (D) (n = 4) and basilar dendritic branching pattern of the layer II cortical neurons (E) (n = 6) between control and irradiated animals. Asterisks indicate differences in the number of intersections in specific radius (*** $p < 0.005$; **** $p < 0.001$).*

Results

Microvascular Morphology and Synaptic Profiles Are Unaltered after Irradiation

Nissl staining performed 2 months after irradiation showed no gross anatomical abnormalities (data not shown). Unbiased stereology did not show any significant differences in the number of septal CA1 neurons (Table 1) or graule cells in the dentate gyrus (Table 2) between control and irradiated gerbils ($p = 0.52$ and 0.77, respectively). Laminin immunohistology and Golgi-Cox impregnation were used to assess brain capillary morphology and synaptic profiles, respectively.[30,33] Laminin staining did not show differences in microvascular morphology between hippocampi from the control and irradiated animals (see Fig 1A). Sholl analysis also failed to show overall differences in the dendritic branching pattern in dentate granule neurons (see Fig 1D) and layer II cortical neurons (see Fig 1E) between these two groups. Furthermore, irradiation did not affect dendritic morphology (see Fig 1B, C) or dendritic length in the dentate granule layer (sham: 705 ± 40μm; irradiation: 728 ± 17μm) and in layer II cortex (sham: 924 ± 42μm; irradiation: 947 ± 88μm).

Irradiation Decreases Ischemia-Induced Neurogenesis in the Dentate Gyrus

The effect of radiation alone (R) ischemia alone (I) and combined radiation plus ischemia treatment (RI) on proliferative cell survival and differentiation in the dentate gyrus GCL was determined by BrdU immunohistochemistry and double immunofluorescence. Ischemia resulted in significantly more surviving new cells (total BrdU-positive cells 2–3 weeks after labeling) and new neurons (total BrdU-TuJ1 double-labeled cells) than all other treatments ($p < 0.01$). Approximately 1 month after ischemia, there was a 4.4-fold increase in the

Table 1. Stereological Estimate of the Total Number of Neurons, Volume, and Cell Density in the Septal CA1 of Adult Male Gerbils

Measure	C	R	I	RI
Cell number ($\times 10^4$)	4.44 ± 0.17	4.96 ± 0.15	2.21 ± 0.21[a]	2.17 ± 0.22[a]
Volume (mm^3)	0.18 ± 0.005	0.20 ± 0.007	0.14 ± 0.007[b]	0.14 ± 0.009[b]
Cell density ($\times 10^5$ cells/mm^3)	2.44 ± 0.82	2.43 ± 0.54	1.60 ± 0.13[c]	1.55 ± 0.92[d]

Total number of NeuN-immunoreactive cells in the septal CA1 per hemisphere was determined by the optical fractionator. Data are mean ± SEM. n = 6 per group. Significant difference in cell number, volume and density was found in I and RI when compared with the C as indicated by asterisks ([b]$p < 0.05$; [d]$p < 0.005$; [c]$p < 0.001$; [a]$p < 0.0001$); between R and I ($p < 0.0001$; $p < 0.001$; $p < 0.001$) and R and RI ($p < 0.0001$; $p < 0.001$; $p < 0.005$).

CA1 = cornu ammonis region 1 of the hippocampus.

Table 2. Stereological Estimate of the Total Number of Granule Cells, Volume, and Cell Density in the Dentate Gyrus of Adult Male Gerbils

Measure	C	R	I	RI
Cell number ($\times 10^5$)	7.5 ± 0.39	6.8 ± 0.29	6.9 ± 0.44	7.4 ± 0.66
Volume (mm^3)	1.05 ± 0.036	0.96 ± 0.092	0.99 ± 0.066	1.04 ± 0.111
Cell density ($\times 10^5$ cells/mm^3)	7.1 ± 0.22	7.1 ± 0.27	7.05 ± 0.30	7.1 ± 0.26

Total granule cell number per dentate gyrus was determined by the optical fractionator. Data are mean ± SEM. n = 6 per group. ANOVA showed no significant group difference in cell number, volume, or cell density ($p = 0.68$; $p = 0.73$; $p = 0.99$).

number of surviving new cells and a 5.2-fold increase of surviving new neurons relative to controls (Fig 2A). After irradiation, the number of surviving new cells in the GCL was decreased by 63.6%, and the surviving new cells with neuronal phenotype were decreased by 83.8% relative to control. Compared with animals that received ischemia only, gerbils that received irradiation followed by ischemia had 76.5% fewer surviving new cells and even a lower proportion of new neurons (21.9% in RI vs 41% in I; see Fig 2A, B). There were very few GFAP-immunoreactive cells in the GCL, and no colocalization of BrdU or GFAP was detected in this region in any of the treatment groups (see Fig 2B).

Irradiation Exacerbates Ischemia-Induced Functional Deficits

In the visible platform trials of the water maze, there was no significant difference in the learning curves among the controls (C), gerbils that received radiation (R), and gerbils that received ischemia (I) treatment alone (Fig 3A). However, gerbils that received irradiation treatment followed by ischemia (RI) demonstrated significant impairments when compared with any of the other groups ($p < 0.01$). In the hidden platform trials, the R group did not show any impairment, whereas the I group showed a significant deficit ($p < 0.01$ vs controls). The RI group demonstrated signifi-

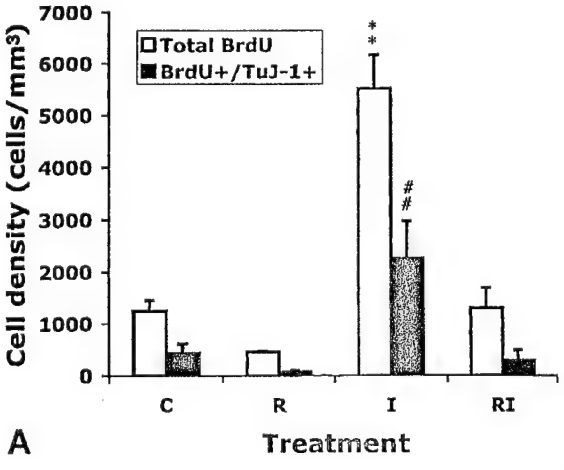

Fig 2. Irradiation inhibits global ischemia-induced neurogenesis in the granule cell layer (GCL). Gerbils with sham treatment (C) (n = 6), irradiation (R) (n = 12), global ischemia (I) (n = 6), and irradiation followed by ischemia (RI) (n = 6) were labeled with BrdU as described in the method. (A) Total number of BrdU immunoreactive and BrdU/TuJ-1 double-positive cells 2 to 3 weeks after BrdU labeling. Global ischemia significantly increases the total newborn cell (*) and new neurons (#). The relative proportion of progenies adopting neuronal fate was reduced in gerbils in R group compared with C group. Reduction of neurogenesis was also noted in the RI compared with the I group. (B) Consecutive 1μm confocal images (×1,000, zoom factor of 8.8 for the BrdU/TuJ-1 panel and 1 for the BrdU/GFAP panel) in z-stacks showing the neuronal identity of newly divided cells in the GCL (arrow) of gerbils treated with irradiation and ischemia (RI). BrdU is labeled as green and cell markers as red. No colocalization of GFAP and BrdU was observed within the GCL in the RI animals. Scale bars = 10μm.

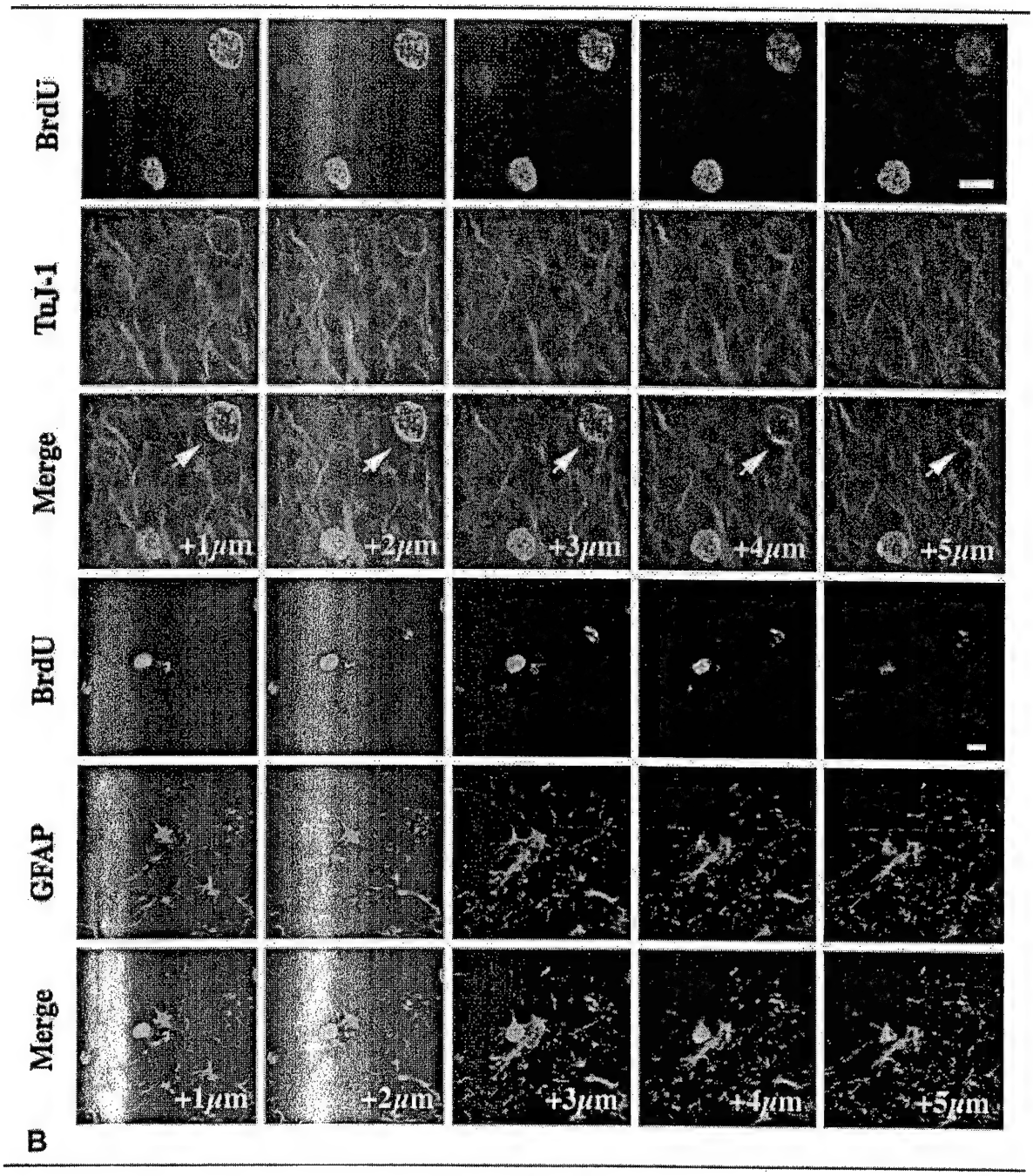

Figure 2 (Continued)

cant impairments in the hidden platform trials ($p < 0.01$ vs controls), and their impairments were significantly worse than those in the I group ($p < 0.05$). We also compared the frequency of trials in which the platform was found within the 60-second trial duration. During the visible platform sessions, this frequency was significantly lower in the RI group than the frequency in the C or R groups ($p < 0.05$; C: 11.29 ± 0.47; R: 10.86 ± 0.73; I: 9.57 ± 0.94; RI: 6.43 ± 1.76). During the hidden platform sessions, this frequency was also significantly lower in the RI group than in the C ($p < 0.01$), I ($p < 0.05$), or R groups ($p < 0.01$; C: 16.86 ± 0.45; R: 14.57 ± 0.87; I: 11.71 ± 2.5; RI: 6.29 ± 2.04). After the hidden platform training, an-

imals were subjected to a probe trial, in which only the C group showed memory retention by spending significantly more time searching in the target quadrant than in any other quadrant ($p < 0.01$; see Fig 3B). The C group also spent significantly more time in the target quadrant than the R ($p < 0.05$), I ($p < 0.05$), or RI groups ($p < 0.01$).

To assess whether impairments in sensorimotor function or reduced activity levels could have contributed to the impairments in water-maze performance after irradiation or ischemia, we tested gerbils for rotor-rod performance and open-field activity, respectively. Neither did irradiation, ischemia, nor combined treatment impair rotor-rod performance relative to controls. There were no group differences in average fall latencies in three consecutive trials ($p = 0.119$). Irradiation, ischemia, or combined treatment did not alter exploratory behavior in the open field. Comparable numbers of rearing events, total path lengths (Fig 4A, B), and total active times (data not shown) reflected normal vertical and horizontal activity levels in all groups. Vertical and horizontal activities declined over a 3-day period in all groups. Lack of overall group differences in open-field activity indicated normal habituation in all groups.

Discussion

The main finding of this study is that functional impairments after cerebral global ischemia are exacerbated by low dose of irradiation, which, in part, inhibits dentate gyrus neurogenesis. Increased neurogenesis from endogenous precursors in the adult brain after cerebral ischemia has been documented in various rodent models.[18–22,34,35] Although evidence based on synaptic morphology and electrophysiological data suggests that the newborn neurons might be functional in the normal dentate gyrus,[23,24] little is known about the functional impact of neurogenesis after an ischemic insult. Here, we show that under conditions of cerebral global ischemia, disruption of neurogenesis is associated with more severe functional impairments.

The extent of spontaneous recovery from cerebral ischemia is highly variable, which might reflect the location and extent of the injury. Motor recovery from cerebral ischemia may be associated with the adjacent cortical areas taking over the function of the damaged areas or utilization of alternative motor pathways.[4,8,10,17,36] Recovery of function outside the sensorimotor system is less well understood. Recent compelling evidence suggests that there is a considerable degree of neurogenesis occurring in some areas affected by cerebral ischemic injury in rodents,[18–21] raising the possibility that the genesis of new neural cells might account for an alternative mechanism in postischemic functional recovery. One approach to determine the functional impact of new neurons after cerebral ischemia is to compare the functional deficits between animals with normal and reduced neurogenesis after the insult. To evaluate the effect of reduced neurogenesis on functional outcome after ischemic injury, we used a split-dose radiation paradigm before the induction of ischemia. Low doses of cranial irradiation have been used previously to ablate neural progenitor cells in the brain.[26,27] Our results confirm that in gerbils, irradiation effectively reduced neurogenesis in the dentate GCL by inhibiting progenitor cell proliferation and neuronal differentiation (see Fig 2). After ischemia, animals that received prior irradiation have much less BrdU incorporation than those that did not receive irradiation (see Fig 2). This suggests that the reduction of endogenous progenitor cells has a profound effect on the central nervous system (CNS) to respond to an ischemia insult and to produce new cells that might participate in repair. The extent of radiation injury in the CNS is dose dependent and the susceptibility of different cell types is variable.[37,38] The normal adult mammalian CNS shows no apparent early or late morphological effects after a single dose of x-irradiation up to 10Gy.[39,40] The radiation paradigm used in this study did not cause any detectable neuronal loss. This is shown by the lack of significant difference between controls and irradiated animals for the number of NeuN-immunoreactive CA1 neurons in the septal hippocampus estimated by unbiased stereology (see Table 1). Five minutes of global ischemia eliminated greater than 50% of the septal CA1 neurons; however, there was no significant difference in the number of septal CA1 neurons between animals that were subjected to ischemia only and the combined treatment of irradiation and ischemia (see Table 1), suggesting that irradiation did not exacerbate ischemic neuronal injury. Furthermore, irradiation did not affect the overall synaptic profile of the dentate granule neurons and layer II cortical neurons (see Fig 1). Global ischemia, however, led to reduced basilar dendritic length of layer II cortical neurons compared with controls (C: $924 \pm 42\mu m$; I: $447 \pm 157\mu m$) and reduced branching patterns (data not shown). Irradiation also did not affect brain capillary morphology at the time of behavioral testing (see Fig. 1). Thus, our results suggest that the radiation treatment used here mainly targeted the neural progenitor cell population and, at least based on morphology, had minimal effect on matured, postmitotic neurons, cerebral microvasculature, and insult threshold.

Five minutes of BCCAO alone obliterated greater than 50% of septal CA1 neurons and likely contributed to learning impairments during the hidden platform training.[3] When preceded by irradiation, ischemia resulted in more severe functional impairments (see Fig 3). However, gerbils that were subjected to the combined treatment also showed significant impairments and slower swim speed during visible platform

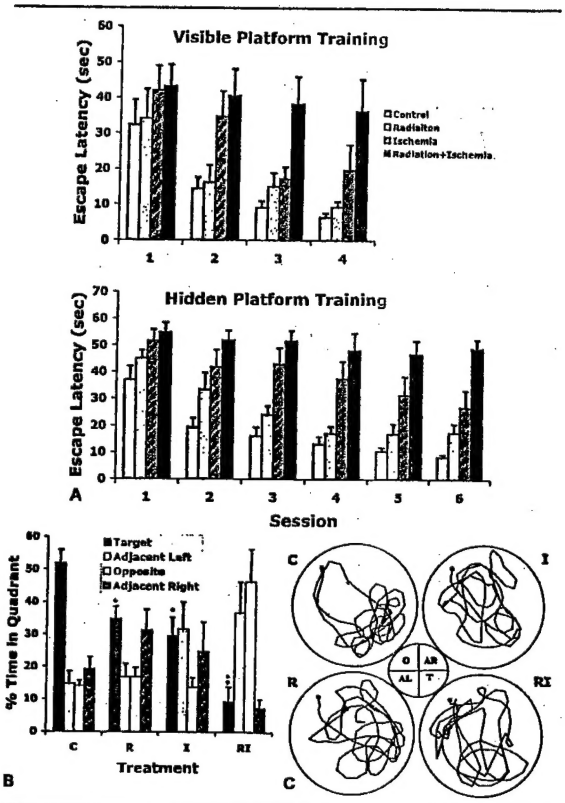

Fig 3. Irradiation exacerbates ischemia-induced encoding of spatial information. Water-maze test was conducted in gerbils that received sham treatment (C) (n = 11), irradiation (R) (n = 9), global ischemia (I) (n = 8), and combined treatment (RI) (n = 7). (A) Latency to find the visible platform (top) and hidden platform (bottom) during acquisition of the water-maze test. During the visible platform session, only RI gerbils demonstrated a significant impairment when compared with any of the other three groups ($p < 0.01$). During the hidden platform sessions, RI gerbils showed a much-worsened deficit compared with I group ($p < 0.05$, RI vs. I). Radiation does not have an effect on the water-maze acquisition. (B) In the probe trial, only the control group spent significantly more time searching in the target quadrant than in any of the other quadrants ($p < 0.05$), indicating retention memory. The R, I, and RI groups spent significantly less time in the target quadrant compared with the C group ($p < 0.05$; **$p < 0.01$). (C) Representative tracks during the probe trial. Quadrants are indicated clockwise as adjacent right (AR), target (T), adjacent left (AL), and opposite (O).*

training compared with any other group. Therefore, the impairments in these animals during the hidden platform training could be partly or completely caused by deficits in task learning in addition to spatial learning and memory.

Does reduced cell regeneration after ischemia contribute to the exacerbated water-maze impairments? Although under conditions of global ischemia reduced neurogenesis was associated with worsened functional outcomes, there was no simple correlation between the amount of dentate gyrus neurogenesis and the water-maze performance among all treatment groups. One direct interpretation would be that water-maze performance does not reflect the level of dentate neurogenesis per se. This is supported by a recent report suggesting that neurogenesis may be associated with the formation of some but not all types of hippocampal-dependent memories.[41] Because the increased dentate gyrus neurogenesis after global ischemia did not prevent water-maze deficits, a second explanation would be that the level of repair in the dentate might be insufficient to compensate the total deficits, and/or mechanisms in addition to dentate neurogenesis might modulate functional recovery. Because the total number of newborn cells constitutes less than 1% of the total granule cells in the dentate gyrus, there were no significant differ-

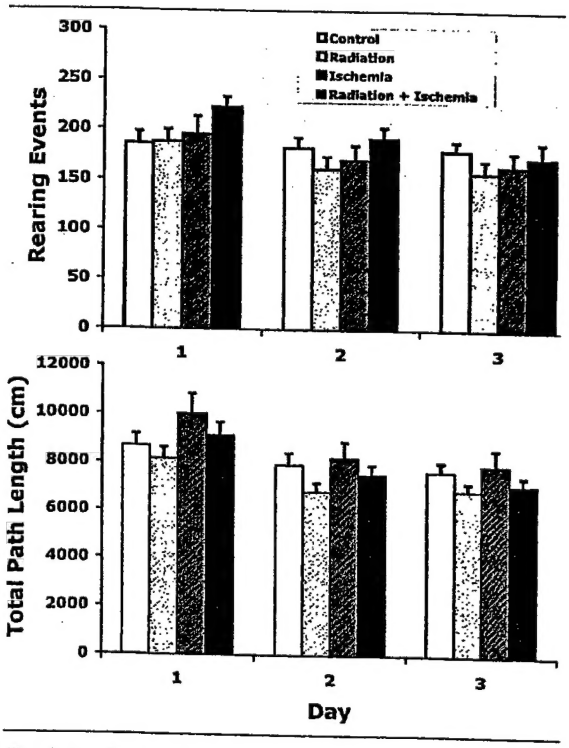

Fig 4. Irradiation or ischemia does not affect overall activity and exploratory behavior in the open field. Gerbils with sham treatment (C) (n = 11), irradiation (R) (n = 9), global ischemia (I) (n = 8), and combined treatment (RI) (n = 7) were tested in the novel open field for 3 consecutive days. Irradiation does not have any significant effect on exploratory behavior in the open field. In all treatment groups, vertical (A) and horizontal activities (B) declined over a 3-day period indicating normal habituation. Lack of significant difference in path length and rearing events reflects normal overall activity in all groups.

ences in the existing granule cell population among all groups (see Table 2). Therefore, the level of dentate gyrus neurogenesis is not sufficient to account for the differences in functional outcome. Because global ischemia damages brain regions besides the dentate gyrus, cells from these regions might be involved in functional outcomes. Alternatively, irradiation might affect pathways involved in reorganization that are not detected by morphological assessment but, however, are necessary for cognitive recovery after ischemia other than neurogenesis.

Nevertheless, irradiation worsened water-maze performance much more so in the ischemic animals than in the naive ones, suggesting that the courses of functional deterioration inflicted by irradiation between a normal and an injured brain are quite different. This is likely because of the deprivation of elevated repair and regeneration needed after ischemic injury by irradiation. Given the widespread distribution of neural progenitors throughout the brain,[42–45] it is possible that enhanced production of new neural cells at sites other than the dentate subgranular zone may well contribute to structural and functional recovery after ischemic injury. One potentially important site involved in cognition is the CA1 pyramidal layer that is able to regenerate after global cerebral ischemia.[34,35] In conclusion, this study suggests that under condition of cerebral ischemia, neurogenesis might play a contributory role in functional recovery. The development of more specific ways to inhibit neurogenesis is warranted to determine the exact role of neurogenesis in mediating cognitive function under baseline conditions and after injury.

This work was supported by the National Institutes of Health (R01 NS40469; J.L.; RO1CA76141, J.R.F.; R21NS40088, J.R.F.; R01 AG20079, J.R.), American Heart Association (SDG003007, J.L.), and the Department of Defense (DAMD17-01-1-0820, J.R.F.).

We thank A. Lim for technical assistance.

References

1. Lai SM, Studenski S, Duncan PW, Perera S. Persisting consequences of stroke measured by the Stroke Impact Scale. Stroke 2002;33:1840–1844.
2. Pulsinelli WA, Brierley JB, Plum F. Temporal profile of neuronal damage in a model of transient forebrain ischemia. Ann Neurol 1982;11:491–498.
3. Block F. Global ischemia and behavioural deficits. Prog Neurobiol 1999;58:279–295.
4. Seil SS. Recovery and repair issues after stroke from the scientific perspective. Curr Opin Neurol 1997;10:49–51.
5. Lee RG, van Donkelaar P. Mechanisms underlying functional recovery following stroke. Can J Neurol Sci 1995;22:257–263.
6. Kotila M, Waltimo O, Niemi ML, et al. The profile of recovery from stroke and factors influencing outcome. Stroke 1984;15: 1039–1044.
7. Chollet F, DiPiero V, Wise RJ, et al. The functional anatomy of motor recovery after stroke in humans: a study with positron emission tomography. Ann Neurol 1991;29:63–71.
8. Carmichael ST. Plasticity of cortical projections after stroke. Neuroscientist 2003;9:64–75.
9. Hess G, Aizenman CD, Donoghue JP. Conditions for the induction of long-term potentiation in layer II/III horizontal connections of the rat motor cortex. J Neurophysiol 1996;75: 1765–1778.
10. Sanes JN, Donoghue JP. Plasticity and primary motor cortex. Annu Rev Neurosci 2000;23:393–415.
11. Witte OW. Lesion-induced plasticity as a potential mechanism for recovery and rehabilitative training. Curr Opin Neurol 1998;11:655–662.
12. Seitz RJ, Azari NP, Knorr U, et al. The role of diaschisis in stroke recovery. Stroke 1999;30:1844–1850.
13. Klocker N, Bahr M. Brain repair—new avenues to an eternal dream? Trends Neurosci 2001;24:3–4.
14. Kruger GM, Morrison SJ. Brain repair by endogenous progenitors. Cell 2002;110:399–402.
15. Gage FH. Neurogenesis in the adult brain. J Neurosci 2002; 22:612–613.
16. Cao Q, Benton RL, Whittemore SR. Stem cell repair of central nervous system injury. J Neurosci Res 2002;68:501–510.
17. Chen S, Cohen SS, Hallett S. Nervous system reorganization following injury. Neuroscience 2002;111:761–773.
18. Liu J, Solway K, Messing RO, Sharp FR. Increased neurogenesis in the dentate gyrus after transient global ischemia in gerbils. J Neurosci 1998;18:7768–7778.
19. Jin K, Minami M, Lan JQ, et al. Neurogenesis in dentate subgranular zone and rostral subventricular zone after focal cerebral ischemia in the rat. Proc Natl Acad Sci USA 2001;98: 4710–4715.
20. Arvidsson A, Collin T, Kirik D, et al. Neuronal replacement from endogenous precursors in the adult brain after stroke. Nat Med 2002;8:963–970.
21. Parent JM, Vexler ZS, Gong C, et al. Rat forebrain neurogenesis and striatal neuron replacement after focal stroke. Ann Neurol 2002;52:802–813.
22. Kee NJ, Preston E, Wojtowicz JM. Enhanced neurogenesis after transient global ischemia in the dentate gyrus of the rat. Exp Brain Res 2001;136:313–320.
23. van Praag H, Schinder AF, Christie BR, et al. Functional neurogenesis in the adult hippocampus. Nature 2002;415: 1030–1034.
24. Shors TJ, Miesegaes G, Beylin A, et al. Neurogenesis in the adult is involved in the formation of trace memories. Nature 2001;410:372–376.
25. Mizumatsu S, Monje M, Morhardt D, et al. Extreme sensitivity of adult neurogenesis to low doses of X-irradiation. Cancer Res 2003;63:4021–4027.
26. Monje ML, Mizumatsu S, Fike JR, Palmer TD. Irradiation induces neural precursor-cell dysfunction. Nat Med 2002;8: 955–962.
27. Parent JM, Tada E, Fike JR, Lowenstein DH. Inhibition of dentate granule cell neurogenesis with brain irradiation does not prevent seizure-induced mossy fiber synaptic reorganization in the rat. J Neurosci 1999;19:4508–4519.
28. West MJ, Slomianka L, Gundersen HJ. Unbiased stereological estimation of the total number of neurons in the subdivisions of the rat hippocampus using the optical fractionator. Anat Rec 1991;231:482–497.
29. Gundersen HJ, Bendtsen TF, Korbo L, et al. Some new, simple and efficient stereological methods and their use in pathological research and diagnosis. APMIS 1988;96:379–394.
30. Gibb S, Kolb S. A method for vibratome sectioning of Golgi-Cox stained whole rat brain. J Neurosci Methods 1998;79:1–4.

31. Raber J, Bongers G, LeFevour A, et al. Androgens protect against apolipoprotein E4-induced cognitive deficits. J Neurosci 2002;22:5204–5209.
32. Raber J, Wong D, Buttini M, et al. Isoform-specific effects of human apolipoprotein E on brain function revealed in ApoE knockout mice: increased susceptibility of females. Proc Natl Acad Sci USA 1998;95:10914–10919.
33. Jucker M, Bialobok P, Hagg T, Ingram DK. Laminin immunohistochemistry in brain is dependent on method of tissue fixation. Brain Res 1992;586:166–170.
34. Schmidt W, Reymann KG. Proliferating cells differentiate into neurons in the hippocampal CA1 region of gerbils after global cerebral ischemia. Neurosci Lett 2002;334:153–156.
35. Nakatomi H, Kuriu T, Okabe S, et al. Regeneration of hippocampal pyramidal neurons after ischemic brain injury by recruitment of endogenous neural progenitors. Cell 2002;110: 429–441.
36. Nudo SS, Wise SS, SiFuentes S, Milliken SS. Neural substrates for the effects of rehabilitative training on motor recovery after ischemic infarct. Science 1996;272:1791–1794.
37. Hopewell JW. Radiation injury to the central nervous system. Med Pediatr Oncol 1998; (suppl 1):1–9.
38. Tofilon PJ, Fike JR. The radioresponse of the central nervous system: a dynamic process. Radiat Res 2000;153:357–370.
39. Hopewell JW, Wright EA. Effect of previous x-irradiation on the response of brain to injury. Nature 1967;215:1405–1406.
40. Hodges H, Katzung N, Sowinski P, et al. Late behavioural and neuropathological effects of local brain irradiation in the rat. Behav Brain Res 1998;91:99–114.
41. Shors TJ, Townsend DA, Zhao M, et al. Neurogenesis may relate to some but not all types of hippocampal-dependent learning. Hippocampus 2002;12:578–584.
42. Palmer TD, Markakis EA, Willhoite AR, et al. Fibroblast growth factor-2 activates a latent neurogenic program in neural stem cells from diverse regions of the adult CNS. J Neurosci 1999;19:8487–8497.
43. Pencea V, Bingaman KD, Wiegand SJ, Luskin MB. Infusion of brain-derived neurotrophic factor into the lateral ventricle of the adult rat leads to new neurons in the parenchyma of the striatum, septum, thalamus, and hypothalamus. J Neurosci 2001;21:6706–6717.
44. Rietze R, Poulin P, Weiss S. Mitotically active cells that generate neurons and astrocytes are present in multiple regions of the adult mouse hippocampus. J Comp Neurol 2000;424: 397–408.
45. Nunes MC, Roy NS, Keyoung HM, et al. Identification and isolation of multipotential neural progenitor cells from the subcortical white matter of the adult human brain. Nat Med 2003; 9:439–447.